THE NATIONAL ACADEMIES PRESS

SHARE f t in ✉

Using Infrared and High-Speed Ground-Penetrating Radar for Uniformity Measurements on New HMA Layers

DETAILS

BUY THIS BOOK

FIND RELATED TITLES

AUTHORS

Sebesta, Stephen; Saarenketo, Timo; and Scullion, Tom

The Second
S T R A T E G I C H I G H W A Y R E S E A R C H P R O G R A M

SHRP 2 REPORT S2-R06C-RR-1

Using Infrared and High-Speed Ground-Penetrating Radar for Uniformity Measurements on New HMA Layers

Stephen Sebesta and Tom Scullion
Texas A&M Transportation Institute
College Station, Texas

Timo Saarenketo
Roadscanners Oy
Rovaniemi, Finland

T R A N S P O R T A T I O N R E S E A R C H B O A R D

Subscriber Categories

Construction
Highways
Materials
Pavements

The Second Strategic Highway Research Program

America's highway system is critical to meeting the mobility and economic needs of local communities, regions, and the nation. Developments in research and technology—such as advanced materials, communications technology, new data collection technologies, and human factors science—offer a new opportunity to improve the safety and reliability of this important national resource. Breakthrough resolution of significant transportation problems, however, requires concentrated resources over a short time frame. Reflecting this need, the second Strategic Highway Research Program (SHRP 2) has an intense, large-scale focus, integrates multiple fields of research and technology, and is fundamentally different from the broad, mission-oriented, discipline-based research programs that have been the mainstay of the highway research industry for half a century.

The need for SHRP 2 was identified in *TRB Special Report 260: Strategic Highway Research: Saving Lives, Reducing Congestion, Improving Quality of Life,* published in 2001 and based on a study sponsored by Congress through the Transportation Equity Act for the 21st Century (TEA-21). SHRP 2, modeled after the first Strategic Highway Research Program, is a focused, time-constrained, management-driven program designed to complement existing highway research programs. SHRP 2 focuses on applied research in four areas: Safety, to prevent or reduce the severity of highway crashes by understanding driver behavior; Renewal, to address the aging infrastructure through rapid design and construction methods that cause minimal disruptions and produce lasting facilities; Reliability, to reduce congestion through incident reduction, management, response, and mitigation; and Capacity, to integrate mobility, economic, environmental, and community needs in the planning and designing of new transportation capacity.

SHRP 2 was authorized in August 2005 as part of the Safe, Accountable, Flexible, Efficient Transportation Equity Act: A Legacy for Users (SAFETEA-LU). The program is managed by the Transportation Research Board (TRB) on behalf of the National Research Council (NRC). SHRP 2 is conducted under a memorandum of understanding among the American Association of State Highway and Transportation Officials (AASHTO), the Federal Highway Administration (FHWA), and the National Academy of Sciences, parent organization of TRB and NRC. The program provides for competitive, merit-based selection of research contractors; independent research project oversight; and dissemination of research results.

Copyright Information

Notice

SHRP 2 Reports

THE NATIONAL ACADEMIES

Advisers to the Nation on Science, Engineering, and Medicine

The **National Academy of Sciences** is a private, nonprofit, self-perpetuating society of distinguished scholars engaged in scientific and engineering research, dedicated to the furtherance of science and technology and to their use for the general welfare. On the authority of the charter granted to it by Congress in 1863, the Academy has a mandate that requires it to advise the federal government on scientific and technical matters. Dr. Ralph J. Cicerone is president of the National Academy of Sciences.

The **National Academy of Engineering** was established in 1964, under the charter of the National Academy of Sciences, as a parallel organization of outstanding engineers. It is autonomous in its administration and in the selection of its members, sharing with the National Academy of Sciences the responsibility for advising the federal government. The National Academy of Engineering also sponsors engineering programs aimed at meeting national needs, encourages education and research, and recognizes the superior achievements of engineers. Dr. Charles M. Vest is president of the National Academy of Engineering.

The **Institute of Medicine** was established in 1970 by the National Academy of Sciences to secure the services of eminent members of appropriate professions in the examination of policy matters pertaining to the health of the public. The Institute acts under the responsibility given to the National Academy of Sciences by its congressional charter to be an adviser to the federal government and, on its own initiative, to identify issues of medical care, research, and education. Dr. Harvey V. Fineberg is president of the Institute of Medicine.

The **National Research Council** was organized by the National Academy of Sciences in 1916 to associate the broad community of science and technology with the Academy's purposes of furthering knowledge and advising the federal government. Functioning in accordance with general policies determined by the Academy, the Council has become the principal operating agency of both the National Academy of Sciences and the National Academy of Engineering in providing services to the government, the public, and the scientific and engineering communities. The Council is administered jointly by both Academies and the Institute of Medicine. Dr. Ralph J. Cicerone and Dr. Charles M. Vest are chair and vice chair, respectively, of the National Research Council.

The **Transportation Research Board** is one of six major divisions of the National Research Council. The mission of the Transportation Research Board is to provide leadership in transportation innovation and progress through research and information exchange, conducted within a setting that is objective, interdisciplinary, and multimodal. The Board's varied activities annually engage about 7,000 engineers, scientists, and other transportation researchers and practitioners from the public and private sectors and academia, all of whom contribute their expertise in the public interest. The program is supported by state transportation departments, federal agencies including the component administrations of the U.S. Department of Transportation, and other organizations and individuals interested in the development of transportation. **www.TRB.org**

www.national-academies.org

SHRP 2 STAFF

Ann M. Brach, *Director*
Stephen J. Andrle, *Deputy Director*
Neil J. Pedersen, *Deputy Director, Implementation and Communications*
James Bryant, *Senior Program Officer, Renewal*
Kenneth Campbell, *Chief Program Officer, Safety*
JoAnn Coleman, *Senior Program Assistant, Capacity and Reliability*
Eduardo Cusicanqui, *Financial Officer*
Walter Diewald, *Senior Program Officer, Safety*
Jerry DiMaggio, *Implementation Coordinator*
Shantia Douglas, *Senior Financial Assistant*
Charles Fay, *Senior Program Officer, Safety*
Carol Ford, *Senior Program Assistant, Renewal and Safety*
Elizabeth Forney, *Assistant Editor*
Jo Allen Gause, *Senior Program Officer, Capacity*
Rosalind Gomes, *Accounting/Financial Assistant*
Abdelmename Hedhli, *Visiting Professional*
James Hedlund, *Special Consultant, Safety Coordination*
Alyssa Hernandez, *Reports Coordinator*
Ralph Hessian, *Special Consultant, Capacity and Reliability*
Andy Horosko, *Special Consultant, Safety Field Data Collection*
William Hyman, *Senior Program Officer, Reliability*
Michael Marazzi, *Senior Editorial Assistant*
Linda Mason, *Communications Officer*
Reena Mathews, *Senior Program Officer, Capacity and Reliability*
Matthew Miller, *Program Officer, Capacity and Reliability*
Michael Miller, *Senior Program Assistant, Capacity and Reliability*
David Plazak, *Senior Program Officer, Capacity*
Monica Starnes, *Senior Program Officer, Renewal*
Onno Tool, *Visiting Professional*
Dean Trackman, *Managing Editor*
Connie Woldu, *Administrative Coordinator*
Patrick Zelinski, *Communications/Media Associate*

ACKNOWLEDGMENTS

FOREWORD

Monica A. Starnes, PhD, *SHRP 2 Senior Program Officer, Renewal*

Obtaining adequate in-place density is vital for achieving pavement durability for hot-mix asphalt (HMA) pavement. While nondestructive testing (NDT) can be used to determine the in-place density and thus help determine the expected pavement durability, rapid NDT techniques can also provide real-time information to paving crews so that corrective action can be taken as the HMA is placed and compacted.

Infrared (IR) imaging and ground-penetrating radar (GPR) are two technologies that can be used to identify in-place density during construction operations. During construction of an HMA pavement, IR techniques are able to evaluate its temperature uniformity, which is critical for avoiding areas of asphalt segregation and thus achieving the needed density. GPR can be used to measure the density of HMA layers, both during and after compaction. The advantages of using these NDT techniques are evident: (1) both techniques provide the needed information regarding expected density and thus durability, (2) both techniques are rapid and provide information in real time, and (3) both techniques provide continuous or near-continuous coverage of constructed HMA pavement in contrast to other existing technologies that take discrete measurements. In all, when used together these two technologies complement each other to deliver the needed information to undertake corrective action during paving operations.

This report presents the findings of the first two phases of SHRP 2 Renewal Project R06C, Using Infrared and High-Speed Ground-Penetrating Radar for Uniformity Measurements on New HMA Layers. The project piloted and evaluated existing IR and GPR technologies for their suitability to assess mat density and their readiness for field use. The report provides a thorough review of the technologies and the four pilots conducted in the United States.

The project also developed a 30-minute training video that gives an overview of the equipment installation, data gathering, and data interpretation for both NDT technologies. The video is available at www.trb.org/Main/Blurbs/167280.aspx.

An additional phase was recently added to this project to develop specifications and pilot them in collaboration with two state departments of transportation. Once completed, the results from this additional scope of work will be published as an addendum to this report.

CONTENTS

Online version of this report: www.trb.org/Main/Blurbs/167280.aspx.

Executive Summary

Introduction

In-place density is a critical factor in determining pavement durability in hot-mix asphalt (HMA). Localized nonuniform zones of mix, termed segregation, often become low-density areas in the mat. Segregation continues to be a major construction-related problem around the nation with a significant adverse impact on pavement service life. Real-time nondestructive testing (NDT) procedures are ideal tools to provide feedback to paving crews, and recent studies have shown that infrared (IR) imaging and ground-penetrating radar (GPR) can be used to assess in-place density during construction while providing nearly 100% testing coverage of the constructed area.

The most common form of HMA segregation, truck-end segregation, occurs where the HMA at the ends of the truckload is colder and sometimes coarser in gradation. These locations show up in the mat as regularly spaced defects at approximately 150-ft intervals along the roadway. Oftentimes, drivers can feel a dip at the segregated locations; over time these locations, with the ingress of water and the influence of traffic loads, fail prematurely. These segregated locations deteriorate early, typically because of their lower density and higher susceptibility to raveling and fatigue cracking. This early distress not only results in poorer ride quality for the traveling public but also requires agencies to use resources earlier than planned to maintain the pavement condition.

Realizing the importance of mitigating segregation in HMA construction, many agencies have implemented segregation check procedures. However, the segregation problem persists and, some would say, is getting worse. Contributing to the problem of detecting and controlling segregation is the increased use of night paving, which makes it difficult to visually see problems. Although many departments of transportation (DOTs) have implemented segregation check procedures, these existing methods typically test only a small portion of the mat. Since HMA segregation is typically localized, spot inspection methods that are currently employed risk overlooking problem areas. It is in the best interest of the DOT, the contractor, and the public to eliminate segregation, so an ideal toolset for combating HMA segregation would include a placement monitoring system that detects segregation quantitatively and in real time, followed by a full-coverage technique after construction for quality assurance. Infrared imaging and ground-penetrating radar technologies are two NDT candidates that previous experience has shown may be able to provide this placement monitoring and postconstruction quality assurance.

Historically, HMA segregation was thought of as a mechanical phenomenon consisting of localized concentrations of coarse gradation. Although this type of segregation certainly exists, the discovery of how thermal signatures from the HMA relate to segregation altered the definition of segregation to include both physical and thermal components. Building on the concept of temperature segregation, several independent agencies have completed research demonstrating

1

that infrared thermography has promise for detecting and quantifying the severity of segregated locations. During evaluation for segregation with infrared thermography, potentially segregated locations show up as cold spots, and the severity of segregation is quantified by the magnitude of the temperature differential at the anomalous location. Although visual inspection certainly remains a part of the solution for combating segregation, in many instances thermography detects anomalies where the human eye cannot discern anything unusual in the HMA mat. Essentially, the cold spots typically result in a low-density location in the finished HMA mat; these cold spots may also exhibit a coarser gradation and lower asphalt cement content.

Another tool that shows promise for evaluating HMA for segregation is GPR. Whereas thermal surveys take place during placement of the HMA, GPR surveys take place after compaction is complete. Historically used for tasks such as estimating pavement layer thickness, GPR measures an electrical property of the HMA that has been shown to correlate well with mat density. By calibrating the GPR to the HMA density, the radar NDT technique may be able to serve as a final quality assurance check on the completed mat. GPR possesses a unique advantage over traditional density-based testing because data collection with GPR is typically performed by a vehicle-mounted system. Nearly 100% of the newly constructed surface area can be tested in a matter of minutes.

Given the current knowledge and promising previous efforts with using infrared and GPR NDT techniques, the objectives of this project were to (a) demonstrate infrared imaging and GPR technologies as NDT techniques to assess HMA density and degree of segregation and (b) make recommendations for how these technologies can be incorporated into existing DOT specifications for verifying construction quality.

A critical requirement for the NDT techniques is that they provide nearly 100% coverage of the constructed surface area. To accomplish the project objectives, a literature search was used to first identify the most promising infrared and GPR technologies for this application. Next, the project team developed test protocols to use in the field. Finally, to demonstrate the technologies, one project in each of the four American Association of State Highway and Transportation Officials (AASHTO) regions was surveyed for uniformity with the recommended infrared and radar systems.

Findings

Numerous techniques exist for collecting thermal profiles of HMA construction. The most promising thermal techniques for full-coverage testing of HMA construction include process control infrared cameras, infrared line scanners, and infrared sensor bars. While all three of these systems could be developed to perform the desired full-coverage testing of HMA construction, only the infrared sensor bar system is currently commercially available. Infrared cameras and line scanners are commercially available, but no commercially available software solution exists to create a distance-based profile view of the thermal data.

GPR systems are commercially available for collecting full-coverage uniformity data. In this study the steps needed to convert the GPR signals into the surface air voids were developed and demonstrated by the research team. This required the development of a regression equation that relates the computed surface dielectric to the air void content measured on field cores. The use of GPR in the United States is complicated because of restrictions placed on the technology by the Federal Communications Commission (FCC). An FCC-compliant GPR system suitable for this application was demonstrated in this study, but additional data-processing capabilities need to be developed to facilitate full implementation for this application. Other grandfathered GPR systems (before the FCC 2002 ruling) are available through service providers.

Based on these findings, researchers conducted field demonstrations in each of the four AASHTO regions on projects representing a variety of placement operations and included two projects using warm-mix asphalt (WMA) technology. The research team used an infrared sensor bar system from MOBA Corporation and the Texas A&M Transportation Institute's 1-GHz radar

system for the thermal and radar surveys. On three projects, a 2.2-GHz air-coupled GPR system from Geophysical Survey Systems, Inc. (GSSI) also provided radar survey data.

The infrared system worked well, installing easily and providing real-time output for review by the superintendent, inspector, and researchers. In terms of level of testing coverage and amount of operator attendance and effort required, the field demonstrations indicated this infrared bar system is clearly superior to the localized thermal profiling methods currently in some DOT test procedures. The thermal data correlated well with in-place mat density, where thermally segregated locations typically became zones of reduced pavement density and in some cases coarser gradation. The final air voids in the mat were found to be a function of both placement temperature and mix properties. For example, the final mat density on one WMA project was strongly influenced by thermal segregation with final air voids at thermally segregated locations of almost 14%, well in excess of allowable limits (typically 9%). On the other demonstration project using WMA, the final mat density was not as strongly influenced by thermal segregation; the cold spots at a similar placement temperature had air void contents of less than 8%.

The GPR systems used performed well for data collection and, with the field calibrations and postprocessing steps described in this report, generated full-coverage density maps of the constructed surface area. The two GPR systems used in this study correlated well with each other and, after calibration to field cores, provided nearly identical results. With calibration, the GPR systems provided a technique to evaluate the density uniformity of nearly 100% of the constructed mat area. The commercially available and FCC-compliant 2.2-GHz system from GSSI should provide the hardware platform for a viable method for uniformity assessment of new overlays.

Conclusions

The work conducted indicates both IR imaging and GPR can be used to collect data over the entire constructed surface area with minimal effort. Infrared measurement systems for profiling hot-mix asphalt construction exist commercially. These systems appear field ready and simple to operate. The results from the demonstrations conducted during this project indicate that states wishing to implement full-coverage thermal profiling may need to perform additional investigations to determine what level of thermal segregation indicates a concern with their mixes. However, as clearly shown in this report, the low-temperature locations were also the locations of highest air voids. The level of air voids is also a function of the compactibility of the mix being placed. Therefore, IR imaging has the capabilities to permit DOTs to identify the critical potential defect locations; field coring (or GPR testing) will then be required to determine if the mix is out of the allowable specification tolerances. This focused coring option will eliminate all of the problems with random coring, which typically does not detect these localized defect areas. Potential users should also be aware of the limitations of the technology. Certain rolling patterns with workable HMA mixes possibly minimize the impacts of thermal segregation; at the other extreme, a thermally uniform mat that does not get compacted properly by a good rolling operation could still exhibit uniformity and density problems. It was certainly interesting to note that warm-mix asphalt technologies (at least the foaming process) had variable success at producing a uniformly compacted mat. On one WMA project, the low temperatures measured with Pave-IR only occurred at locations of paver stops. The actual placement temperature was higher, but a cold zone was detected once the paving train resumed since that mix was sitting on the ground for the duration of the paver stop. This cold zone did not become high air voids after compaction. On the other WMA project, low temperatures occurred due both to severe thermal segregation (i.e., actual placement temperatures) and due to paver stops, and all of these locations of low temperature became regions of high air voids after compaction.

GPR is less developed for full implementation into specifications. Even though commercial systems and service providers do exist, with GPR the major limitations are the level of expertise required and the lack of data-processing automation. Generally, several steps of processing are

4

required before the user can generate the full-coverage data output. Additional work is needed to streamline the process of transforming GPR data into a meaningful uniformity assessment for overlays. For typical lift thicknesses of surface mixes (2 in. or less), the 1- and 2.2-GHz GPR systems should be acceptable solutions for GPR data collection. In practice, until further hardware is developed, because of FCC restrictions, new users will need to rely on the 2.2-GHz GPR system.

The goal of investing in either of these NDT technologies is to foster higher quality, more uniformly constructed, and longer-lasting new surfacings. With state agency manpower continuing to be strained because of budget conditions, the use of an automated thermal profiling system offers a system for passive inspection. From the contractor's standpoint, the ability to obtain information on the uniformity of the mat during placement allows for real-time action to improve overall product uniformity. Assuming adequate compaction takes place, a more uniform mat increases the probability of the quality control/quality assurance cores resulting in a bonus.

Successful implementation of the GPR technology would allow agencies to have a complete picture of the overall quality of the completed HMA product. Such a picture provides much more information about the quality of the final product than the current random coring methods typically employed. As highway administrators are becoming increasingly concerned with both ensuring and documenting the homogeneity of HMA construction, infrared and GPR techniques offer potential solutions for accomplishing that goal. All the NDT data could be stored in a database for use if and when pavement defects appear.

Recommendations

Based on the findings in this project, thermal segregation detection using an infrared bar should be considered for implementation into agency specifications for uniformity assessment. The system demonstrated in this report provides the agency with color profile maps of placement temperatures and the number and duration of paver stops. The additional use of Global Positioning System (GPS) technology ensures that these potential problem areas can be accurately located for additional follow-up testing. The following activities should be considered to aid in expediting implementation of the IR imaging systems:

- Conduct additional demonstration projects including the full-scale validation coring described in this report. At least six additional DOTs (including one Canadian province) contacted the research team during this study asking to be included in the demonstration testing; however, this project restricted demonstration to four states. This level of interest clearly shows that thermal segregation is a recognized major concern for many (if not all) DOTs.
- Conduct webinars and other presentations at national conferences to inform potential users.
- Arrange visits to specific states to meet with key decision makers. These decision makers are typically state material engineers, paving contractor association representatives, IR equipment suppliers, and selected contractors. The purpose of these visits should be to explain this technology in detail and to provide information on implementation options. The specific goals of these visits will be to identify reporting requirements that will meet the DOT's objectives of constructing more uniform, longer-lasting overlays; developing draft specifications; establishing pilot implementation projects where the new technology can be used in parallel with existing processes; and identifying how the existing system can be customized to meet each agency's reporting needs.

Chapter 4 and the appendices discuss specification approaches that agencies could use to implement this technology. These approaches include using the thermal profile

- For passive inspection, in which the thermal profile largely serves as information to the contractor and agency to promote uniformity;

- To trigger other action when thermal segregation exists, in which locations with thermal segregation receive spot testing with a density profile to determine if substantial density differentials exist;
- To measure compliance with placement temperature tolerances, in which the thermal profile simply measures if the placement temperatures stay within the range required by the agencies' specifications; and
- For focused coring, in which, instead of random coring, the engineer selects a core location for placement pay factors based on the thermal profile.

From the findings in this research project, GPR has an advantage over IR imaging because it is used on the final mat after compaction. If problems are found in the GPR analysis, then these will be low-density areas where future failures can be anticipated. However, additional development is needed to streamline the steps from data collection to project uniformity evaluation before successful implementation can occur. This process will require partnering with industries and working with their radar systems to integrate the data collection and processing functions into a full-featured system tailored toward uniformity assessment of new asphalt pavement layers. Chapter 4 presents additional details on how this integration may be accomplished.

CHAPTER 1

Background

Problem Statement and Research Objective

For hot-mix asphalt (HMA) pavement, in-place density is a critical determining factor for pavement durability. Real-time nondestructive testing (NDT) procedures are ideal tools to provide immediate feedback to paving crews so that corrective action can be taken. Promising recent studies have shown that infrared (IR) imaging and ground-penetrating radar (GPR) technologies can be used to identify in-place density during construction operations. Both technologies can be used to provide nearly 100% coverage of constructed layers in contrast to other existing technologies such as nuclear density gauges and electrical impedance devices that take discrete measurements.

Temperature uniformity is critical for achieving the needed density. Temperature segregation continues to be a frequently reported defect in new HMA overlays, and such segregation is difficult to detect with traditional techniques during mat placement. Thermally segregated areas result in periodic low-density areas in new mats that let water enter lower layers, significantly shortening the performance life of new overlays. IR imaging techniques are already being implemented by some transportation agencies for quality assurance (QA) purposes.

GPR can also be used to measure in real time the density of HMA layers, both during and after compaction. Although this technology is not new, very little progress has been made in implementing GPR in construction specifications. The Finland Road Authority, for example, has used GPR and implemented a test procedure in 2002 as an accepted method of measuring HMA layer density. No department of transportation (DOT) in the United States, however, has implemented GPR for QA of HMA layers.

The objective of this project was to demonstrate IR and GPR technologies as NDT techniques to assess HMA density and segregation and to make recommendations for how these technologies can be incorporated into existing DOT specifications for construction QA. The IR and GPR technologies under investigation should provide nearly 100% coverage of the constructed surface area.

Scope of Study

This project focused on seeking off-the-shelf IR and GPR technologies that are best suited for collecting nearly 100% coverage data on HMA construction. Researchers reviewed equipment specifications and test procedures prior to recommending which IR and GPR equipment to consider for demonstration. Working with DOTs and equipment manufacturers, the research team showcased the NDT equipment on one project in each of the four AASHTO regions.

C H A P T E R   2

Research Approach

This project employed IR imaging and GPR technologies best suited for developing a profile view of the quality and uniformity of HMA construction. With the IR technology, this profile view consists of HMA placement temperatures presented spatially over the new HMA mat area. With GPR, after data processing, this profile view consists of HMA surface densities for the entire mat.

Both IR and GPR techniques have been used by numerous agencies with success to identify surface and subsurface defects in flexible pavements. In this project, a series of nine tasks, highlighted below, enabled the research team to demonstrate IR and GPR techniques for performing nearly 100% coverage evaluation of the uniformity of HMA construction projects.

Project Tasks

The following is a description of the project tasks:

- *Task 1.* Conduct an international literature search to identify applicable IR and GPR NDT technologies for assessing HMA density and segregation during construction activities.
- *Task 2.* Based on the findings from Task 1, evaluate and recommend the most promising NDT equipment and testing protocols for assessing HMA density and segregation during pavement construction. The recommendations

need to include detailed evaluations of the practical performance values, such as speed, accuracy, precision, ease of use, and so forth, of these technologies and techniques for their successful implementation.
- *Task 3.* Develop and submit to SHRP 2 detailed plans for field demonstration and validation of the recommended NDT techniques.
- *Task 4.* Conduct a field demonstration of these techniques in one transportation agency and conduct validation of the results using core testing to determine actual densities.
- *Task 5.* Prepare and submit to SHRP 2 an interim report documenting Tasks 1 through 4. The interim report should include recommendations to demonstrate the techniques in the three remaining AASHTO regions. Additionally, the report should include any recommendations regarding modifications to testing procedures that could improve the performance of these technologies.
- *Task 6.* Conduct field demonstrations in the remaining three AASHTO regions recommended in Task 5.
- *Task 7.* Document testing protocols and prepare training materials for these technologies based on the lessons learned during the field demonstrations.
- *Task 8.* Prepare a draft final report documenting the entire project and submit it to SHRP 2 for review.
- *Task 9.* Prepare and submit a revised final report that responds to reviewer comments.

CHAPTER 3

Findings and Applications

Several IR technologies may be able to provide nearly 100% coverage of HMA construction; these include infrared cameras, infrared line scanners, and infrared sensor bars. With GPR, commercial availability in the United States is largely limited to one system because of Federal Communications Commission (FCC) regulations. Some agencies already have thermal profiling procedures adopted and implemented, and one agency in Europe (Finland) has adopted a procedure for uniformity assessment of HMA construction with GPR. The research team determined that the most promising commercially available NDT equipment is an infrared system from MOBA Corporation and a 2.2-GHz GPR system from Geophysical Survey Systems, Inc. (GSSI).

The research team performed field demonstrations with infrared and radar NDT in each of the four AASHTO regions and collected a minimum of 10 field cores for laboratory validation testing at each demonstration project.

After shakedown testing in Texas, full-scale testing was performed in the states of Florida, Minnesota, and Maine. Full details of the results obtained and the conclusions drawn are presented in this chapter. In summary, both the IR imaging system and the GPR system performed well at measuring the uniformity of the overlays being placed. Recommendations for full-scale implementation are provided in the next chapter.

Literature Search Findings

Summary

Departments of transportation typically adjust pay for field placement of HMA based on how core densities compare with a set target value. However, these coring programs are spot specific and likely miss localized areas of low quality. In the 1990s, researchers began experimenting with IR imaging and GPR technologies for collecting full-coverage quality evaluations on new HMA construction. Both IR and GPR technologies have matured and can now effectively screen

HMA construction for quality. IR technologies have been implemented for this purpose in some U.S. state DOTs and in Sweden, and GPR has been implemented in areas of Europe. This literature search details problems occurring from localized segregation, outlines current IR and GPR devices available for evaluating hot-mix construction uniformity, and summarizes current implementation approaches in use for both IR and GPR technologies.

The Problem

For HMA placement quality assurance, most transportation departments sample by coring only a small fraction of the mat area placed. The core air void contents are used to determine placement acceptance and pay-adjustment factors. This practice is in place largely because of time requirements for testing and not necessarily a lack of desire for more extensive testing coverage. In fact, most agencies would like to obtain more extensive testing coverage to reduce agency risk, evaluate uniformity, and reduce the public's exposure to the risk of sizeable portions of the work not complying with specifications.

In HMA paving, operational variances and problems with segregation can significantly alter the uniformity of the in-place product, resulting in isolated areas at risk of early distress. For example, Figure 3.1 shows cyclic segregation in HMA. These segregated locations typically result in reduced density, increased holding of water after rain events, and high risks of early pavement distress such as raveling and cracking.

Historically, anomalous, or segregated, locations have been identified primarily through visual assessment. This subjective approach leaves ample room for error and disputes, so agencies seeking to push the state of the art have turned to IR and GPR techniques to obtain quantitative, full-coverage evaluations of new HMA layers. IR techniques exist that can provide full-coverage data collection of mat placement

Figure 3.1. Segregated location after rain event.

temperatures behind the screed, and GPR techniques exist that can provide full-coverage quality assurance evaluations of the final compacted HMA product. For example, Figure 3.2 shows an IR image and a corresponding visual image of an HMA mat with cyclic segregation. GPR captures the reflected energy of waves transited by the GPR antenna. The reflected energy from the surface can easily be processed to compute the surface dielectric of the top layer. For a very uniform (nonsegregated) mat, this reflected energy should also be very uniform; Figure 3.3 contrasts dielectric plots collected with GPR of both uniform and segregated HMA mats. Sudden localized drops in surface dielectric are clear indicators of classical truck-end segregation.

Current IR Technologies

Background

IR technology has made numerous inroads in the past 20 years. IR imaging has been used to attempt to find subsurface defects in highways, bridges, and tunnels. Much interest in new methods of detecting segregation resulted when, in 1996, Stephen Read suggested temperature differentials in HMA were related to segregation (*3*). Since that time, several research efforts have validated the relationship between temperature differentials in the pavement mat and HMA properties such as density, asphalt content, and gradation. Among these efforts was work at the National Center for Asphalt Technology (NCAT), additional work in Washington State, and work in Texas (*4–6*). Owing to the continued development of thermal measurement instruments, it is possible to obtain continuous accurate measurements of the mix once it leaves the paver and thereby provide a means to ensure that the whole production line is under control (*7*).

IR sensors operate by detecting the amount of electromagnetic energy emitted from the target. As the temperature of the target increases, the amount of emitted energy increases.

Photos courtesy of the Washington State Department of Transportation.

Figure 3.2. Thermal profile and visual image showing pavement condition of cold spots (1).
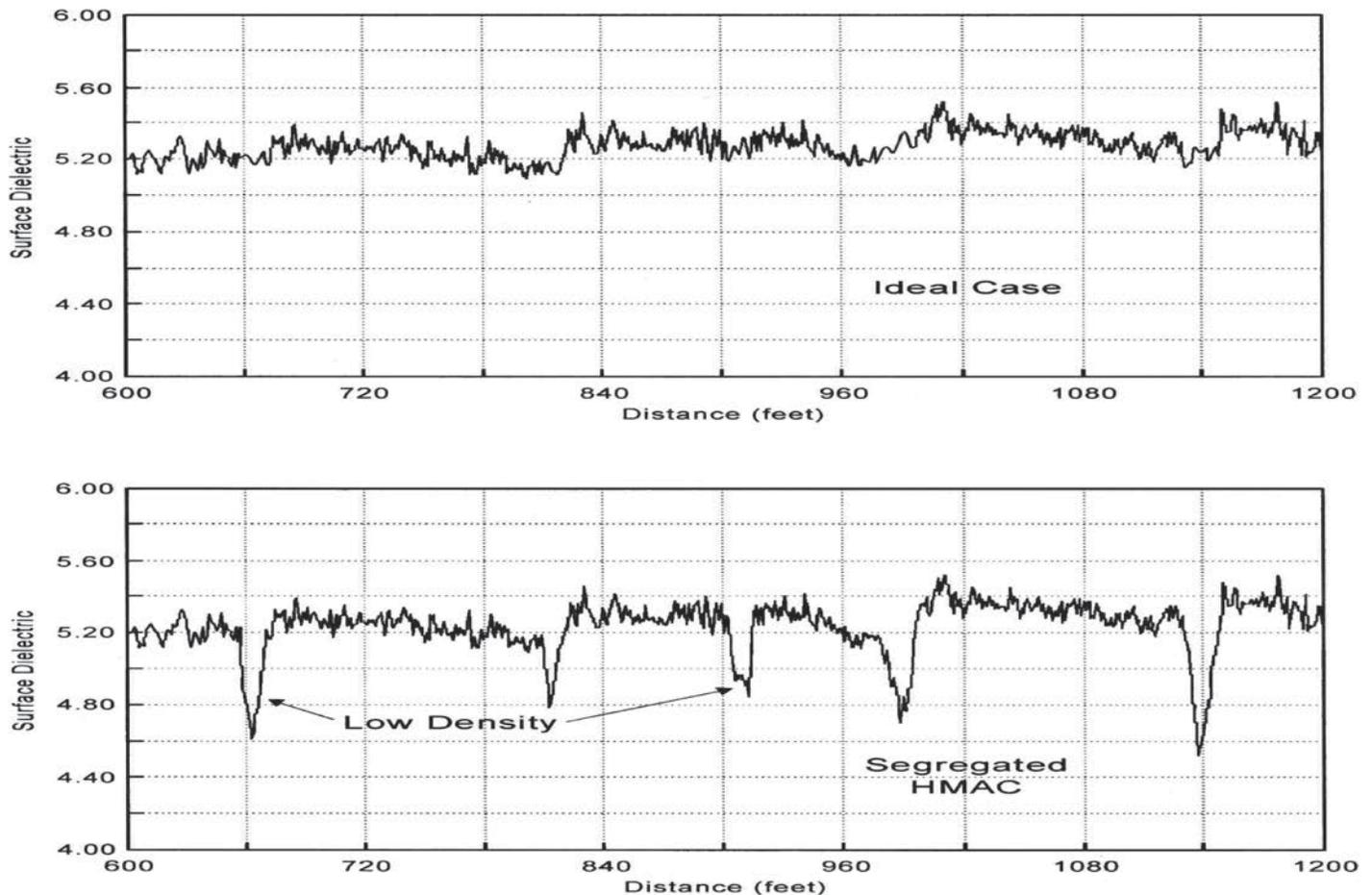
Figure 3.3. Comparison of surface dielectrics measured with GPR of uniform (top) and cyclically segregated (bottom) HMA (2).

The basic relationship between the target temperature and the output of a radiation thermometer is

$$V(T) = \varepsilon K T^N$$

where

  $V(T)$ = thermometer output with temperature,
  ε = target emissivity,
  K = constant,
  T = target temperature,
  N = N factor [= $14388/(\lambda T)$], and
  λ = equivalent wavelength.

For the operating conditions and temperatures encountered during HMA paving, a sensor with a spectral response of 8 to 14 μm provides an optimal balance of accuracy, measurement range, and resistance to effects of atmospheric transmittance.

Available IR Systems

Spot radiometers, infrared cameras, infrared line scanners, and infrared sensor bars are four techniques available for collecting thermal data. Figures 3.4 and 3.5 show technologies known to have been used on HMA projects.

Spot radiometers are handheld temperature "guns" and are useful for testing small areas, but they are not practical for collecting full-coverage data of an entire project. IR cameras, line scanners, and sensor bars all have the capability of collecting true full-coverage data behind the screed with minimal operator attendance. In the simplest form of use, IR cameras take snapshots and, through postprocessing, provide temperature distribution statistics of individual images. Temperature contour plots can be developed by merging multiple images. Noted drawbacks of using IR cameras include the necessity for constant operator attendance, poor precision in identifying the location on the mat that the picture captures, and the need to merge numerous snapshots to analyze an entire project (6).

Although discussions with industry manufacturers during the course of this project indicate an IR camera could be used to provide full-coverage, automated temperature profiling, such application would require a third-party software solution. Currently, no such solution is known to be commercially

Figure 3.4. Spot radiometer, IR camera, and IR bar measurement systems.

available. However, software packages that integrate GPR and thermal camera data are under development in Finland.

An IR line scanner could image the entire lane width and, as long as a software solution exists to collect and process the data as required, could provide adequate data-collection and data-processing features for uniformity measurements. Figure 3.5 shows a paver with a line scanner installed to collect thermal profile data. The IR line scanners have been used in Sweden for years in certain road regions. The Swedish National Road Administration has published a method description. Appendix A presents an English translation.

IR bar systems specifically for HMA uniformity measurement are currently available commercially. These systems can image the entire production run without operator attendance while providing real-time feedback to the paver operator, project superintendent, and inspector. The IR bar system provides a two-dimensional contour plot as the output in both real time and postprocessing without the need to merge

numerous files. However, areas of the mat may exist where data points are interpolated rather than directly measured, depending on the number of sensors selected, the sensor spacing, and the sensor distance-to-spot (d:s) ratio.

Table 3.1 summarizes potential IR data collection devices and the strengths and limitations of each. Table 3.2 lists some manufacturers of these devices.

Example IR Case Studies

Numerous agencies have examined thermal uniformity criteria for HMA paving. While NCAT defined severities of segregation based on thermal temperature differentials, the Washington State DOT (WSDOT) and Texas DOT (TxDOT) selected 25°F as the upper limit before the section is deemed at risk of not meeting uniformity specifications.

Figure 3.6 illustrates how TxDOT developed this threshold temperature differential value. Based on existing specifications

Photo courtesy of Mats Wendel, Swedish National Road Administration (SNRA).

Figure 3.5. IR line scanner performing thermal profiling.

Table 3.1. IR Devices for Data Collection

IR Device	Approximate Cost (US$)	Strengths	Potential Drawbacks
Handheld spot radiometer	150–500	Inexpensive, compact Already suitable for some DOT test procedures	Requires constant attendance Only logs high, low, and average
IR camera (such as FLIR InfraCAM)	4,000	Inexpensive, compact Already suitable for some DOT test procedures	Requires constant attendance Only records snapshots; not practical for full-coverage testing
IR line scanner (such as Raytek MP150)	19,000[a]	Directly measures entire mat width with up to 1,024 measurement points per line Does not require constant operator attendance System developed and in use in Sweden	Unknown if turnkey software is commercially available Must be mounted onto paver
IR camera (a process monitoring system such as FLIR A320)	13,000[a] 17,000 with required options[a]	Capable of full-coverage testing and streaming of temperature-rich video Does not require constant operator attendance	No turnkey software solution currently available for full-coverage HMA uniformity testing Must be mounted onto paver
IR sensor bar (such as MOBA Pave-IR)	18,000	System developed and in use in Texas Does not require constant operator attendance Incorporates GPS Turnkey system available for HMA testing	Sensor geometry and d:s ratio may result in portions of mat not being directly measured Must be mounted onto paver

[a] The cost is the base price of the equipment. Availability of a software solution for HMA profiling may affect the price.

for density uniformity, numerous projects were tested with thermal imaging equipment, and then cores at locations of varying temperature were collected. On average, a temperature differential exceeding 25°F produced density variations exceeding the specification maximum (*6, 8*). WSDOT selected 25°F because it discovered approximately 90% of field nuclear density profiles failed to pass their density uniformity specification when the temperature differential exceeded 25°F (*1, 5*).

Through research and implementation efforts, researchers in Texas have conducted thermal investigations on more than a dozen paving projects. Many of these results have been documented elsewhere through either research reports or technical memoranda. As an example case study, Figure 3.7 shows an excerpt of thermal profile results from a Type D mix placed in January 2005. This project used end-dump trucks into a material transfer device (MTD), and the thermal survey using

Table 3.2. Thermal Imaging Manufacturers

Manufacturer	Device Most Suited to IR Profiling of HMA	Contact
DIAS Infrared GmbH	IR cameras[a]	www.dias-infrared.de/index.php/content/view/4/37/lang,en/
FLIR	IR cameras[a]	www.flir.com/US/
Infrared Cameras, Inc.	IR cameras[a]	www.infraredcamerasinc.com/
Infratec GmbH	IR cameras[a]	www.infratec.com
IRCAM GmbH	IR cameras[a]	www.ircam.de/startseite/startseite_d.php
IRCameras	IR cameras[a]	www.ircameras.com/
IRCON	Line scanner[a]	http://ircon.com/
MOBA	IR bar	www.moba.de/en.html
Raytek	Line scanner[a]	www.raytek.com/Raytek/en-r0/
ShedWorks, Inc.	IR bar[a]	www.shedworks.com/
Sierra Pacific Innovations	IR cameras[a]	www.x20.org/thermal/index.htm
Xenics	Line scanner, IR cameras[a]	www.xenics.com/

[a] Commercial availability of a software solution for automated, full-coverage HMA thermal profiling is unknown for these devices.

pcf = pounds per cubic foot
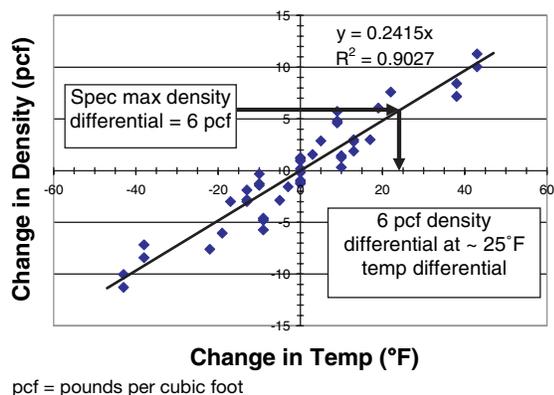
Figure 3.6. Example relationship between temperature differential and core density differential (6).

an IR sensor bar system revealed significant temperature differentials along the longitudinal profile typical of truck-end segregation. Based on the survey, TxDOT met with the contractor and worked to improve the quality and uniformity of the project through better control at the plant, use of a different model MTD, and altered rolling patterns.

After modifying operational procedures, thermal profiles exhibited significantly improved mat placement uniformity. Figure 3.8 contrasts the resultant thermal profiles after the contractor implemented changes to the original profile shown in Figure 3.7.

Figures 3.9 and 3.10 illustrate how the changes in operations significantly tightened the measured placement temperature distribution. With the initial operation, approximately 95% of measured temperatures fell within a 90°F window. With the new operation based on the recommendations from the thermal survey, approximately 95% of measured temperatures fell within a 40°F window. Based on recommendations from the initial thermal profile survey, the modified operation reduced the range of mat placement temperatures by more than 50%. Without the thermal survey, the extent of variability in the initial paving operation likely would not have been discovered.

In Europe, thermal imaging was recently performed on a resurfacing project in the Netherlands. Researchers used two

IR cameras and collected more than 400 images from the side of the mat at predetermined 10-m intervals (*10*). Extensive postprocessing of the images allowed researchers to compile contour plots with distance of the mat temperatures (*10*). Figure 3.11 shows one of the thermal plots generated from the IR camera. Researchers in the Netherlands performing this work also evaluated a line scanner and indicated they preferred the line scanner because it was easier to use and produced contour pictures immediately (A. Doree, unpublished data).

IR technology is more developed in Sweden, where line scanners have been adopted for use to collect thermal profiles. Figure 3.5 shows a paver equipped with a line scanner system, and Figure 3.12 shows example output from this system.

Figure 3.13 illustrates another case study from thermal profiling on a Texas project using an IR sensor bar system. The paving train exhibited truck-end thermal segregation, which showed up as cold spots in the IR profile. Figure 3.14 contrasts the surface appearance of a cold spot with the appearance of a location with normal placement temperature. In this case, the contractor elected to use a different MTD the next day, which produced the profile shown in Figure 3.15. The original operation produced placement temperature differentials of 50°F to 80°F; the new operation reduced these differentials to 30°F or less.

Current IR Implementation Status

Currently, WSDOT and TxDOT are the only agencies known to have adopted thermal uniformity criteria in the United States. WSDOT uses SOP 733 to check for pavement areas with thermal differentials greater than 25°F. This procedure uses either an IR camera or a handheld IR thermometer to view at least five consecutive truckloads of HMA. When temperature differentials exceeding 25°F exist, the WSDOT procedure checks the density of the cold spot with a nuclear density gauge using the direct transmission mode. If four or more locations with a density less than 89% of the reference maximum density exist in a lot, the lot bid price is penalized 15%. In the WSDOT specification, only one location of low density per truckload gets counted toward the cumulative number of failing locations.
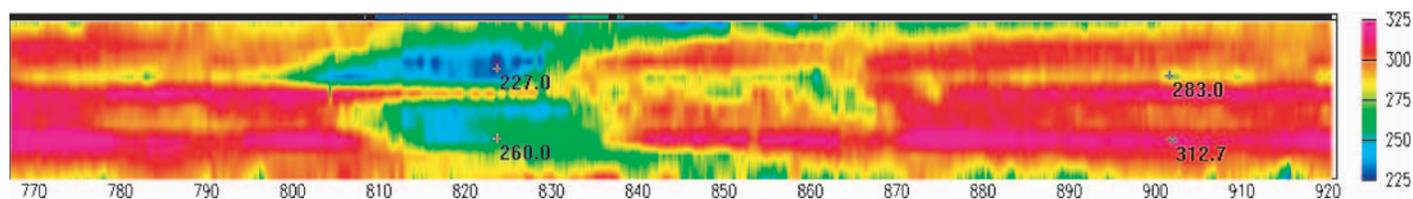
Figure 3.7. Example thermal profile from initial paving operation (9).
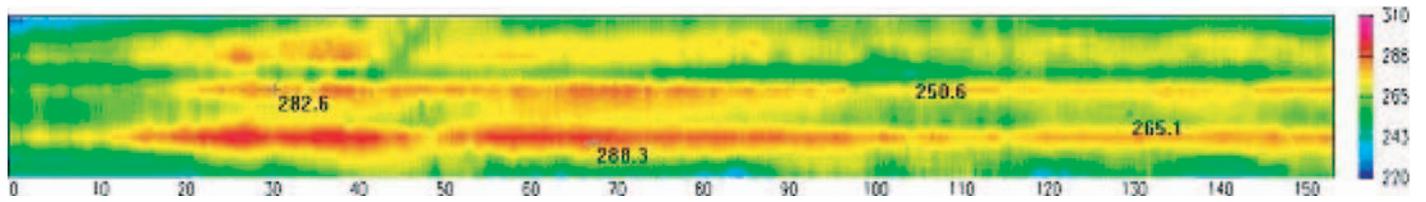
Figure 3.8. Example thermal profile from modified paving operation (9).
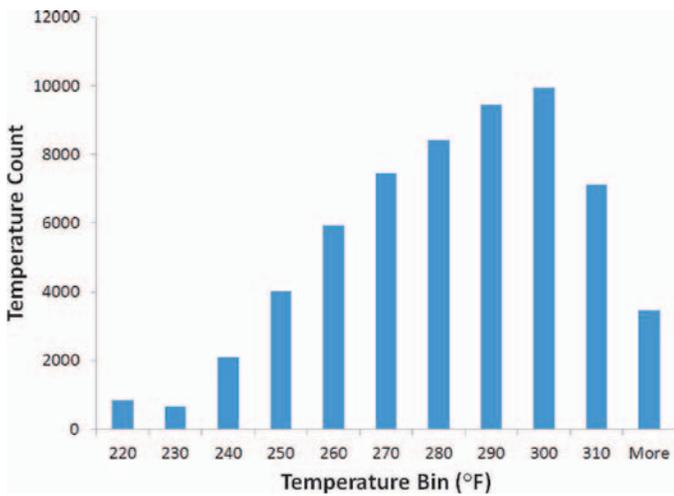
Figure 3.9. Histogram of measured mat placement temperatures from initial paving operation (9).
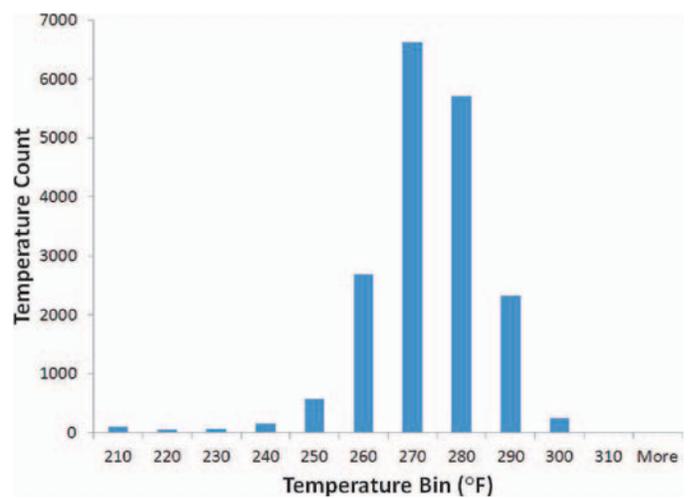
Figure 3.10. Histogram of measured mat placement temperatures from modified paving operation (9).
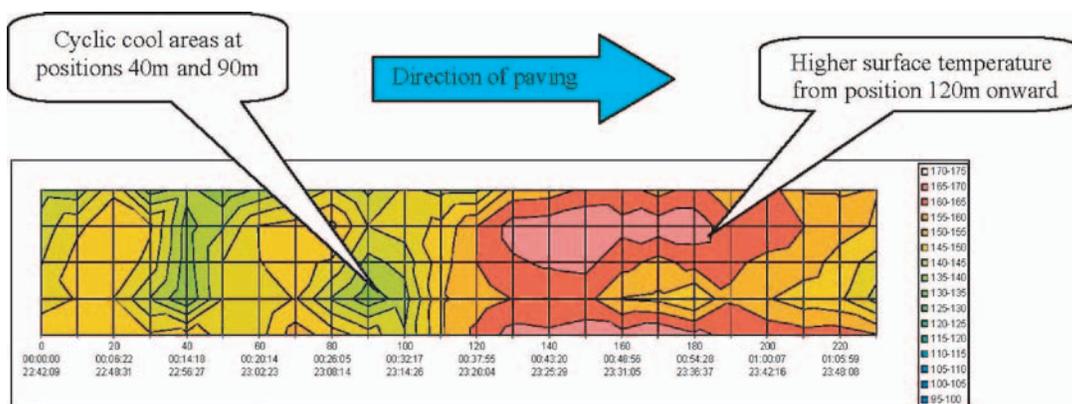
Figure 3.11. Surface temperature profile from the University of Twente (10).
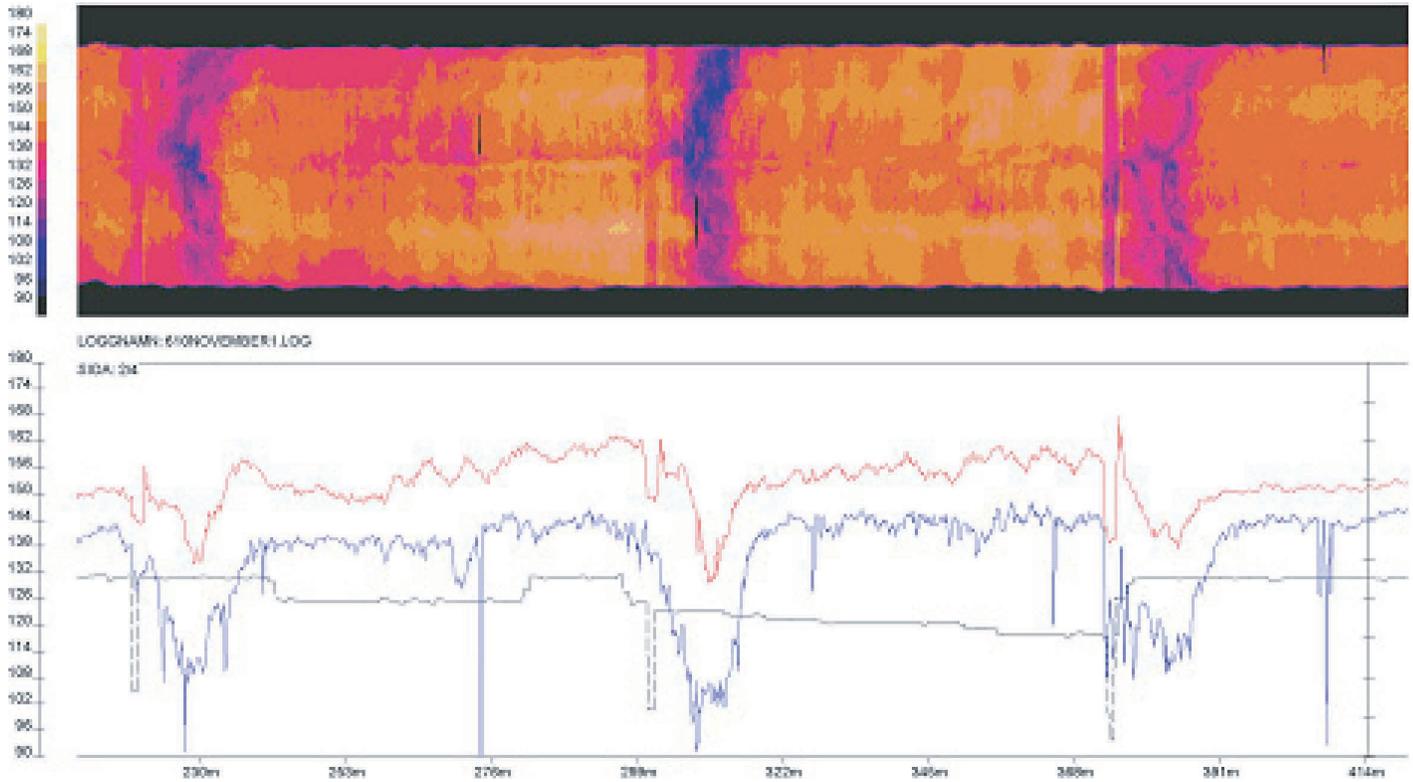
Image courtesy of Mats Wendel, SNRA.

Figure 3.12. Thermal profile output from line scanner system in Sweden.
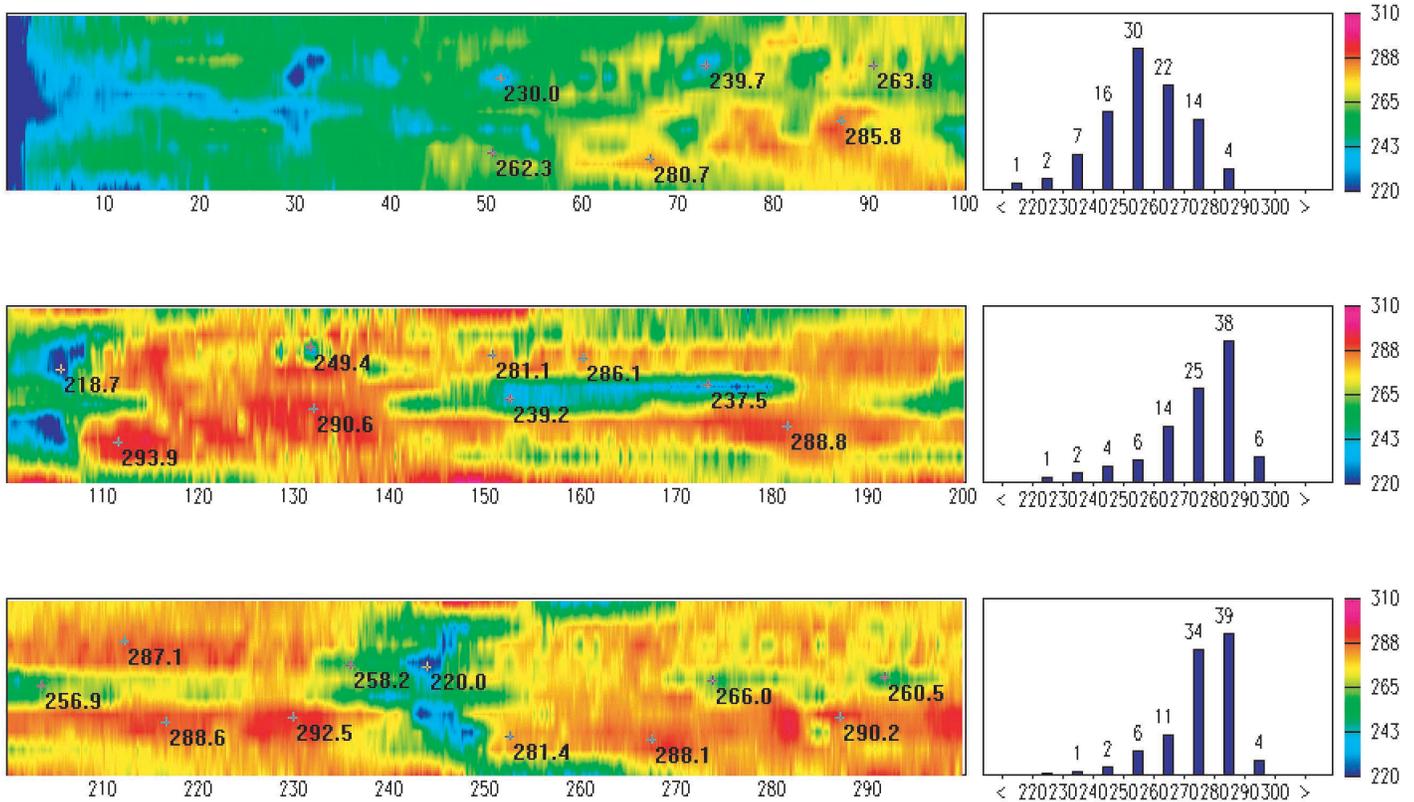
Figure 3.13. Initial paving operation thermal profile (11).
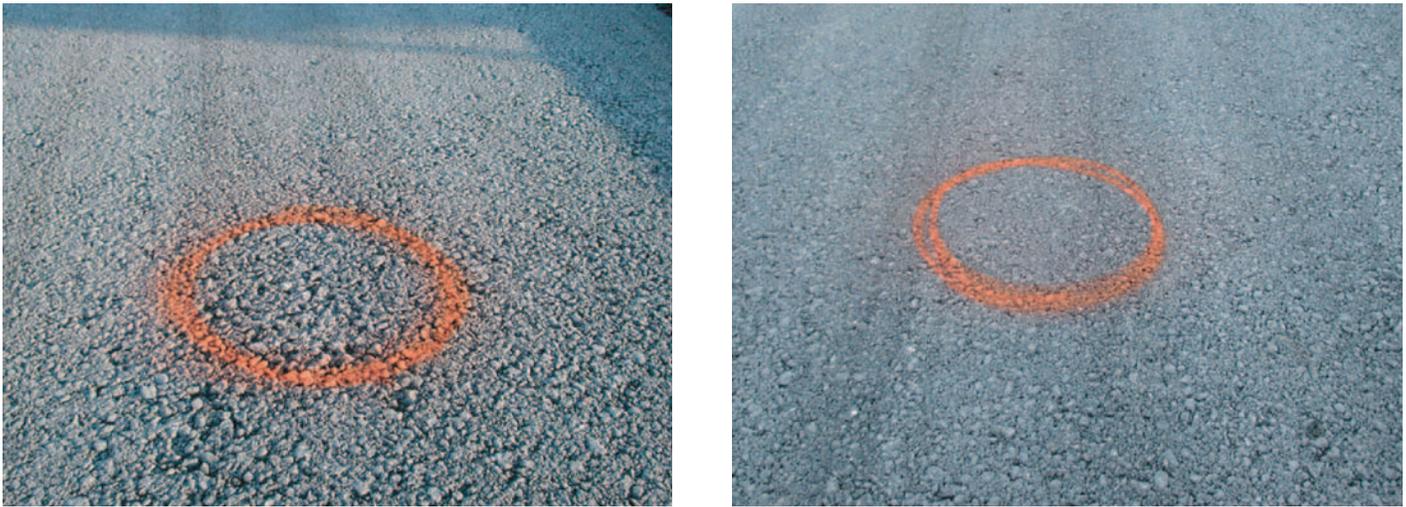
Figure 3.14. Thermal cold spot (left) and normal (right) locations on HMA mat (11).

(continued from page 13)

TxDOT uses a similar approach, in which Test Method Tex-244-F evaluates the project using a handheld IR thermometer to check for areas with temperature differentials exceeding 25°F. Tex-244-F profiles the mat temperature for a distance of 150 ft, or two truckloads, and TxDOT specifications call for at least one test per sublot. Locations with thermal segregation are evaluated for density differentials using Test Method Tex-207-F, Part V. TxDOT specifications eliminate any production or placement bonus for any sublot with a failing density profile. Table 3.3 shows TxDOT's current density profile criteria.

In Europe, despite thermal sensors being widely used in the asphalt-laying process, additional research has been done only in Sweden and the Netherlands, and there are only a few publications regarding the technology and survey results. IR technology is most implemented in Sweden, where Region Stockholm has used it for more than 15 years and has used a bonus and fines system for about 10 years.

Current GPR Technologies

Background

GPR sends discrete electromagnetic pulses into the pavement and then captures the reflections from layer interfaces in the pavement structure. Radar is an electromagnetic wave and therefore obeys the laws governing reflection and transmission of electromagnetic waves in layered media. At each interface within a pavement structure, a part of the incident energy is reflected, and a part is transmitted. Figure 3.16 shows a
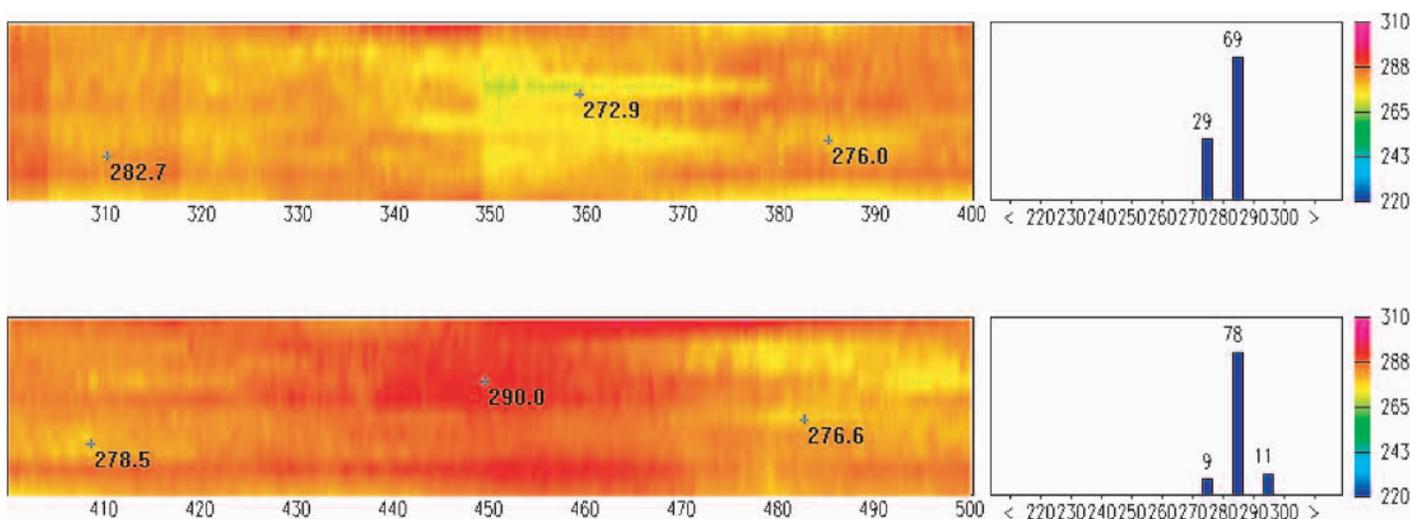
Figure 3.15. Modified operation thermal profile (11).

Table 3.3. TxDOT Density Profile Criteria

Mixture Type	Highest to Lowest Maximum Allowable Density Range (lb/ft³)	Average to Lowest Maximum Allowable Density Range (lb/ft³)
Types A and B	8.0	5.0
Types C, D, and F	6.0	3.0

typical plot of captured reflected energy versus time for a single GPR pulse.

The amplitude of radar reflections and the time delay between reflections are used to calculate layer thicknesses and layer dielectrics. For purposes of this study, the surface layer dielectric is of most interest. As will be described, the surface dielectric is the parameter that is used as an indicator of segregation. The surface dielectric is calculated as follows (*12*):

$$\varepsilon_a = \left[\frac{1 + A_1 / A_m}{1 - A_1 / A_m} \right]^2$$

where

ε_a = dielectric of the surface layer,
A_1 = amplitude of surface reflection (V), and
A_m = amplitude of reflection from a large metal plate (V) (this represents 100% reflection).

The use of GPR for quality control (QC) in HMA pavements has been largely headed by European efforts. The first GPR tests on roads in Europe were done in the late 1970s and early 1980s in Scandinavia. These GPR tests were performed using ground-coupled antennas in Sweden (*13–15*) and in Denmark (*16*). Although the results were promising, the method did not receive general acceptance at that time (*17*). However, after the mid-1980s, the method rapidly became a routine survey tool in various road design and rehabilitation projects in Finland (*18–21*). The first tests on asphalt were done in the late 1980s when high-frequency antennas were tested in pavement thickness measurements and for detecting transverse crack growth in pavements (*20*).

In Central Europe, according to Hobbs et al. (*22*), the first civil engineering tests with GPR in the United Kingdom were done in 1984. Since then, the published GPR research has focused especially on concrete structures (*23*) and pavement testing (*24–26*). In France, the main focus has been on pavement testing (*26*). In the Netherlands, the main application on roads has been layer thickness measurements (*27*).

The idea for using the GPR technique to measure asphalt air void content was tested in Rovaniemi, Finland, for the first time in the summer of 1993 in a project financed by the Finnish Technology Development Centre (TEKES)(*28*). This involved testing a multichannel GPR system manufactured by the Canadian company Road Radar, Ltd. The tests were conducted on experimentally paved asphalt pedestrian paths along HW 4 between Rovaniemi and Saarenkylä, which contained void
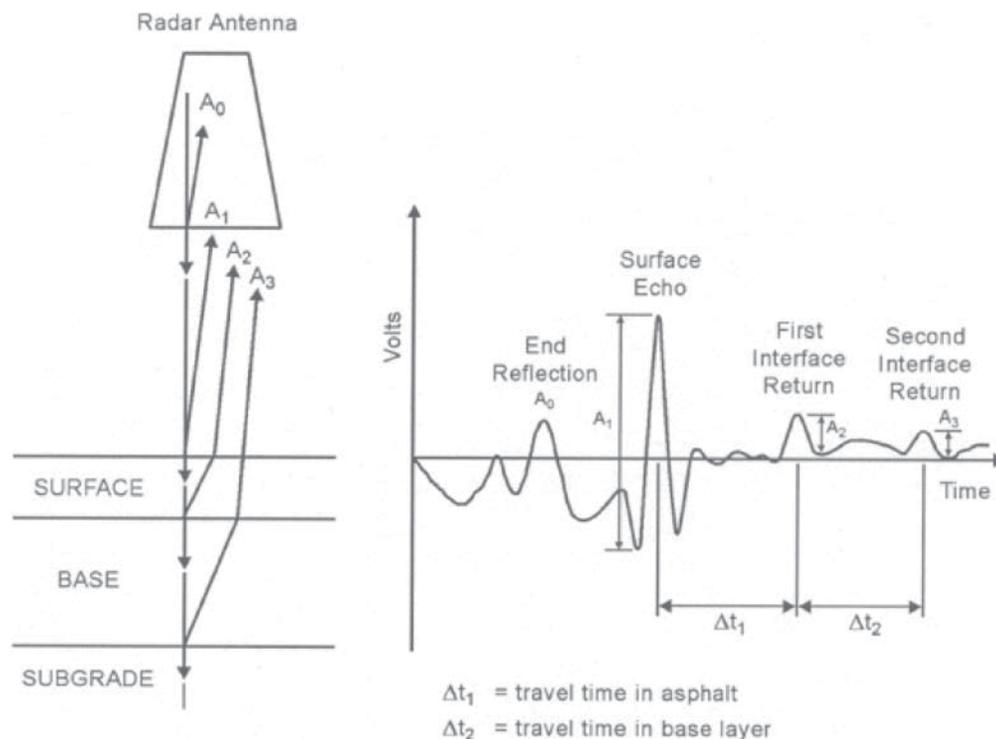
*Figure 3.16. Example signal from a GPR pulse (*12*).*

spaces of different types depending on the number of times the pavements had been rolled. The results were not encouraging, although this was mainly because of technical problems with both hardware and software.

However, following some promising results achieved through laboratory research in 1994 and 1995 at the Texas A&M Transportation Institute (TTI), the research in Finland was continued in the summer of 1996 in the form of a joint project initiated by the Finnish National Road Administration, the University of Oulu, and Neste Oy (*17, 28–30*). This project involved testing the measurement methods in laboratories and at actual pavement-laying sites in southern and northern Finland. Tests were also carried out to determine whether GPR could be used in real-time compaction monitoring, as Figure 3.17 shows. The GPR equipment used in these tests was GSSI 1-GHz antennas. Based on the laboratory tests, a model for the correlation between dielectric value and air void content was developed. After the final laboratory and field tests were completed in 1997, the surface reflection technique was accepted as the standard quality control method for asphalt pavements in Finland.

In 2004, the Finnish transport agency Finnra (*33*) published the first specifications concerning the use of GPR techniques in road rehabilitation projects. Research has also begun on the transfer and use of GPR results by automated road construction machinery (*34*).

Available GPR Systems

GPR antennas can be divided into ground-coupled and air-coupled systems. The leading commercial manufacturers of ground-coupled antennas used in road, airport, and railway surveys are GSSI (United States), IDS (Italy), MALÅ (Sweden), Penetradar Corporation (United States), Sensors and Software (Canada), and UTSI Electronics (United Kingdom). In addition, the 3D-Radar stepped-frequency GPR system can be classified into the ground-coupled category.

In pavement quality control, air-coupled systems have certain advantages over ground-coupled systems. The greatest advantage of these air-coupled systems is the repeatability of their measurements since the antenna coupling does not change with changes in the pavement properties. This allows them to be used to measure changes in the material properties in asphalt quality control surveys (*17*). Another advantage is that, because they are mounted above the pavement, data collection can be done at full traffic speeds and, as such, not interfere with traffic. Currently, horn antenna air-coupled systems are manufactured by GSSI, Penetradar, Pulse Radar, and Wavebounce, all from the United States, and butterfly dipole systems are manufactured by Radar Team Sweden Ab. Euradar air-coupled GPR systems have also been used in pavement surveys in the Netherlands (*27*).

In Finland, Sweden, Estonia, and Germany, where the pavement quality control tests have been conducted, the main control system used was the GSSI SIR-10 with a 1-GHz horn antenna, which was later replaced by the SIR-20 system. Some tests have also been carried out in Finland and Sweden using a GSSI 2.2-GHz horn antenna. In the United States, DOTs with active GPR programs, such as TxDOT and the Florida DOT, use 1-GHz systems from GSSI, Wavebounce, or Pulse.

GPR Hardware Specifications

In Europe, Finland is the only country routinely using GPR in HMA quality control, and it is the only country that has set specifications for the GPR hardware. Sweden has also described a method for the use of GPR, and its GPR hardware calibration procedure follows Finnish standards. The tests are slightly modified GPR system tests developed by TTI for TxDOT's 1-GHz air-coupled systems (*35*). Appendix B shows the TTI/TxDOT GPR specifications, which measure the following parameters:

- Noise-to-signal (N/S) ratio;
- Signal stability (amplitude and time jitters);
- Travel-time linearity;
- Long-term stability (time window shifting and amplitude stability); and
- Penetration depth.

All of the hardware systems that are used in HMA quality control in Finland have to pass these tests annually and meet the criteria shown in Table 3.4. Based on the test results, a GPR

Figure 3.17. Testing the use of GPR in HMA compaction guidance in Finland.

Table 3.4. Specifications of Finnish GPR Systems for Asphalt Quality Control Surveys

Tester	Class A GPR Systems Can Be Used in All Finnra Surveys (%)	Class B GPR Systems in Finnra Surveys Can Be Used According to Special Terms and Instructions (%)
Noise-to-signal ratio	5	10
Short-term amplitude stability	1	3
Long-term amplitude stability	3	6
Long-term time stability	5	10
Travel-time linearity	5	7.5

system can receive one of two classifications, A or B, according to these criteria. Class A systems can be used in all Finnish Road Administration (Finnra) surveys, whereas Class B systems can only be used if special protocols are followed. Figure 3.18 shows a system undergoing verification testing.

In addition to the functional specifications already mentioned, an additional concern with GPR surveys is the repeatability of results. Several repeatability tests have been made over the years with different GPR survey systems, and when tests have been conducted during the same day, the repeatability has been excellent, as Figure 3.19 shows.

Example GPR Case Studies

Asphalt air void content is one of the most important factors affecting the life span and deformation properties of pavements. Measuring void content using dielectric values relies on the dielectric value of the asphalt pavement being a function of volumetric proportions and the dielectric values of its components (*28*). Compaction of the asphalt reduces the proportion of low-dielectric-value air in the asphalt mixture, and it increases the volumetric proportions of bitumen and

Figure 3.18. GPR system testing.

rock and thus results in higher dielectric values of asphalt (*17, 21, 31*). The observed relationship between dielectric value and air void content is logarithmic, as Figure 3.20 shows.

EUROPEAN EXPERIENCES WITH GPR FOR HMA QUALITY CONTROL
The GPR measurements in the field are performed using a 1-GHz horn antenna. At that frequency, the thickness range of measured density is normally 0 to 30 mm. Higher frequency (2.2-GHz) antennas can and should be used to measure the density of thinner overlays. Preliminary tests have shown that the 2.2-GHz systems seem to work better, especially with remix pavements, but they are also more sensitive to variations in asphalt surface texture and to external noise (*36*).

Dielectric values of asphalt surfacing are calculated by using the surface reflection technique. Following the GPR field evaluation, one or two calibration cores are taken, and these cores are returned to the laboratory for traditional void content determination. For each type of aggregate and mix design, similarly shaped relationships have been developed (*31*). The calibration cores are used to establish the link for each specific project. In 1999, GPR was accepted for use as a quality control tool, among other pavement density measurement techniques, on all new surfacing projects in Finland. Since 2004, GPR has been the only method allowed on high-traffic-volume roads because it does not obstruct traffic. In addition to quality control or quality assurance surveys of new asphalt pavement, GPR has, during the past few years, been applied increasingly in quality control surveys of other road structures (*37*).

A description of the current Finnish method for the use of GPR in asphalt air void content measurement is presented in Appendix C. Five companies in Finland can perform these surveys. According to reports from industry personnel, the benefits of the GPR systems are the continuous profile provided, the fact that data collection does not interrupt traffic, the safety offered to workers, and that the survey is nondestructive. Another benefit is that problem locations can easily be identified from the GPR profiles and, in turn, be tracked to places in the field. This allows the contractor to not only repair these sections but also improve his or her work methods and practice.
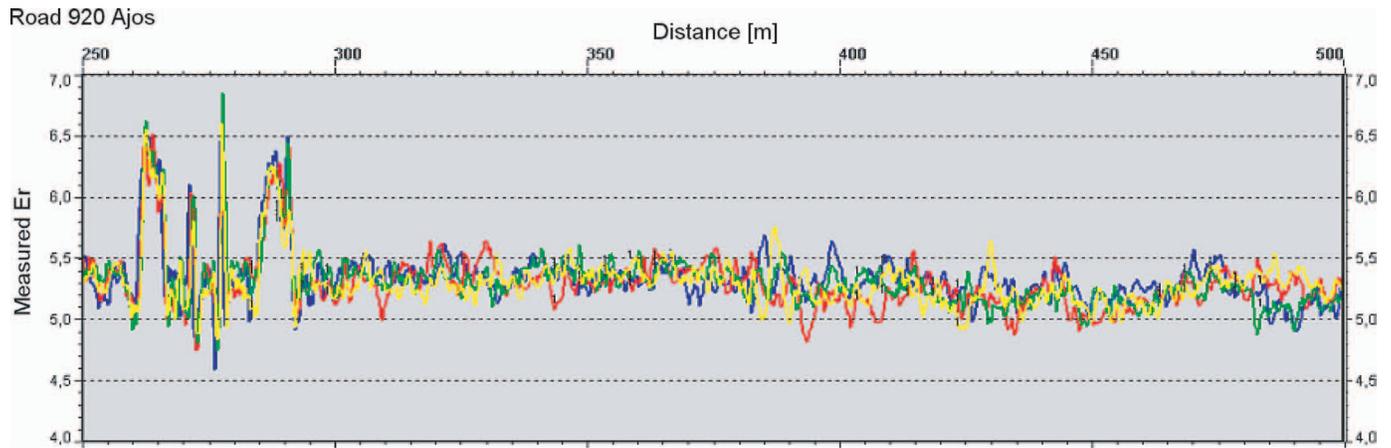
Figure 3.19. Repeatability tests of four GPR runs with 2.2-GHz GSSI system (36).

Currently, the greatest problem, especially among Finnra personnel, is that there is a slight mistrust of the results. In addition, the single equation in current use is not totally applicable to all mixtures and aggregates. One reason for these problems is that the measurement and analysis process is not described precisely enough. Other problems reported by the contractors and survey consultants include the following:

- The GPR survey cannot be performed when pavement is wet, resulting in long wait times during rainy days.
- When the outer wheelpath is measured, there are differences in the results because of compaction of the asphalt by heavy traffic.
- Drilling reference samples is dangerous on busy roads. In practice, it has to be done at night.
- Reference drill core analysis is not always reliable. Two cores from the same location can give different results.
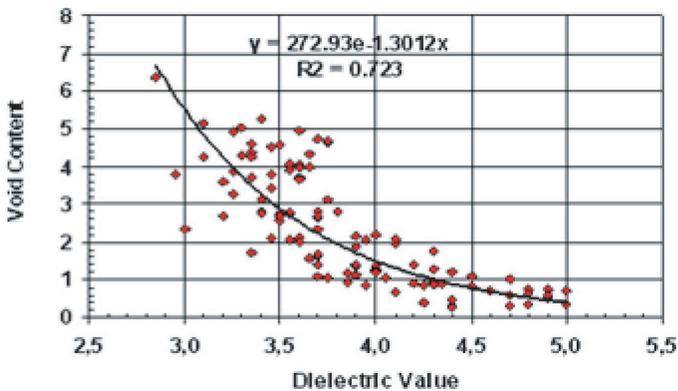
Figure 3.20. Relationship between HMA void content and dielectric values (31). Note that dielectric values are measured with capacitance-based Percometer surface probe.

- Slag or other additives in the HMA mix may cause dielectric values to be too high, and consequently the model does not work.
- Old asphalt affects the results too much with thin pavements in remix pavements.
- The model may not work with really thin (<30 mm) pavements.
- Bridges may skew the results.
- Utility works in urban areas may affect the results.

For the aforementioned reasons, Finnra, the Rovaniemi University of Applied Sciences, and GPR consultants are planning to establish a new research project to improve mathematical models for pavement void content calculations and rewrite the specifications. Furthermore, the Swedish and Norwegian road administrations and GPR contractors may join the research project.

In addition to being used for quality control for density measurement, GPR is also a great tool for detecting asphalt segregation, even though it has not been used routinely in these surveys. Figure 3.21 presents a good example of the use of GPR to detect problems with asphalt segregation. In the GPR data, a reduction in dielectric value was observed at the end of each truckload and at other places where an experimental paver had problems. The experimental paver causing these problems was replaced by a conventional machine at 2,700 m, and after that point the quality improved. The measurement results, taken from the inner and outer wheelpaths, also show a commonly encountered trend: Dielectric values are always slightly higher in the outer wheelpath than in the inner wheelpath as a result of the compaction effect of heavy traffic.

Figure 3.22 presents an example of segregation detection using GPR and videos in Sweden, and Figure 3.23 presents an example of using a three-dimensional GPR technique and time slices to map the segregated areas in an airport runway.
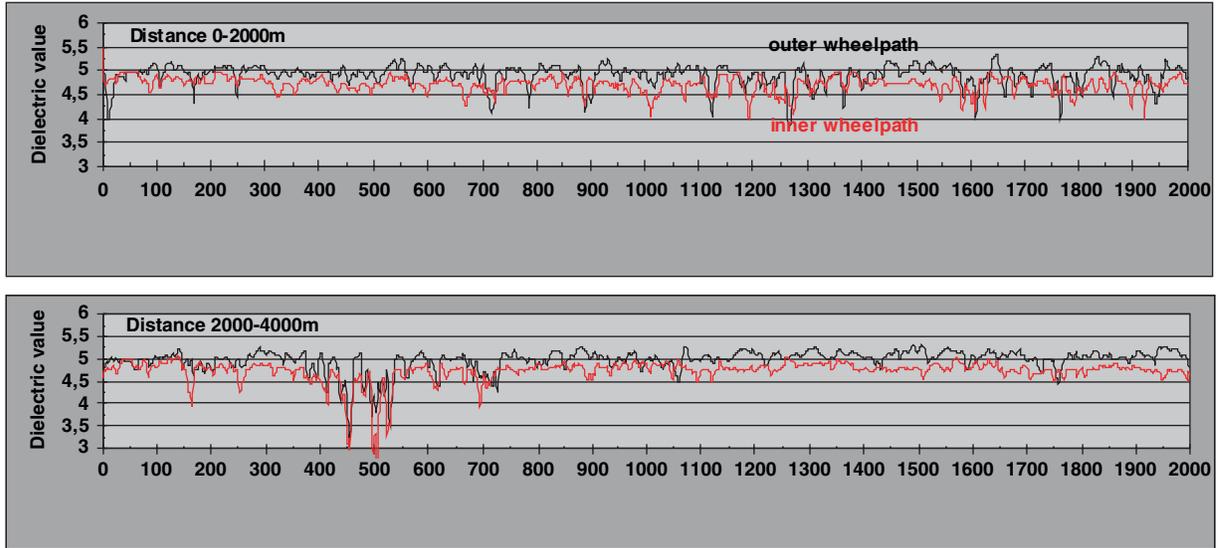
Figure 3.21. Dielectric value of asphalt at Ylinampa (17).
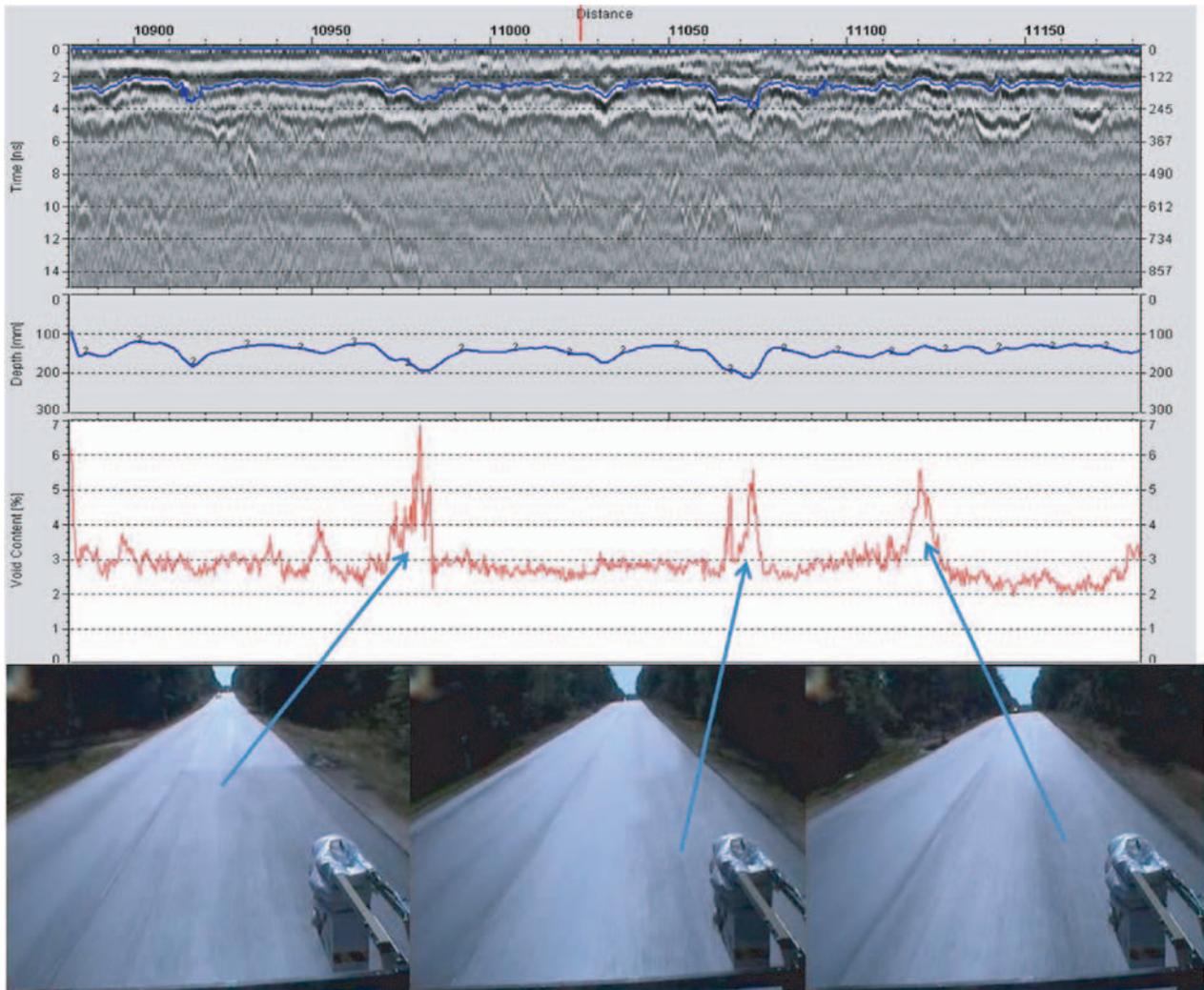
Figure courtesy of Roadscanners Oy.

Figure 3.22. HMA segregation measured with GPR and calculated as void content. Note that this figure also presents GPR data and HMA thickness information at the top.
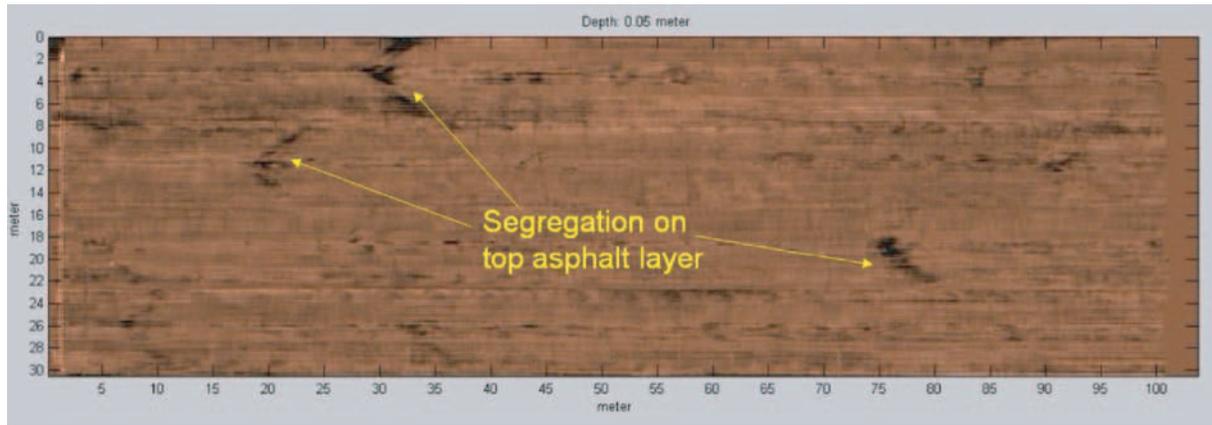
Figure 3.23. Segregation detection with three-dimensional GPR (28). Note that segregation of the larger area is deeper in the asphalt, which can also be seen in the three-dimensional radar GPR time-slice view calculated from a depth of 50 mm. This case presents a 100 m × 30 m area of an airport runway.

GPR FOR QUALITY CONTROL IN THE UNITED STATES

Unlike in Finland, GPR has not been officially adopted for quality control in the United States. However, states such as Texas and Florida do have GPR programs in which the technology is used routinely for pavement surveys to look for stripping damage and trapped water and to detect layer thickness and changes in structure. Additionally, work in Texas has followed in the path of the Finnish experience by beginning to employ GPR for compaction measurement and segregation detection (8, 9). Researchers use the following relationship for relating the measured HMA surface dielectric value to air voids:

$$\% \text{ Air Voids} = A \times e^{B \times \text{Surface Dielectric}}$$

where A and B are laboratory-determined constants.

As an example, Figure 3.24 shows the GPR and core data used to calibrate the GPR surface layer dielectric value to air void content on a Type C mix in Texas. After making this calibration, density profiles such as those shown in Figure 3.25 can be developed for the entire section. Texas researchers have performed these analyses on more than a dozen projects across the state; however, the efforts remain largely in the research realm. Currently, such an analysis is not an official DOT method.

Status of Implementation of GPR

In Europe, the GPR technique has been routinely used in Finland, but the Swedish National Road Administration has also arranged extensive tests of the technique and has prepared a description of the technique. Other countries where the GPR technique has been tested in asphalt quality control are Estonia

and Germany. The most implementation has occurred in Finland, where pay schedules exist based on the GPR measurements. Appendix C presents the current Finnish Päällystalan neuvottelukunta (PANK) method.

In the United States, several DOTs have active GPR programs. However, these programs primarily use GPR for layer thickness measurement, identification of section breaks, detection of trapped water or excessively wet materials, and investigation for signs of HMA stripping. Use of GPR for HMA construction quality control is not an official method in any DOT in the United States.

Supplemental NDT Devices

While full-coverage data collection relies on devices such as IR and GPR, several spot-test devices are available as checks on the other NDT data. For example, the nonnuclear Pavement
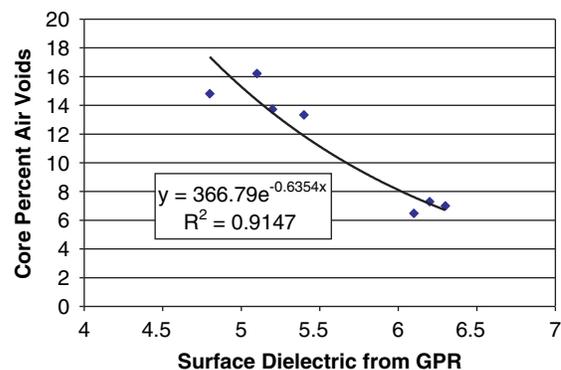
Figure 3.24. Calibration of GPR surface dielectric to core air void content (6).
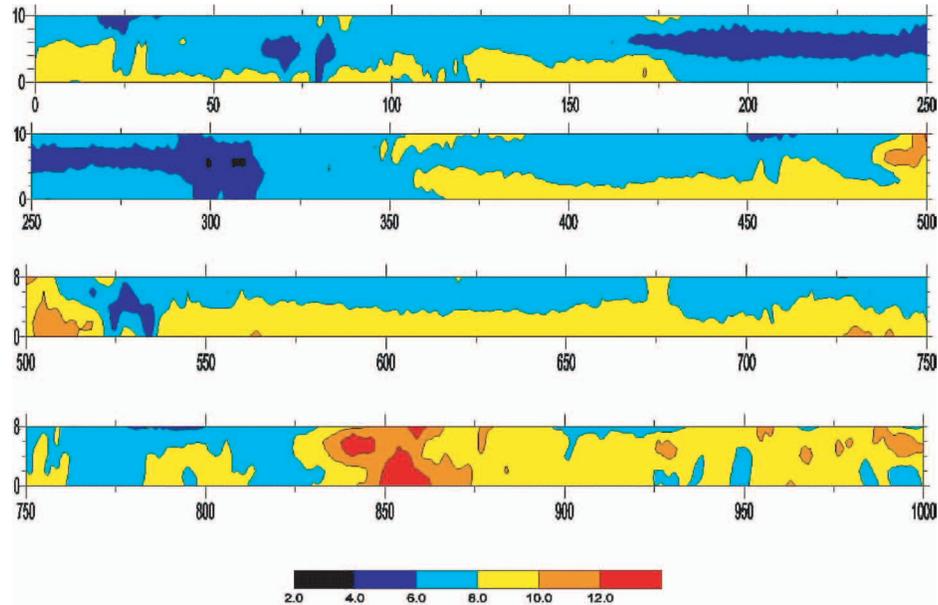
Figure 3.25. In-place percent air voids of new overlay measured with GPR (6).

Quality Indicator (PQI), nuclear density gauge, and nonnu-clear Pavetracker Plus (each shown in Figure 3.26) can be used for spot density measurements and have been used in the United States and Europe. Problems reported with these devices are usually caused by large variations in surface texture.

Additionally, a handheld GPR called the Spot, made by Wavebounce, can quickly measure the surface dielectric value at a test location. Figure 3.27 shows the Spot. All of these spot-test devices could be used to complete the data set at field validation locations prior to cutting cores.

Sweden has developed a density-on-the-run (DOR) system, as shown in Figure 3.28. This system uses three sensors in an HMA quality survey. Its advantage is a continuous profile, but like other contact measurement devices it is sensitive to changes in surface texture. Also, this system cannot be used when the pavement is wet.

Figure 3.26. PQI, nuclear density gauge, and Pavetracker Plus.

Figure 3.27. Spot handheld GPR.

Photo courtesy of Svante Johansson.

Figure 3.28. Swedish DOR system for continuous pavement density.

Conclusions from Literature Search

In North America, HMA construction is governed by agency specifications in which placement acceptance is largely based on core results. However, some agencies have implemented thermal uniformity testing. These procedures rely on hand-held radiometers, IR cameras, or IR bar systems. The use of GPR for HMA construction quality control is not an official method in any DOT in the United States. The practice of using GPR for density measurement has been employed, but only in a research capacity.

In Europe, methods for quality control and quality assurance are governed by national standards and specifications. In the new performance-based contracts, all of the quality-related issues have also been made the responsibility of the contractor. In such cases, contractors are only interested in on-site, real-time quality assurance and guidance. For this work, thermal cameras, line scanners, and other thermal sensors can provide valuable data that can be used to detect segregation. According to this search, these techniques are most widely used in Sweden and the Netherlands. However, the greatest part of HMA is paved in Europe through normal contracts, and drill cores remain the primary method of quality assurance. Only in Finland is the GPR technique in routine use.

A key task for road administrations in the future will be to ensure and to document the homogeneity of HMA construction. This can be achieved during the placement process through the use of thermal measurement systems. IR bar and IR line scanner solutions exist for collecting the placement data. The homogeneity of HMA density can be verified after compaction using multichannel GPR techniques that facilitate the measurement of a newly paved lane surface in its

entirety with a single pass. All the data can then be stored in a database that can be used if and when pavement defects appear in certain road sections.

Recommended NDT Equipment and Test Protocols

Summary

Based on a review of the available equipment and the strong desire of the SHRP 2 project team to focus on full-coverage testing, the IR sensor bar represents the most commercially developed solution for thermal profiling. Both IR line scanners and IR cameras would have offered a feasible solution if commercially available systems for thermal profiling HMA construction had been available. However, during the course of this SHRP 2 project, neither system became available as an integrated package ready for deployment for testing asphalt-mixture construction.

With GPR, the multiple-antenna systems provide the ideal setup of profiling because they collect data across the entire mat width in one pass. However, the use of a single-channel system also offers an acceptable solution. The following sections detail the IR and GPR equipment and test protocols recommended for use in the demonstrations that researchers conducted in this project.

Recommended IR Equipment

The most commercially developed IR imaging equipment for full-coverage testing is the IR bar system. Such a system is commercially available from MOBA Corporation; shown in Figure 3.29, this unit was used in the field demonstrations. Appendix D presents the current test method for using this equipment; this method was used for the field demonstration.

Photo courtesy of MOBA Corporation.

Figure 3.29. MOBA Pave-IR.

The IR line scanner solution shown in Figure 3.5 was developed and field proven in Sweden, but it did not become commercially available during the duration of this project. Appendix A presents the method used in Sweden with this system.

The IR camera solution is the least-developed method for full-coverage thermal profiling of HMA construction. Although the automation camera can generate a temperature-rich plan view with custom software development, during the course of this project no known software solution became available on the market.

Recommended GPR Equipment

The single-channel GPR system, such as GSSI's SIR-20 system with a 1-GHz antenna (shown in Figure 3.18), is what Finland has implemented for quality control measurements. However, demonstration in the United States is complicated by the fact that the primary GPR systems used internationally for such applications currently are not FCC compliant.

In light of this fact, whenever available, the 2.2-GHz GSSI system was demonstrated in the field. The research team used the basic method implemented in Finland and presented in Appendix C. On all demonstration projects, the research team also demonstrated TTI's 1-GHz air-coupled radar system using the procedures outlined in Appendix E.

In addition to their demonstrating TTI's 1-GHz and GSSI's 2.2-GHz radar systems, the project team attempted to demonstrate other systems, including the Penetradar multiple-channel integrated radar inspection system (IRIS), shown in Figures 3.30 and 3.31, and the 3d-Radar (now owned by Curtiss-Wright) system, shown in Figures 3.32 and 3.33. The Penetradar and 3d-Radar systems have the advantage of being able to collect full-coverage data with one pass of the

Photo courtesy of Penetradar Corporation.

Figure 3.30. Penetradar multiple-channel IRIS system.

vehicle over the newly constructed HMA mat; however, neither system was available for any of the demonstration projects. Arrangements to demonstrate the Penetradar system never materialized, largely because of scheduling and budgetary constraints. Demonstration of the 3d-Radar system was precluded largely by the extended lead times necessary to obtain required FCC approvals.

Detailed Test Plan

Summary

This section describes details of the test plan used to demonstrate IR and GPR technologies for uniformity measurements of new HMA layers. Researchers used the paver-mounted IR bar system as the primary means of IR data collection and spot radiometers for periodic verification of temperature measurements. A commercial package for thermal profiling of HMA layers with the IR line scanner or camera systems never became commercially available during the course of this project.
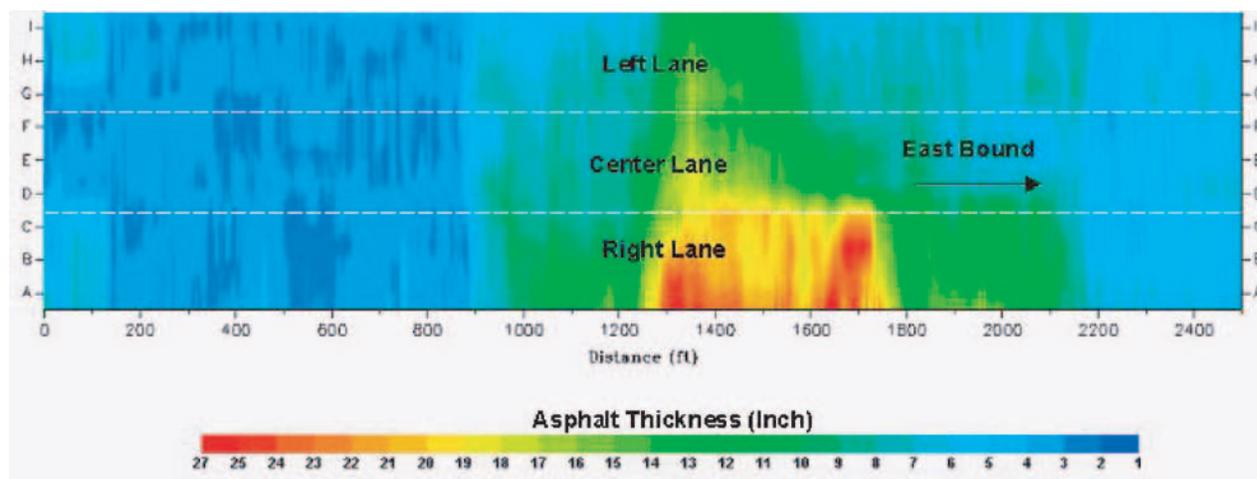

Image courtesy of Penetradar Corporation.

Figure 3.31. Plan profile output from Penetradar IRIS mapping software.

Photo courtesy of Roadscanners Oy.

Figure 3.32. 3d-Radar system.

Researchers used a GPR system meeting the performance requirements shown in Appendix B to collect the radar profiles. The default system used was TTI's 1-GHz system; on some projects, GSSI's 2.2-GHz system was also available and demonstrated. The multiple-channel Penetradar IRIS and the 3d-Radar systems were not available for the demonstrations.

The research team used a field evaluation of the GPR data to select core locations, which were tested in the laboratory to validate the significance of the IR and GPR surveys. Details of the proposed test plan follow.

Participating DOTs

Researchers performed demonstrations in cooperation with the Texas, Florida, Minnesota, and Maine DOTs to demonstrate the NDT technologies in all four AASHTO regions. During the course of this project, interest in participation was also received from Washington State, New Jersey, Virginia, and the province of Quebec.

Type of Project

All demonstration projects took place on surface mixes. The Texas project used a stone mastic asphalt (SMA), while the remaining projects used Superpave SP-12.5 mixtures. The first demonstration took place in Texas in September 2009. Two projects used windrow elevators, one project used bobtail trucks to dump the mix directly into the paver hopper, and one project used a material transfer device.

Equipment Necessary

The research team used the following equipment for primary NDT field data collection: a MOBA Pave-IR with GPS and a GPR system meeting the performance requirements shown in Appendix B. The following supplementary pieces of equipment were used for spot testing and coring: spot radiometers, a thin-lift nuclear density gauge, and a coring rig.

Collecting IR and GPR Data

In the field, the project team relied on the IR bar system for thermal profile collection and TTI's 1-GHz GPR system for the radar surveys. The GSSI 2.2-GHz radar system was also demonstrated on some projects.

Collecting IR Data

The protocol used for collecting the IR bar data followed the procedure adopted in TxDOT Test Method Tex-244-F (shown in Appendix D). The following is a summary of the IR bar data collection procedure:

- Install the IR bar system onto the paver in accordance with the manufacturer's instructions. If the system has adjustable sensor spacing, set the outer sensors no closer than 2 ft from the mat edge.
- Calibrate the distance encoder on the IR system over a length of at least 100 ft.


Image courtesy of 3d-Radar.

Figure 3.33. Plan profile output from 3d-Radar system.

- Document the mixture type, contractor, haul distance, haul truck type, target placement temperature, environmental conditions, and paving train equipment.
- Initiate data collection upon the starting of the paving train, setting the IR system to collect a scan at no more than 6-in. intervals.
- The IR bar system automatically collects and displays the thermal profile once data collection is initiated.

Collecting GPR Data

The GPR data collection followed the Finnish and Texas methods included in Appendices C and E, respectively. The following procedure summarizes the process:

- At the project site, set up the GPR equipment and allow the antenna to warm up according to the manufacturer's instructions.
- After placement and completion of finish rolling on the new HMA mat, collect GPR data in each wheelpath and the pavement centerline within the desired section limits. Collect data based on distance with a GPR trace collected at a maximum spacing of 1 ft.
- Collect the complete reflection (metal plate) data file.

Selecting and Documenting Locations of Calibration Cores

The research project team selected core locations based on field observations of varying temperature (from the IR survey) and dielectric (from the GPR survey). Core locations from the IR survey were selected by reviewing the thermal profile data in the field and then identifying at least five locations where the temperatures represented by the core locations spanned the observed placement temperatures.

The project team selected core locations from the GPR survey by first performing a field review of the GPR profiles and identifying the span of dielectric values represented. Next, at least five locations where the surface dielectric values represented by the core locations spanned the observed dielectrics were identified.

Supplemental Measurements

Several tools exist to supplement the IR and GPR surveys. The project team used spot radiometers to supplement the automated IR measurements. After core locations were selected, a thin-lift nuclear gauge provided a mechanism for estimation of density.

Laboratory Testing

The primary laboratory test of interest conducted on the cores was the determination of bulk specific gravity (ASTM D2726) and air void content (ASTM D3203). This is because density plays such a large role in the performance of the mat, and the thrust of interest in the NDT demonstrations was to assess the uniformity of the new mat. When possible, the research team also performed a performance test on the cores. Tests considered included the Hamburg Test (Test Method Tex-242-F), which is a rutting test; the Overlay Test (Test Method Tex-248-F), which is a crack-resistance test that indirectly relates to fatigue properties; and the indirect tensile strength test (ASTM D6931).

Demonstration Project in AASHTO Region 4

Summary

The first demonstration project took place September 29, 2009, in AASHTO Region 4 on US-190 near Woodville, Texas. The researchers used a MOBA Pave-IR system to collect thermal profile data and supplemented the measurements with a handheld spot radiometer for collecting placement temperature data at core locations. At the time of testing, no commercially available IR package using either a line scanner or a thermal camera was available.

TTI's 1-GHz system was used for the GPR data collection. The GSSI 2.2-GHz air-coupled system with radio frequency (RF) filter was also demonstrated. Efforts were made to secure participation of Penetradar and 3d-Radar systems. Scheduling conflicts, however, precluded Penetradar from participating, and 3d-Radar needed a longer window of opportunity to secure FCC clearance.

Job Mix Formula

The contractor placed a 1.5-in. lift of SMA-D constructed under TxDOT Standard Specification Item 346. The mix used PG 76-22 binder with 0.20% fibers. Table 3.5 shows the gradation job mix formula (JMF) for the mix produced the day of testing. Table 3.6 shows the JMF and QC/QA results for asphalt content.

Paving Operation

The contractor produced the mix in Livingston, Texas, resulting in a haul distance of approximately 30 mi. Belly dump trucks and a Lincoln 660 AXL windrow elevator were used to convey mix into an Ingersoll Rand PF 3200 paver. The contractor overlapped the truck windrows by approximately 30 ft and paved the eastbound inside lane from Station 166 + 11 to 177 + 80. Heavy rains at the plant resulted in cutting the workday short. Figure 3.34 shows the paving train.

Table 3.5. Job Mix Formula for SMA-D on Region 4 Demonstration

Sieve Size	Current JMF Cumulative Percent Passing	JMF Individual Retained Limits, Percent	TxDOT QC/QA Test Data Cumulative Percent Passing	Contractor QC/QA Test Data Cumulative Percent Passing
¾ in.	100.0	0–5	100.0	100.0
½ in.	86.0	9–19	82.0	89.3
⅜ in.	57.5	23.5–33.5	56.6	60.8
No. 4	23.5	29–39	23.0	24.5
No. 8	23.6	0–4.9	19.2	20.2
No. 16	19.0	1.6–7.6	15.9	16.8
No. 30	15.6	0.4–6.4	13.7	14.8
No. 50	12.8	0–5.8	12.4	13.8
No. 200	10.5	0–5.3	10.2	10.4

Note: Data courtesy of TxDOT.

Thermal Survey Result

Figure 3.35 shows the MOBA Pave-IR collecting thermal profile data on the project. Figure 3.36 shows the thermal profiles from the project. The thermal data show reduced temperatures at the truck ends with temperature differentials typically around 30°F. Ten locations were marked for further investigation, as annotated in Figure 3.36. Table 3.7 presents the measured temperatures and transverse and longitudinal distances to these locations.

GPR Survey Result

After the contractor completed finish rolling, the researchers collected GPR data over both wheelpaths and the centerline with TTI's 1-GHz and GSSI's 2-GHz systems. Figure 3.37 shows the GPR data collection in progress. The GPR data produced measurements of the surface HMA dielectric constant spatially over the test area, as Figures 3.38 and 3.39 show. The purpose of these dielectric measurements was to calibrate with the HMA density for full-coverage prediction of in-place HMA density. The 1-GHz system was used to collect stationary GPR data directly over the 10 locations previously marked from the thermal data for calibration to density. Table 3.8 shows the GPR-measured surface dielectric values for the 10 cores.

NDT Validation Test Results

To validate the meaning of the NDT data, a field sequence and a laboratory sequence were performed on the 10 locations. In the field, researchers collected nuclear density readings with a Troxler 3450 using a 60-s count time. In the laboratory, researchers determined the bulk specific gravity of the cores followed by permeability with the constant head method and then used the Overlay Test for a performance evaluation. Laboratory testing concluded with asphalt content by ignition oven and gradation determination. Table 3.9 presents the density data, permeability, and asphalt content results merged with the temperature and GPR measurements, and Table 3.10 presents the gradation results. The cores did not reach the failure criteria in the Overlay Test.

Figure 3.34. Paving operation on Region 4 demonstration.

Table 3.6. Asphalt Content JMF and QC/ QA Results from Region 4 Demonstration

JMF (%)	TxDOT QC/QA Result (%)	Contractor QC/QA Result (%)
6.1	6.4	6.2

Note: Data courtesy of TxDOT.

Figure 3.35. Pave-IR collecting thermal profile data on Region 4 demonstration.

Table 3.7. Core Locations with IR-Measured Temperature for Region 4 Demonstration

| Core	IR Temperature (°F)	Longitudinal Distance (ft)	Transverse Offset from Inside Joint (in.)
1	290	163	41
2	250	310	28
3	300	347	50
4	265	817	29
5	292	836	47
6	245	977	103
7	274	980	25
8	300	1,015	39
9	239	1,156	50
10	265	1,156	30
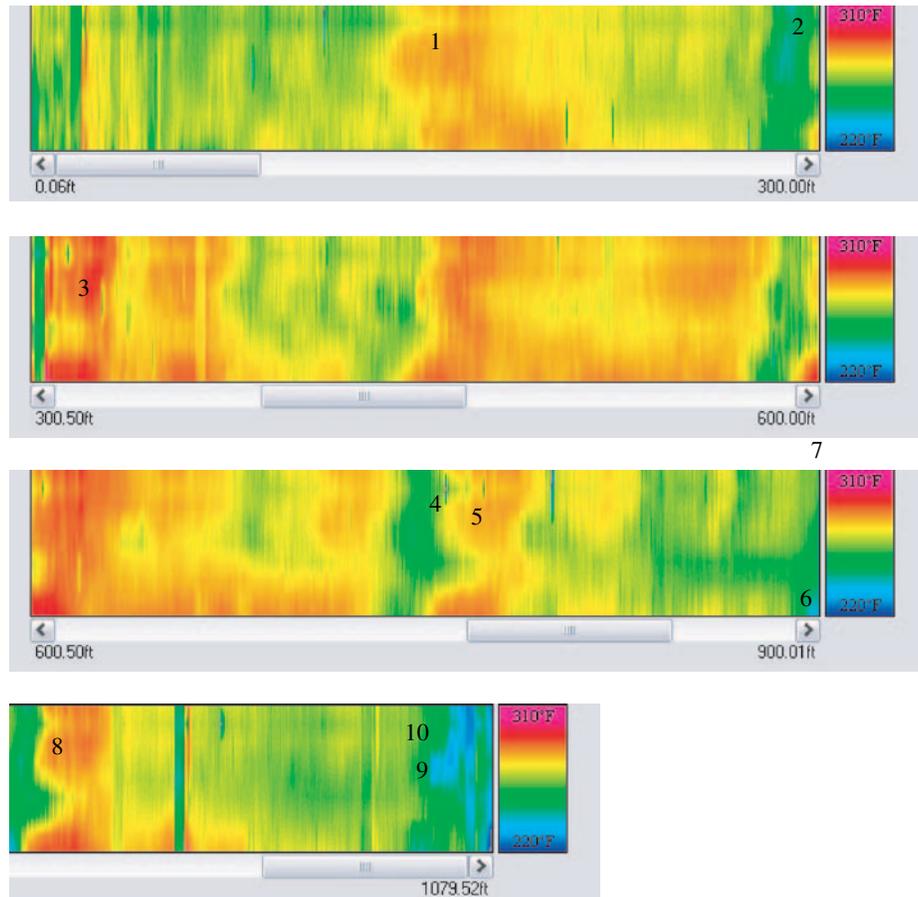
Figure 3.36. Thermal profile of SMA-D from Region 4 demonstration.

Figure 3.37. 1-GHz (left) and 2-GHz (right) GPR data collection.
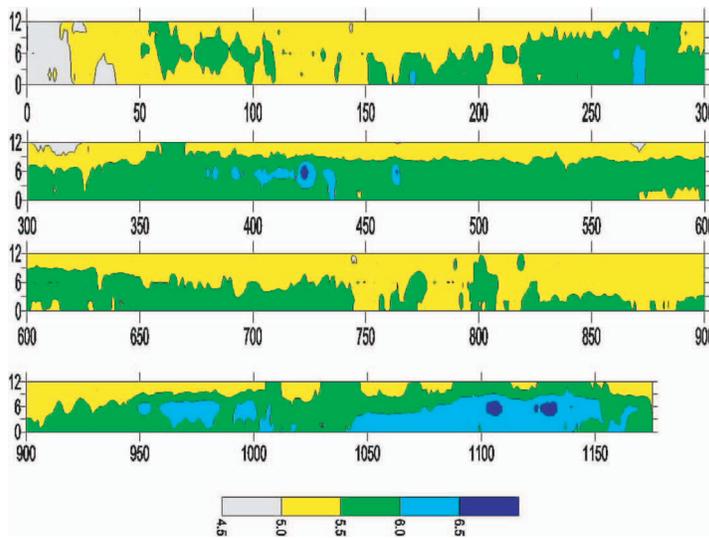

**Figure 3.38. Surface dielectric measured with 1-GHz GPR system on Region 4 demonstration.**
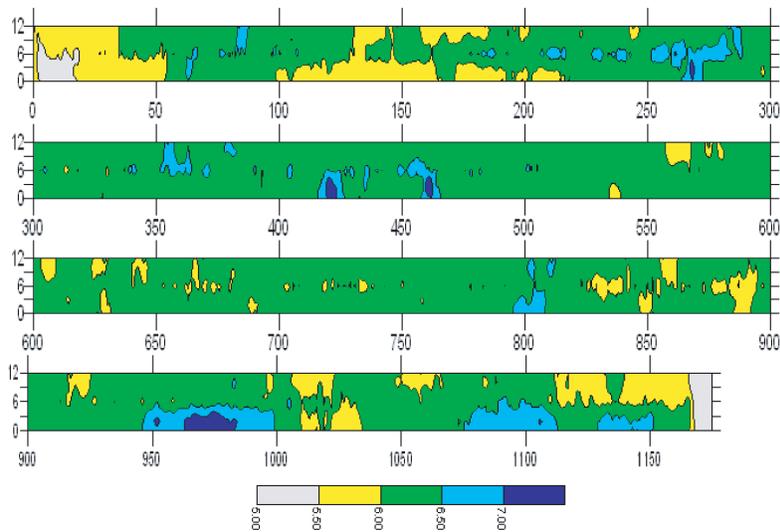
Figure 3.39. Surface dielectric measured with 2-GHz GPR system on Region 4 demonstration.

Table 3.8. GPR-Measured Core Dielectric Values from 1-GHz System on Region 4 Demonstration Project

Core	1	2	3	4	5	6	7	8	9	10
GPR ε	4.9	4.5	4.9	5.0	4.6	5.4	4.9	4.8	4.8	4.8

With the core data complete, researchers analyzed the IR and GPR data in conjunction with the core validation results to investigate the significance of the NDT readings. Appendix F of this report presents correlation matrices for the data, along with results from tests for the significance of the observed correlation values.

Significance of Thermal Data

Historically, thermal cold spots typically show up as low-density locations in the mat. Therefore, the first thing investigated was whether the temperature data or thermal differentials correlated to density or density changes, respectively. Figures 3.40 and 3.41 illustrate that on this project the temperature data did not correlate with density or changes in density.

As the correlation matrices in Appendix F show, the temperature data did correlate with several gradation parameters. The hotter locations were finer in gradation from the No. 16 and smaller sieves; however, from a practical perspective, the gradation results in Table 3.10 show that virtually all the cores are within the DOT allowable operational tolerances for these sieve sizes.

Significance of GPR Data

Low surface dielectric values typically indicate higher air voids in the compacted HMA. On this project, as illustrated

Table 3.9. Region 4 Core Density and Overlay Test Results with Field NDT Data

Core	Field IR Temperature (°F)	Field ε from GPR	Field Nuclear Density (lb/ft³)	Laboratory Density (lb/ft³)	Laboratory Percent Air Voids[a]	Permeability (cm/s)	Asphalt Content (%)
1	290	4.9	133.8	139.8	7.2	3.493 E-05	5.6
2	250	4.5	127.0	140.7	6.6	2.662 E-04	5.6
3	300	4.9	136.1	143.7	4.6	No flow	5.8
4	265	5.0	132.1	135.8	9.9	4.742 E-05	6.1
5	292	4.6	130.2	139.8	7.2	2.237 E-04	5.8
6	245	5.4	136.9	145.7	3.3	No flow	6.0
7	274	4.9	133.2	131.4	12.8	1.31 E-07	5.8
8	300	4.8	131.9	142.1	5.7	1.688 E-04	5.5
9	239	4.8	132.2	138.9	7.9	2.138 E-05	6.0
10	265	4.8	129.9	135.3	10.3	5.535 E-04	6.4

[a] Based on TxDOT QC/QA-determined maximum theoretical specific gravity of 150.7 lb/ft³.

Table 3.10. Region 4 Core Gradation Results[a]

Core	2	3	4	5	6	7	8	9	10	JMF
¾ in.	100.0	100.0	100.0	100.0	100.0	100.0	100.0	100.0	100.0	100.0
½ in.	86.1	89.6	88.4	89.2	89.7	**91.7**	85.6	89.1	87.6	86.0
⅜ in.	61.2	**69.7**	65.7	65.5	**68.9**	**67.8**	63.0	**66.7**	64.7	57.5
No. 4	26.3	**32.0**	28.8	27.1	29.0	28.9	26.6	29.1	29.9	23.5
No. 8	20.0	**24.4**	21.7	20.5	21.2	20.8	19.9	22.2	23.4	23.6
No. 16	**15.6**	19.9	17.6	16.6	17.1	16.6	16.4	17.8	18.9	19.0
No. 30	13.3	17.3	15.2	14.3	14.7	14.1	14.1	15.0	16.3	15.6
No. 50	11.4	15.3	13.3	12.6	12.9	12.2	12.3	12.7	14.3	12.8
No. 200	8.1	11.8	10.1	9.5	9.6	9.1	9.0	8.5	10.7	10.5

Note: Entries in bold are outside the JMF percent passing operational tolerances.
[a] Percent passing. Results for Core 1 not available due to sample-handling accident.
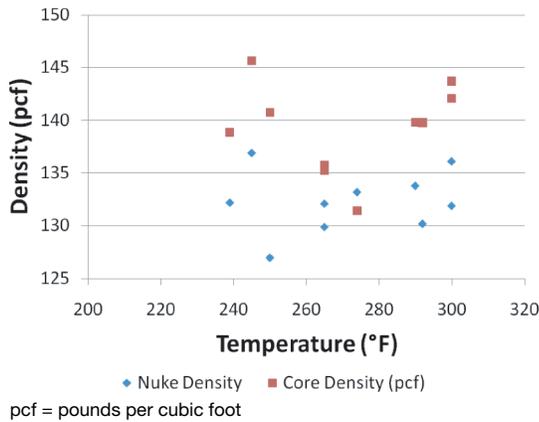
Figure 3.40. Lack of correlation between temperature and density with Region 4 data.

Figure 3.42. Lack of correlation between GPR and laboratory density with Region 4 data.

by Figure 3.42, the GPR-measured surface dielectric constant correlated well with field nuclear density readings; however, neither the GPR nor the nuclear gauge correlated with the laboratory-measured core densities. More research needs to be conducted to determine why the GPR did not correlate with the laboratory densities. This project represented the first time these GPR quality control procedures were attempted on this mix type; it is unknown if the mix type, the presence of fibers, or the rain at the plant contributed to the lack of correlation between the GPR and core densities.

As with the thermal data, the GPR result did relate to changes in some of the gradation parameters. As shown in the correlation data in Appendix F, increases in the GPR-measured HMA dielectric correlated with increases in percent passing the ½-in., No. 4, and particularly the ⅜-in. sieve, as shown in Figure 3.43. This increase in percent passing these sieve sizes was accompanied by increases in the individual percent retained on the No. 4 and No. 8 sieves.

If GPR will ever be a feasible option for uniformity measurement on a national scale, the equipment must be commercially available. In the United States, the GSSI 2-GHz system represents the most likely candidate because of its compliance with FCC regulations. Because of this, researchers evaluated the output from the GSSI system in comparison with the measured surface dielectrics from TTI's 1-GHz system for each of the three GPR passes. As Figure 3.44 illustrates, although the GSSI-measured values are typically around 0.5 higher, good correlation exists between the two systems.

Conclusions from Test Site

At the US-190 demonstration site, the infrared NDT operated well and succeeded in covering nearly 100% of the constructed


Figure 3.41. Lack of correlation between temperature and density differentials with Region 4 data.
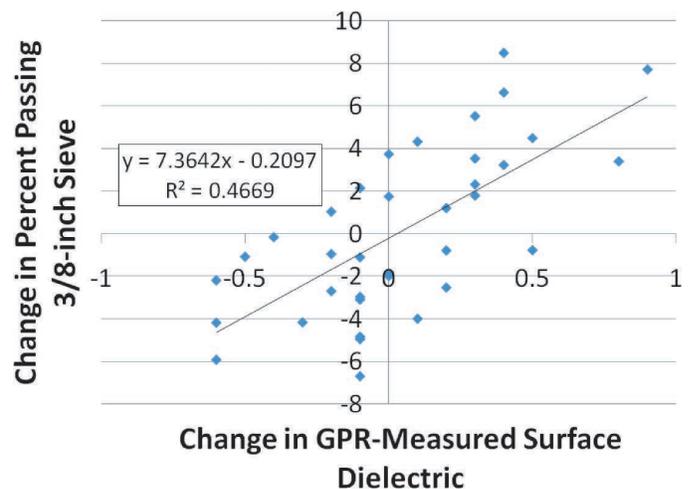
**Figure 3.43. Gradation changes with changes in measured dielectric value with Region 4 data.**
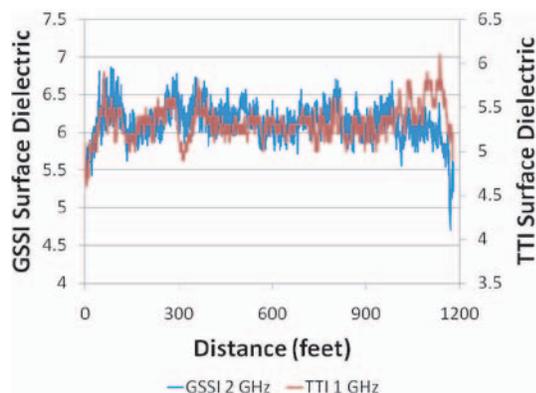
Figure 3.44. Surface dielectrics measured with 1-GHz and 2-GHz systems on Region 4 demonstration project.

Table 3.11. Job Mix Formula for SP-12.5 on Region 2 Demonstration Project

Sieve Size	Current JMF Cumulative Percent Passing	JMF Individual Retained Limits, Percent	Primary Control Sieve
¾ in.	100.0	100	
½ in.	98.0	90–100	
⅜ in.	89.0	–90	
No. 4	65.0		
No. 8	48.0	28–58	39
No. 16	38.0		
No. 30	30.0		
No. 50	20.0		
No. 100	9.0	2–10	
No. 200	4.8		

area. With cores collected at locations representing a range of temperatures from 239°F to 300°F, a cross-section analysis did not find a correlation between the temperature and core density. The GPR data similarly worked well and succeeded in providing a view of nearly 100% of the constructed area but did not correlate with core density.

This project represented the first time these NDT procedures were employed on this mix type. Historically, work with the IR and GPR tests has focused on dense-graded mixes. It is unknown if the mix type, the presence of fibers in the mix, the rain at the plant during production, or some other factor resulted in the lack of correlation between the NDT and laboratory core densities on this project. If possible, this mix type should be tested again. Future work may be needed to identify whether these NDT procedures should be restricted to certain mix types or placement processes.

Demonstration Project in AASHTO Region 2

Summary

This demonstration took place on June 14–15, 2010, in AASHTO Region 2 on Lake Underhill Drive near Orlando, Florida. The researchers used a MOBA Pave-IR system to collect thermal profile data and supplemented the measurements with a handheld spot radiometer for collecting placement temperature data at core locations. At the time of testing, no commercially available IR package using either a line scanner or a thermal camera was available.

TTI's 1-GHz system was used for the GPR data collection on the first night of demonstrations. The TTI 1-GHz system and the GSSI 2.2-GHz air-coupled system with RF filter were used on the second night of demonstrations.

Job Mix Formula

The contractor placed a 1.5-in. lift of SP-12.5 traffic level C. The mix was designed at 75 gyrations and used 30% crushed reclaimed asphalt pavement (RAP) and 3.5% RA 1000 to obtain the optimum asphalt content of 5.2%. Table 3.11 shows the gradation job mix formula.

Paving Operation

The contractor produced the mix near Kissimmee, Florida, resulting in a haul distance of approximately 30 mi, and used tarped bobtail trucks to transfer the mix into a Cat AP 100D paver. Two Sakai R2H rollers in tandem provided breakdown rolling, and an IR DD-112 was used for finish rolling. Figure 3.45 shows the paving train.

Figure 3.45. Paving operation on demonstration project in Region 2.

Thermal Survey Result

Figure 3.46 shows the thermal profile from the project. The thermal data were collected from 81.25279 W, 28.53927 N to 81.2489 W, 28.53941 N. The profiled section began just west of the intersection with Econlockhatchee Trail and proceeded east for approximately 1,270 ft. The thermal data show reduced temperatures at the truck ends with temperature differentials typically between 70°F and 90°F. Locations spot tested are annotated in the profile, and Table 3.12 presents their placement temperatures.

GPR Survey Result

After the contractor completed finish rolling, the researchers collected GPR data at five different transverse offsets over the mat width. Figure 3.47 shows the GPR data collection in progress with TTI's 1-GHz air-coupled system. The GPR survey began 110 ft east of the starting point of the thermal survey to avoid the intersection with Econlockhatchee Trail. After collecting data from the five passes, the 1-GHz system was then used to collect stationary GPR data directly over the 10 locations marked in the thermal data for calibration to
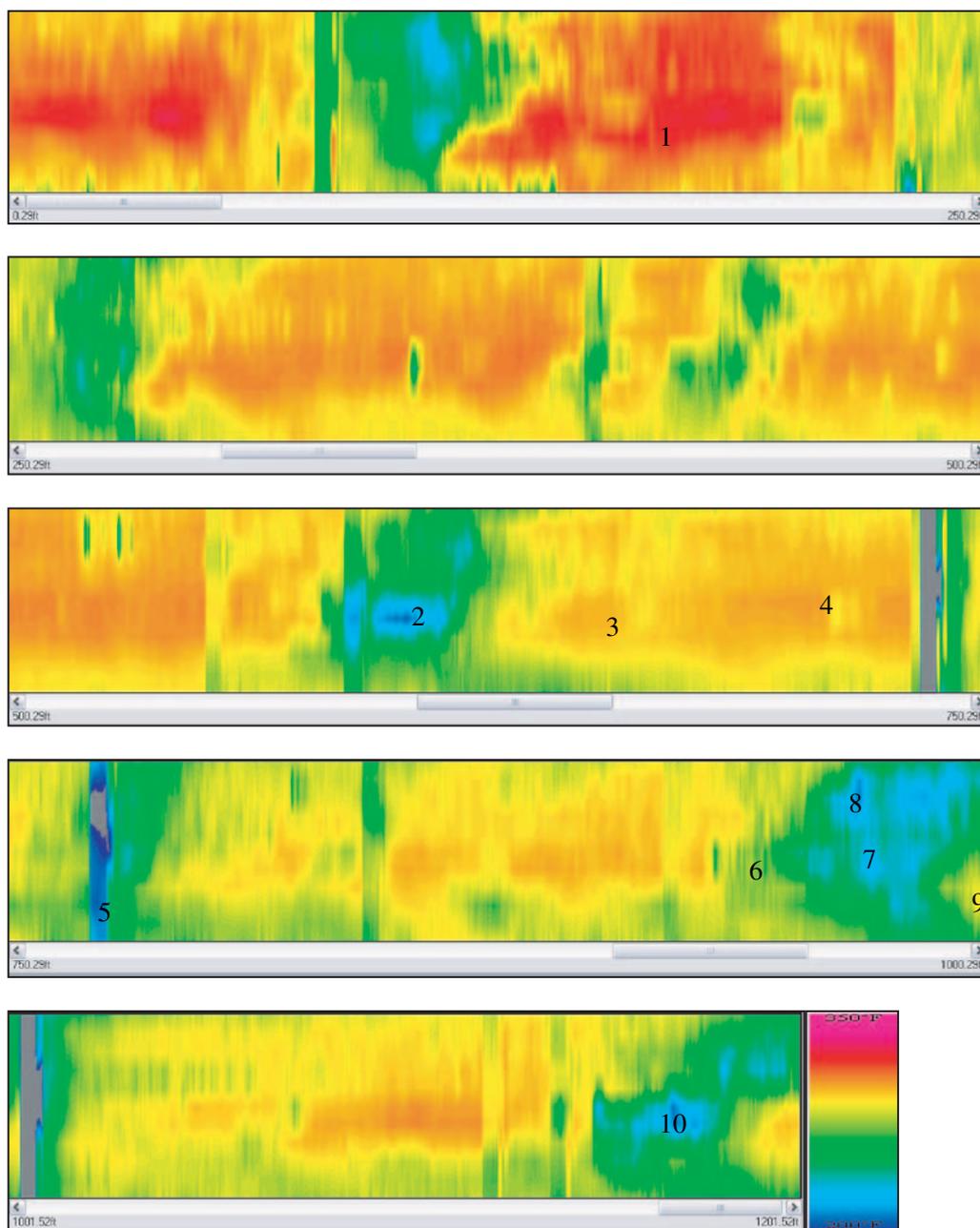

Figure 3.46. SP-12.5 thermal profile. Note that the true distance profiled was 1,270 ft.

Table 3.12. Region 2 Core Locations with IR-Measured Placement Temperature

Core	1	2	3	4	5	6	7	8	9	10
IR Temperature (°F)	283	218	299	301	215	284	228	212	292	206

Figure 3.47. GPR data collection on Region 2 project.

density. Table 3.13 shows the GPR-measured surface-layer dielectric values for the 10 cores.

NDT Validation Test Results

To validate the meaning of the NDT data, a field sequence and a laboratory sequence were performed on the 10 locations. In the field, researchers collected nuclear density readings with a Troxler 3450 using a 60-s count time. In the laboratory, researchers determined the bulk specific gravity of the cores and measured the maximum theoretical density

Table 3.13. Core Dielectric Values from 1-GHz GPR on Region 2 Project

Core	1	2	3	4	5	6	7	8	9	10
GPR ε	4.8	4.2	4.9	4.7	4.4	5.1	4.4	4.0	4.5	4.1

of a sample of loose mix collected from the job site to convert the densities to air void contents. Table 3.14 presents the density data results merged with the temperature and GPR measurements. Appendix G presents correlation matrices for the data, along with results from tests for the significance of the observed correlation values.

Significance of Thermal Data

Figure 3.48 illustrates a statistically significant correlation between the measured placement temperature and in-place air voids. Figure 3.49 shows the correlation between the observed density differentials and the measured temperature differentials.

Significance of GPR Data

Low surface dielectric values typically indicate higher air voids in the compacted HMA. On this project, as illustrated

Table 3.14. Core Density and Overlay Test Results with Field NDT Data from Region 2 Project

Core	Field IR Temperature (°F)	Field ε from GPR	Field Nuclear Density (lb/ft³)	Laboratory Density (lb/ft³)	Laboratory Percent Air Voids[a]
1	283	4.8	126.7	140.5	8.4
2	218	4.2	126.2	136.2	11.2
3	299	4.9	139.2	144.0	6.2
4	301	4.7	141.9	144.2	6.0
5	215	4.4	134.7	137.3	10.5
6	284	5.1	141.2	143.4	6.5
7	228	4.4	133.9	140.0	8.9
8	212	4.0	128.8	135.8	11.5
9	292	4.5	134.1	137.6	10.3
10	206	4.1	127.4	131.9	14.0

[a] Based on maximum theoretical specific gravity of 153.5 lb/ft³.
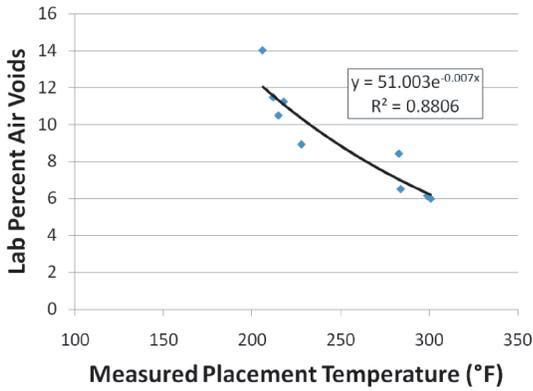
Figure 3.48. Relationship between temperature and core density from Region 2 data.

by Figure 3.50, the GPR-measured surface dielectric constant correlated well with laboratory core densities. Figure 3.51 shows how density differentials correlated with changes in the GPR-measured dielectric.

With the relationship shown in Figure 3.50, both the statistical and geospatial distributions of air voids can be developed by converting each GPR trace into an air void content prediction, yielding more than 4,500 measurement points. Figure 3.52 presents the expected air void distribution, and Figure 3.53 presents the expected geospatial distribution of air voids on the section surveyed by GPR.

Focusing on the worst (air voids > 12%) regions in Figure 3.53 and comparing these locations to the thermal profile in Figure 3.46 reveals that the areas with the highest air voids also had significant temperature differentials:

- The red zone at the start of the GPR data in Figure 3.53 corresponds to approximately 105 ft in the thermal profile figure. The thermal data showed a temperature differential of approximately 70°F at this location.

Figure 3.50. Calibrating GPR to predict in-place air voids from Region 2 data.

pcf = pounds per cubic foot
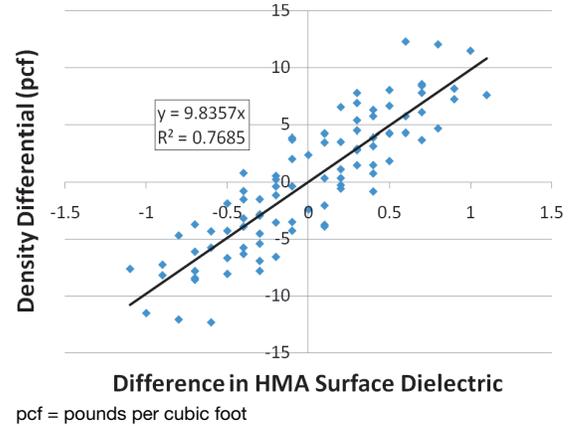
Figure 3.51. Density differentials versus dielectric differentials from Region 2 data.

pcf = pounds per cubic foot
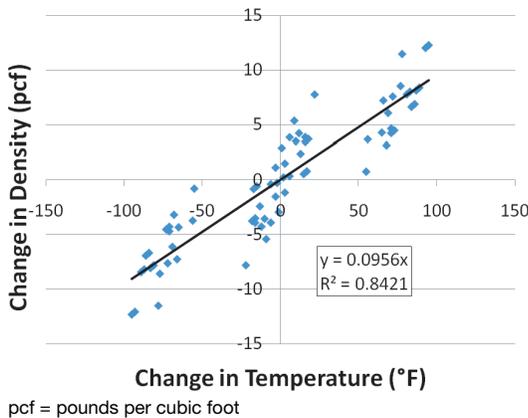
*Figure 3.49. Density differentials versus temperature differentials from Region 2 data.*
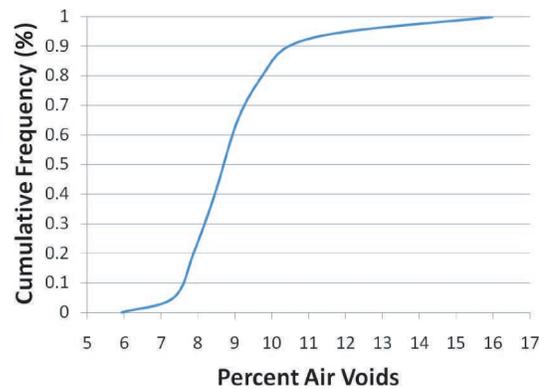
Figure 3.52. Expected air void distribution for SP-12.5 HMA in Region 2.
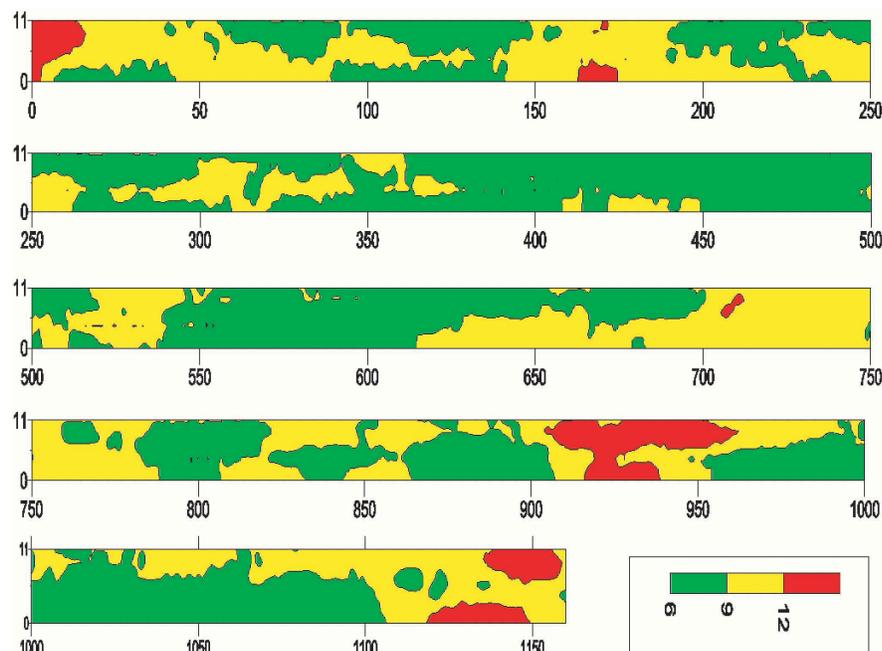
Figure 3.53. Geospatial distribution of air voids for SP-12.5 HMA in Region 2.

- The red zone at approximately 170 ft in Figure 3.53 corresponds with a 60°F temperature differential at 268 ft in the thermal profile.
- The localized high void region at approximately 710 ft in Figure 3.53 matches the location of the paver stop at 774 ft in the thermal profile; at this location, the mix surface temperature was approximately 190°F in the thermal profile.
- The large zone of high air voids centered around 925 ft in Figure 3.53 corresponds with temperature differentials from 60°F to 90°F centered around 977 ft in the thermal profile. At this location, the mix placement temperature ranged from 210°F to 230°F.
- The high-void region from 1,110 to 1,150 ft in Figure 3.53 matches the cold spot centered around 1,170 ft in the thermal profile. The cold zone ranged in temperature from approximately 210°F to 230°F; the surrounding mix that was not thermally segregated typically ranged in temperature from 270°F to 300°F.

Conclusions from Test Site

At the demonstration site in AASHTO Region 2, the infrared NDT operated well and succeeded in covering nearly 100% of the constructed area. The data showed a defensible statistical correlation between the placement temperature and the mix density. Although the thermal survey cannot capture the effects of rolling delays or other issues that may occur after placement, the GPR survey occurs after all finish rolling to serve as a final quality check. At this demonstration site, the GPR correlated well with in-place density and succeeded at providing a view of nearly 100% of the constructed area.

Additional data analysis revealed that the locations of highest air voids, as evaluated with GPR, also exhibited significant temperature differentials in the thermal profile. The NDT technologies produced similar results in identifying the poorest areas of the mat.

Demonstration Project in AASHTO Region 3

Summary

This demonstration took place on September 20, 2010, in AASHTO Region 3 on the second lift of the eastbound driving lane of TH-60 just east of Worthington, Minnesota. The project team used a MOBA Pave-IR system to collect thermal profile data and supplemented the measurements with a handheld spot radiometer for collecting placement temperature data at core locations. TTI's 1-GHz system was used for the GPR data collection. The morning following the demonstration, the Minnesota DOT (MnDOT) collected GPR data over the test section with its GSSI 2.2-GHz air-coupled system. The data showed thermal variations correlated strongly with density differentials, and the GPR worked well for evaluating the density uniformity of the section.

Table 3.15. Job Mix Formula for SP-12.5 on Region 3 Demonstration Project

Sieve Size	Composite Formula	Broadband
¾ in.	100	100–100
½ in.	96	85–100
⅜ in.	85	35–90
No. 4	63	30–80
No. 8	54	25–65
No. 16	39	
No. 30	26	
No. 50	13	
No. 100	6	
No. 200	3.7	2–7
Spec. voids	4.0	3.0–5.0
% AC	5.0	4.6

Figure 3.54. Paving operation during Region 3 demonstration.

Job Mix Formula

The contractor placed a 1.5-in. lift of MnDOT SPWEB440E. This is a gyratory design wearing course with a 4.0% air void requirement, a ¾-in. maximum aggregate size, and PG 64-28 binder. The day of the demonstration, the second of three lifts was placed, and the mix was produced as WMA using the foam process. Table 3.15 shows the job mix formula, which included 30% plant RAP.

Paving Operation

The total project length was approximately 15 mi, with the plant located approximately midway along the project, for a haul distance of approximately 6 mi. The contractor used a combination of belly dump, tandem axle, and flow boy trucks to windrow the mix. A Barber Green pickup machine transferred the mix into a CAT AP 1000D. A CAT CB 64 and Hamm HD 140 in tandem performed breakdown rolling, a Dynapac CP 27 and CAT PS 360 in tandem performed intermediate rolling, and a Dynapac CC 522 performed finish rolling. Figure 3.54 shows the paving train.

Thermal Survey Result

Figure 3.55 shows the thermal profile from the project. The thermal data that the evaluation focused on were collected from Stations 245 to 270, which resulted in a test section approximately 2,500 ft long. The thermal data show a few

instances of severe truck-end temperature differentials (with temperature differentials around 60°F) occurring just before Station 238, just after Station 249, and at Station 267. A drop in the mean placement temperature occurred just after Station 259, and a long paver stop lasting approximately 35 min occurred at approximately Station 265 + 60. Locations spot tested for densities are annotated in the profile, and Table 3.16 presents their placement temperatures.

GPR Survey Result

After the contractor completed finish rolling, the researchers collected GPR data at five different transverse offsets over the mat width using TTI's 1-GHz air-coupled system. Figure 3.56 shows the GPR data collection in progress. After collecting the five passes, the 1-GHz system was then used to collect stationary GPR data directly over the 10 locations marked in the thermal data for calibration to density. Table 3.17 shows the GPR-measured surface dielectric values for the 10 cores.

NDT Validation Test Results

To validate the meaning of the NDT data, a field sequence and a laboratory sequence were performed on the 10 locations. In the field, researchers collected nuclear density readings with a Troxler 3450 using a 60-s count time. Then, two 4-in.-diameter cores were collected side by side in the field at the 10 spot-test locations. In the laboratory, researchers determined the bulk specific gravity of the cores, followed by the indirect tensile strength, asphalt content by ignition, and then aggregate gradation. Table 3.18 presents the NDT data
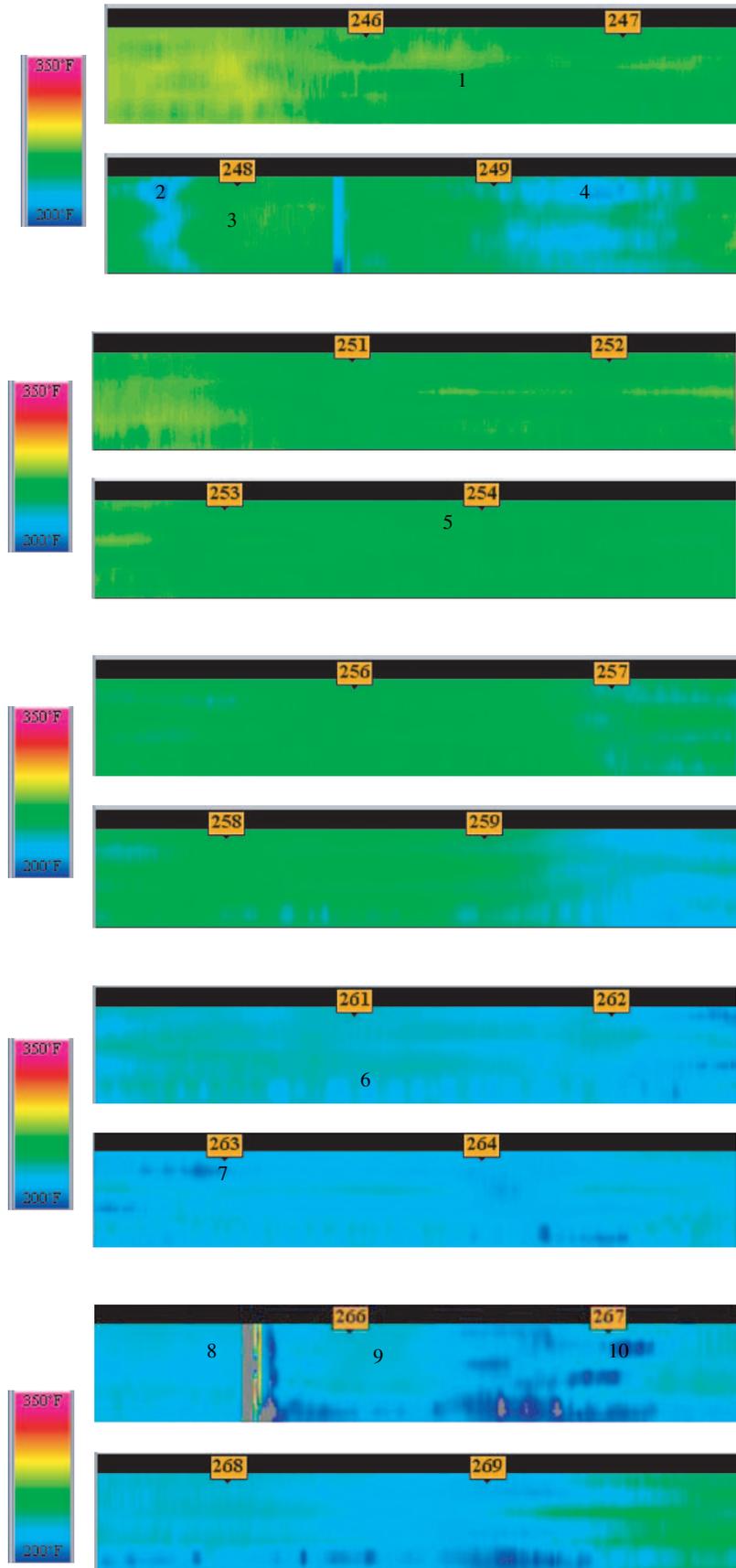
Figure 3.55. Thermal profile from Region 3 project.

Table 3.16. Region 3 Core Locations with IR-Measured Placement Temperature

Core	1	2	3	4	5	6	7	8	9	10
IR Temperature (°F)	264	220	266	212	261	238	218	228	235	177

merged with the core results. The core density and indirect tension (IDT) values presented are the average of the two side-by-side cores at each location. For asphalt content and gradation, the side-by-side cores were combined into one larger sample.

With the core data complete, researchers analyzed the IR and GPR data in conjunction with the core validation results to investigate the significance of the NDT readings. Appendix H presents correlation matrices for the data, along with results from tests for the significance of the observed correlation values.

Significance of Thermal Data

Figure 3.57 illustrates how the thermal cold spots typically correlated with both a segregated mat appearance and an eventual low-density location in the completed mat. These thermally segregated locations corresponded to truck ends. Figure 3.58 illustrates a statistically significant correlation observed between the measured placement temperatures and in-place air voids from the project, and Figure 3.59 presents the relationship between density and temperature differentials. Figures 3.58 and 3.59 exclude core 8 because after placement this location was not rolled for approximately 35 min due to the location's proximity to a paver stop.

Figure 3.56. GPR data collection on Region 3 demonstration project.

At the location of the paver stop, which occurred at approximately Station 265+60, the paver remained idle for approximately 35 min. Immediately leading up to this point, the mean mixture temperature was about 230°F. However, because of the paver stopping, a portion of the placed mat did not get rolled until the paving train resumed. Additionally, the paver burners continued to heat the mat underneath the screed. The net effects were that the location not rolled during the paver stop became low in density regardless of the temperature at the time of placement. A visual mark taking the shape of the burners occurred in the pavement, and riders felt a bump in the completed mat at the location of the paver stop. Figure 3.60 illustrates these occurrences.

Figure 3.61 shows significant thermal segregation (with a temperature differential of approximately 60°F) that occurred shortly after the paving train resumed. At this location, the mean mix temperature was still reduced to approximately 220°F to 230°F. (The mix earlier in the day typically averaged 250°F to 260°F.) As in other instances of thermal segregation, the cold streaks showed up visually in the mat and became a low-density location. An important observation from this section of the mat is that although the mean mixture temperature dropped about 20°F into the 230°F range, the density achieved at the "normal" temperature in this section was still reasonable at ~6.5% air voids. This observation matches previous experiences in the literature of thermal profiling, which indicates that, from a stochastic viewpoint, thermal differentials are more meaningful when observed over short paving distances.

In addition to the correlation with air voids, the test data also revealed that the thermally segregated locations exhibited substantially reduced indirect tensile strengths. Figure 3.62 illustrates the correlation observed in the data set. The data show an approximately 1-psi reduction in tensile strength for each degree of temperature drop at the time of placement.

Finally, the correlation matrices in Appendix H reveal that the thermal data correlated to the mixture gradation. The data showed a positive correlation between the temperature and percent passing. In addition to exhibiting reduced density and reduced tensile strengths, the thermally segregated locations tended to also be coarser in gradation. The data did not show a statistically significant correlation between the measured placement temperature and the asphalt cement content.

Table 3.17. Core Dielectric Values from 1-GHz GPR on Region 3 Project

Core	1	2	3	4	5	6	7	8	9	10
GPR	4.15	3.7	4.1	3.9	4.05	4.05	3.85	3.55	4.15	3.8

Table 3.18. NDT Data with Core Results from Region 3 Demonstration

Core	1	2	3	4	5	6	7	8	9	10
IR temperature (°F)	264	220	266	212	261	238	218	228	235	177
Dielectric	4.15	3.7	4.1	3.9	4.05	4.05	3.85	3.55	4.15	3.8
Nuclear density (lb/ft^3)	140.7	124.2	137.4	132.2	137.0	136.4	133.2	123.2	138.3	121.4
Core voids (%)[a]	6.0	11.5	5.8	12.2	6.8	7.2	9.4	15.0	6.4	14.8
IDT (psi)	135.6	71.9	120.1	66.9	116.9	103.5	78.8	50.7	109	39.1
% AC	5.95	4.97	5.51	5.67	5.51	5.97	5.07	5.49	5.27	5.05
Percent Passing										
¾ in.	100.0	100.0	100.0	100.0	100.0	100.0	100.0	100.0	100.0	100.0
½ in.	94.9	91.8	92.6	93.9	94.5	95.5	89.5	92.8	91.9	90.1
⅜ in.	86.8	79.9	85.6	81.9	86.4	86.8	76.4	81.6	83.3	77.9
No. 4	65.8	56.8	63.7	62.0	66.1	66.7	56.8	62.6	61.2	58.3
No. 8	56.8	48.1	54.2	53.6	56.2	56.7	48.6	52.8	51.4	48.3
No. 16	43.6	36.9	41.7	42.6	43.1	43.4	37.3	40	39	35.6
No. 30	30.2	25.9	28.6	31.1	29.5	29.7	25.6	26.8	26.3	23.5
No. 50	16.2	14.2	14.9	19.0	15.9	15.9	13.6	14.0	13.8	12.0
No. 100	7.6	6.9	6.9	11.7	7.9	7.7	6.6	6.8	66	5.6
No. 200	4.7	4.2	4.1	9.1	5.2	5.0	4.2	4.3	4.1	3.5

[a] Based on maximum theoretical specific gravity of 152.6 lb/ft^3 obtained from MnDOT records.
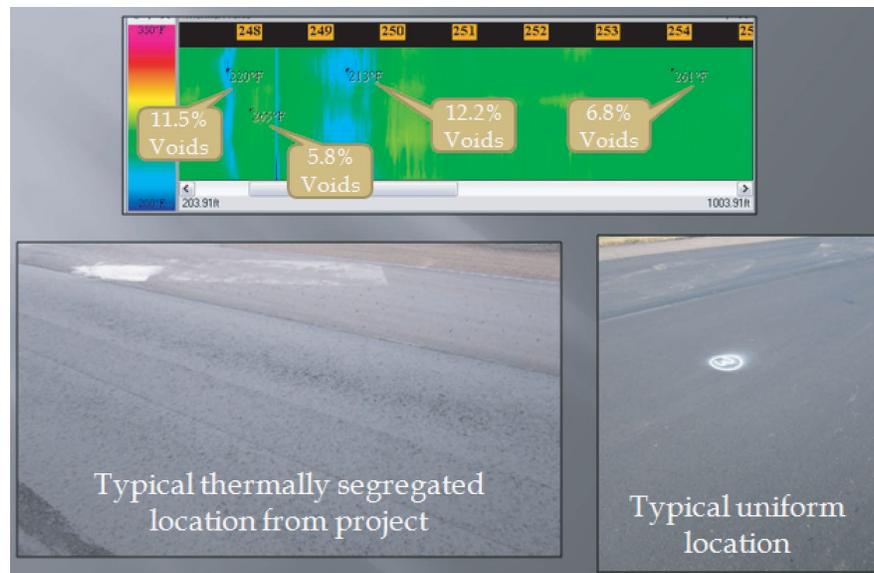
**Figure 3.57. Example of core densities and mat appearance with thermal segregation from demonstration in Region 3.**
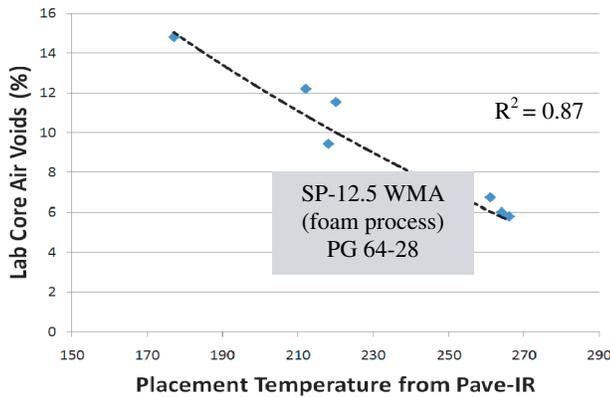
Figure 3.58. Air voids versus placement temperature from Region 3 project.



pcf = pounds per cubic foot
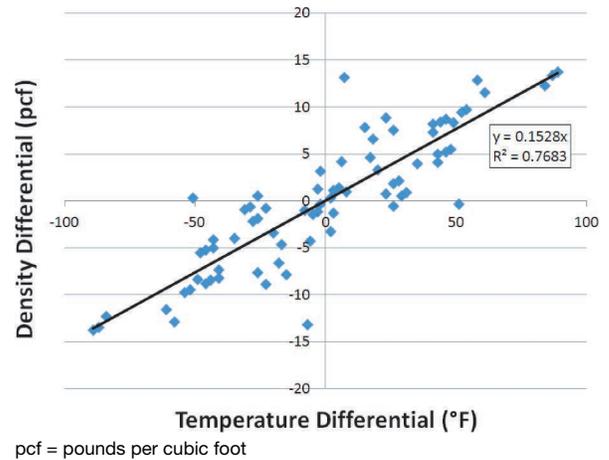
Figure 3.59. Density versus temperature differentials from Region 3 project.

Significance of GPR Data

Low surface dielectric values typically indicate higher air voids in the compacted HMA. On this project, as illustrated by Figure 3.63, the GPR-measured surface dielectric constant correlated well with laboratory core densities. Figure 3.64 illustrates that a reduction in density of about 12 lb/ft³ is expected to occur for each drop of 0.5 in the measured surface dielectric constant.

Using the calibration between radar and air voids shown in Figure 3.63, each of the GPR measurements was converted to an air void measurement, resulting in more than 8,000 measurements of air voids geospatially over the section evaluated. These data served to generate the statistical

and geospatial distribution of air voids, as Figures 3.65 and 3.66 illustrate.

In Figure 3.66, the air voids are color coded according to MnDOT's pay schedule: below 7% air voids is the bonus region, from 7% to 8% air voids is pay unity, and air voids exceeding 8% result in a penalty. Table 3.19 presents the locations of the highest air void regions (red) in Figure 3.66. A joint review of the GPR and thermal profile outputs suggests that, in general, the cold spots observed in the thermal profile match well with the locations of low density observed in the GPR output. Additionally, the GPR output suggests the low-density locations typically occur at intervals averaging
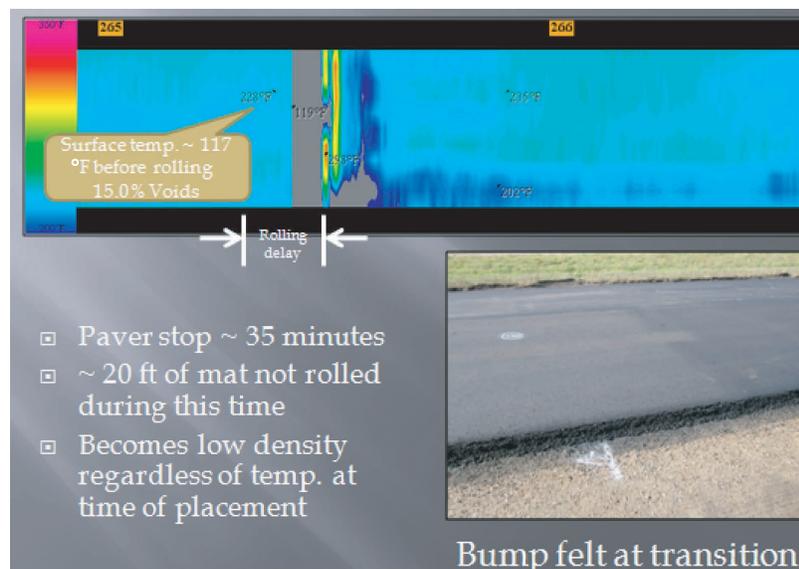
Figure 3.60. Influence of prolonged paver stops from Region 3 demonstration project.
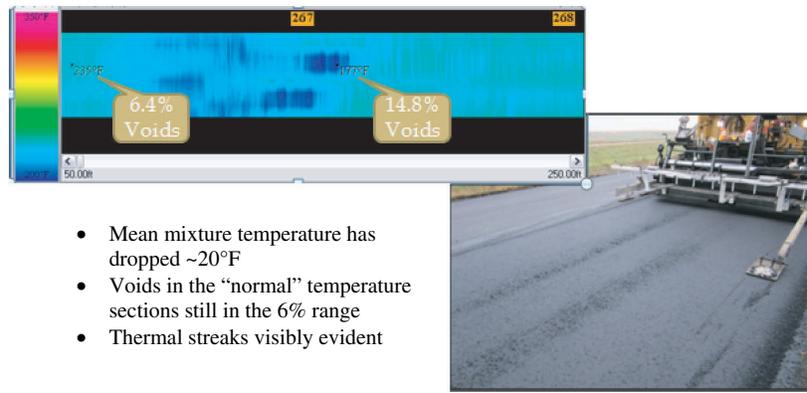
- Mean mixture temperature has dropped ~20°F
- Voids in the "normal" temperature sections still in the 6% range
- Thermal streaks visibly evident

Figure 3.61. Significant thermal segregation on Region 3 demonstration.
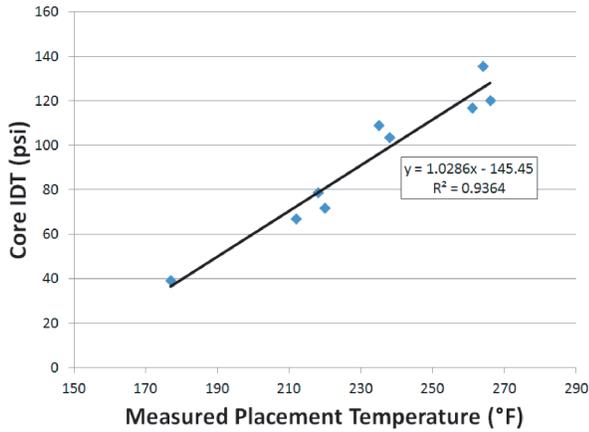
Figure 3.62. Core IDT versus measured placement temperature from Region 3.

$y = 1.0286x - 145.45$
$R^2 = 0.9364$

pcf = pounds per cubic foot

Figure 3.64. Density differentials versus dielectric differentials from Region 3 data.

$y = 24.396x$
$R^2 = 0.813$

Figure 3.63. Calibrating GPR to predict in-place air voids from Region 3 data.

$y = 6,334.7614e^{-1.6702x}$
$R^2 = 0.8285$
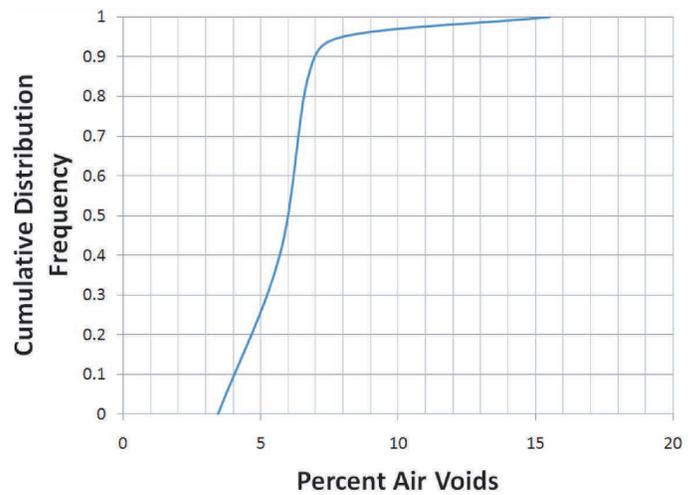
Figure 3.65. Expected air void distribution on Region 3 project. Note that the average predicted void content is 6.5%.
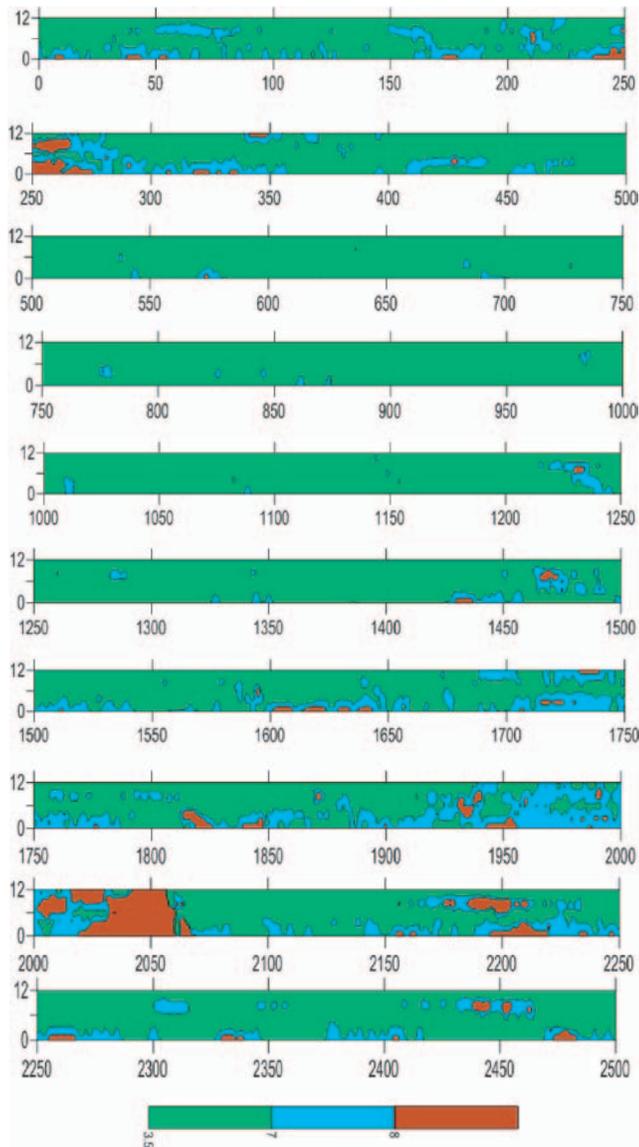
Figure 3.66. Geospatial distribution of air voids on Region 3 demonstration.
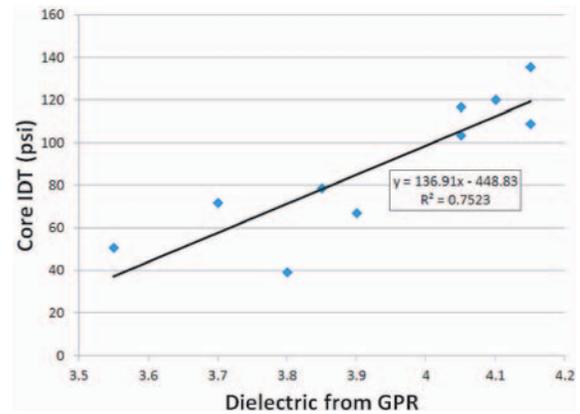
**Figure 3.67. Core IDT versus dielectric from Region 3 project.**

either approximately 120 ft or 240 ft. These intervals are consistent with the windrow lengths one would expect from tandem axle trucks and belly dump or flow boys, respectively, suggesting the cyclic low density largely resulted from truck-end segregation.

In addition to the correlation with air voids, the GPR correlated well with the indirect tensile strength, where locations with higher dielectric values also exhibited increased strength values. Figure 3.67 illustrates this observation.

The correlation matrices in Appendix H also show a relation between the radar data and the percent passing the $3/8$-in. sieve, where increases in the dielectric correlated with increases in percent passing. The data did not show a statistically significant correlation between the measured surface dielectric constant and the asphalt cement content.

Conclusions from Test Site

At the demonstration site in AASHTO Region 3, the infrared NDT operated well and succeeded in covering nearly 100% of

Table 3.19. Summary of Low-Density Locations from GPR on Region 3 Project

Distance in GPR (Station 245 Is Zero in GPR)	Station	Distance (ft) from Previous Low-Density Location	Comment
260	247 + 60	Not applicable	Cold spot in IR
1,240	257 + 40	980	
1,475	259 + 75	235	Cold spot in IR
1,725	262 + 25	250	Cold spot in IR
1,840	263 + 40	115	
1,940	264 + 40	100	Leading up to paver stop
2,050	265 + 50	110	Paver stop
2,200	267 + 00	150	Cold spot in IR
2,440	269 + 40	240	May match IR ~ Station 269
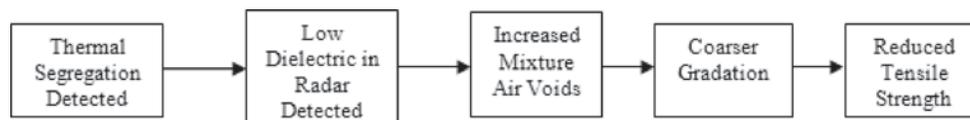
Figure 3.68. Flow diagram relating NDT to mixture properties.

the constructed area. The data showed a defensible statistical correlation between the placement temperature and mix density. Although the thermal survey cannot capture the effects of rolling delays or other issues that may occur after placement, the GPR survey occurs after all finish rolling to serve as a final quality check. At this demonstration site, the GPR correlated well with in-place density and succeeded at providing a view of nearly 100% of the constructed area. The effect of roller delay resulting in low density, regardless of placement temperature, was clearly observed on this project.

Additional data analysis revealed that the locations of highest air voids, as evaluated with GPR, also generally exhibited significant temperature differentials in the thermal profile. The two NDT technologies produced similar results in identifying the poorest areas of the mat.

In performance-related testing, indirect tensile tests revealed defensible relationships between the NDT, core density, and measured indirect tensile strength. The thermally segregated and low-dielectric locations, which were low density, also exhibited reduced tensile strength. Based on these observations, Figure 3.68 presents a flowchart illustrating how the NDT could be viewed as relating to mixture properties.

Demonstration Project in AASHTO Region 1

Summary

This demonstration took place on August 10, 2011, in AASHTO Region 1 on the southbound inside lane of I-295 near Freeport, Maine. The project was a mill and inlay overlay process, and Figure 3.69 illustrates the existing pavement condition in the outside lane. The existing mix was placed in the mid-1990s and exhibits cyclical raveling and pothole failures at approximately 150-ft intervals; these failures result in a poor ride and are typical of cyclical segregation. Between these failed locations, the HMA layer was in good condition, so the new overlay was required largely because of cyclical segregation problems in the old mat.

On the new overlay, the project team used a MOBA Pave-IR system to collect thermal profile data and supplemented the measurements with a handheld spot radiometer for collecting placement temperature data at core locations. TTI's 1-GHz and GSSI's 2.2-GHz air-coupled radar systems were used for the GPR data collection. The results showed a significant correlation between the temperature data and eventual in-place core density, where colder locations detected in the thermal profile generally exhibited lower in-place density after compaction. Additionally, both GPR systems worked well for evaluating the density uniformity of the demonstration section.

Job Mix Formula

The contractor placed a 1.5-in. lift of HMA Mix-12.5MM (WMA) with 15% RAP. This Superpave mixture was designed at 75 gyrations with 5.7% binder. Of the total binder content, 5.0% was new PG 64-28. Table 3.20 shows the job mix formula.

Paving Operation

The plant produced the WMA using a foam process with a reported target production temperature of 300°F. After a haul distance of approximately 25 mi, the contractor predominantly used end-dump trucks to deliver the mix into a Roadtec SB 2500D, which then transferred the mix into a CAT AP 1055D to pave a mat 16 ft wide. Figure 3.70 shows the paving train.

Figure 3.69. Damage from segregation in old HMA mat on I-295.

Table 3.20. Job Mix Formula for SP-12.5 on Region 1 Test Site

Sieve Size	Aim	Specification
¾ in.	100	100
½ in.	98	90–100
⅜ in.	85	–90
No. 4	66	NA
No. 8	47	28–58
No. 16	34	NA
No. 30	23	NA
No. 50	14	NA
No. 100	8	NA
No. 200	4.8	2–10
% Binder	5.7	NA

Note: NA = not available.

Thermal Survey Result

Because the mat width was 16 ft, Pave-IR was set up to focus data collection over the area of the inside lane and excluded the area that would become the inside shoulder. The thermal data the evaluation focused on was collected from Station 243 to Station 228, which resulted in a test section approximately 1,500 ft long. The paving train used 2 h and 18 min to pave this section, with an average speed of 10.9 ft/min.

Figure 3.71 shows the thermal profile from the project. Locations spot tested for densities are annotated in Figure 3.71, and Table 3.21 presents their measured placement temperatures. The largest anomalies in the thermal profile appear to be a result of the three paver stops at Stations 242.65, 240.5, and 239.64. The combined idle time from these three paver stops was approximately 14 min.

Figure 3.70. Paving operation at Region 1 demonstration.

By narrowing the color-scale range in the thermal profile, Figure 3.72 highlights other thermal patterns observed in the operation: (a) when observed, the colder zones in the mat occurred near the center of the mat area appeared typical of colder zones from truck exchanges; (b) from Station 240 to Station 230, enough of a pattern was observed to suggest each truck paved approximately 94 ft on average; and (c) two zones, centered near Station 237.60 and Station 234.50, existed where the mean truck mix temperature exceeded the placement temperatures typically observed in the operation.

Figure 3.73 illustrates the distribution of placement temperatures measured in the demonstration section. The Maine DOT construction specification requires temperature tolerances of ±20°F at the paver. Figure 3.73 is based on data collected at placement immediately behind the screed and suggests substantial compliance with the specification requirement.

GPR Survey Result

After the contractor completed finish rolling, the researchers collected GPR data at five different transverse offsets over the lane width using TTI's 1-GHz and GSSI's 2.2-GHz air-coupled systems. Figure 3.74 shows the GPR data collection in progress. After collecting the five passes, each system collected stationary GPR data directly over the locations planned for calibration to density. Table 3.22 shows the GPR-measured surface dielectric values for the 11 field cores.

NDT Validation Test Results

To validate the meaning of the NDT data, a field sequence and a laboratory sequence were performed on the 11 core locations. In the field, researchers collected nuclear density readings with a Troxler 3450 using a 60-s count time. Then 6-in.-diameter cores were collected at each spot-test location. In the laboratory, researchers determined the bulk specific gravity of the cores. Table 3.23 presents the NDT data merged with the core results.

With the core data complete, researchers analyzed the IR and GPR data in conjunction with the core validation results to investigate the significance of the NDT readings. Appendix I presents correlation matrices for the data, along with results from tests for the significance of the observed correlation values.

Significance of Thermal Data

Figure 3.75 illustrates how the thermal cold spots during normal placement typically became higher air void locations in the mat. This figure omits cores 1 and 2 because those locations were in the hand-worked portion at the construction
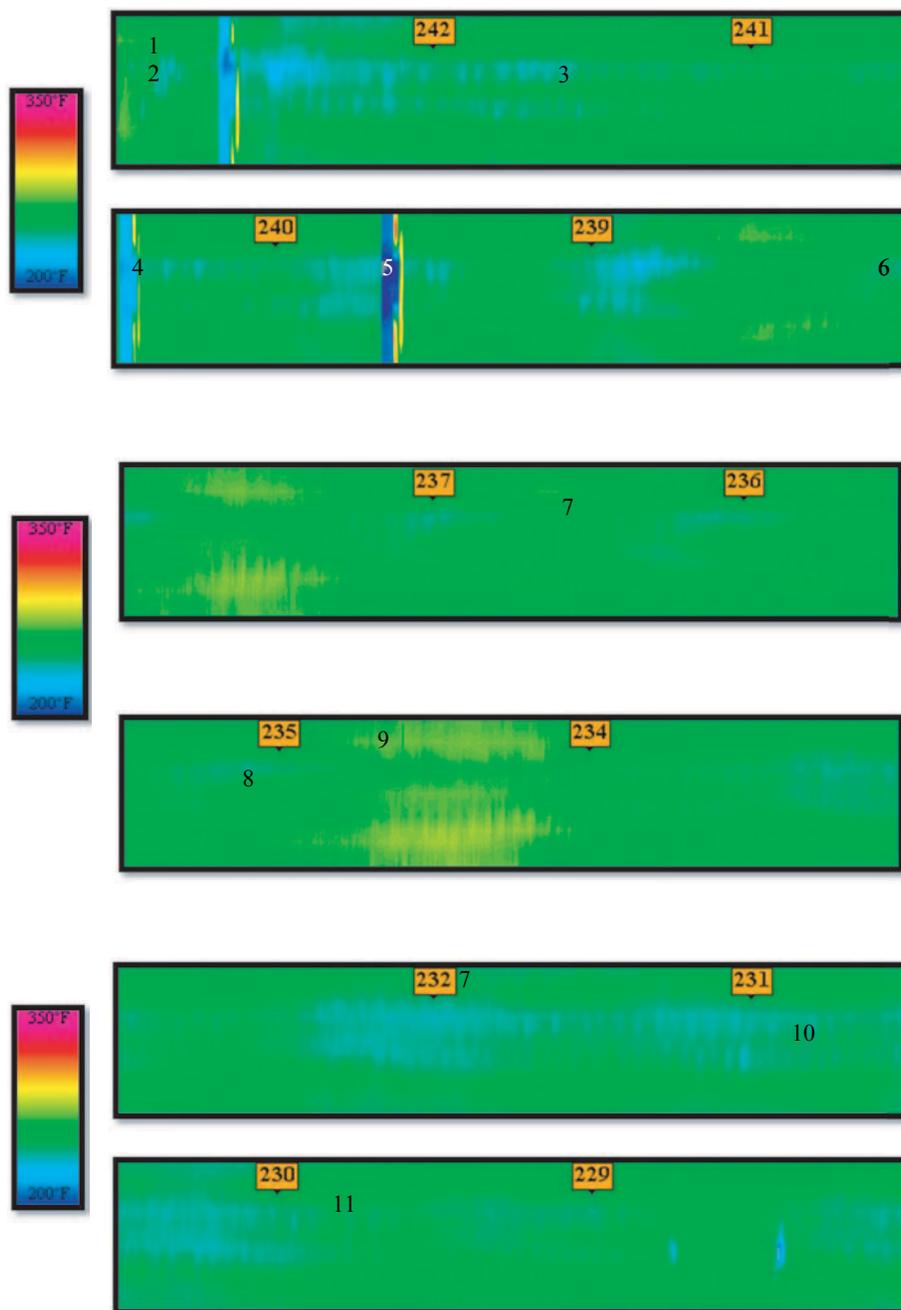
Figure 3.71. Thermal profile from Region 1 demonstration.

Table 3.21. Core Locations with IR-Measured Placement Temperature from Region 1

Core	1	2	3	4	5	6	7	8	9	10	11
IR Temperature (°F)	237	263	232	217	196	244	269	242	267	243	249
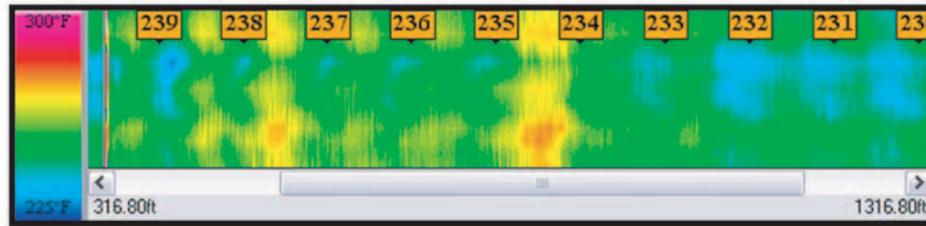
Figure 3.72. Patterns Observed in Region 1 Thermal Profile.

Mean: 254 °F
Median: 254 °F
σ: 7.54 °F
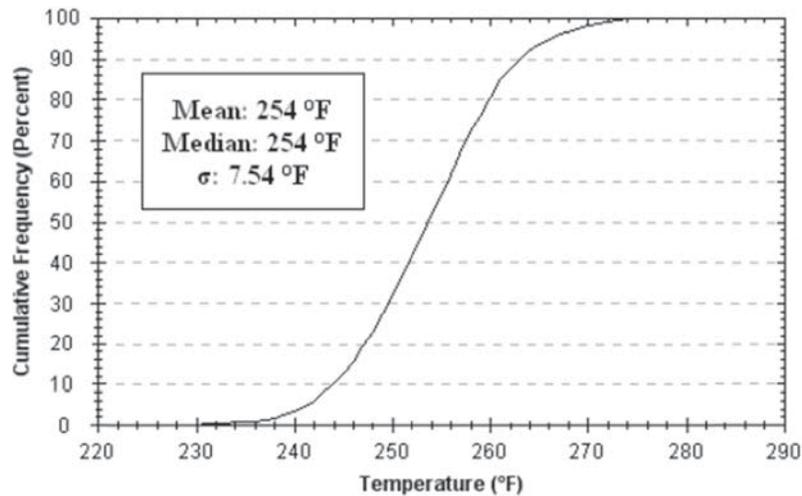
Figure 3.73. Distribution of placement temperatures at Region 1 demonstration.

joint beginning the pull, which would not be representative of the normal placement operation. Figure 3.76 shows the statistically significant relationship observed between the measured density and temperature differentials.

For this mix design, the Maine DOT specification requires a target density of 95.0%, with lower and upper specification limits of 92.5% and 97.5%, respectively. Based on the data in Figures 3.75 and 3.76, a temperature differential of 80°F would be required before the mixture density would deviate from the target beyond the specification limits.

Figure 3.74. GPR data collection for Region 1 demonstration.

Significance of GPR Data

Low surface dielectric values typically indicate higher air voids in the compacted asphalt mixture. On this project, as illustrated by Figure 3.77, both GPR systems correlated well with the laboratory core densities. Using the respective calibration equations, each of the GPR measurements was converted to an air void content measurement. This process resulted in thousands of spot measurements over the test area and served to generate the statistical distribution of air voids, as Figure 3.78 shows. The data show that even though the actual measured dielectric values differed slightly between the two systems, after calibration to the project's field cores, the results nearly match. Both systems estimate approximately 95% of the demonstration mat area qualifies for pay bonus with air void contents between 2.5% and 7.5%.

Because the geospatial position of each radar measurement was also known, the data could serve to generate a contour plot of the expected air voids over the mat area. Figures 3.79 and 3.80 present these plots for the I-295 project from the 1-GHz and 2.2-GHz radar systems, respectively.

Conclusions from Test Site

At the demonstration site in AASHTO Region 1, the infrared NDT operated well and succeeded in covering nearly 100% of

Table 3.22. GPR-Measured Core Dielectric Values from I-295

Core	1	2	3	4	5	6	7	8	9	10	11
GPR ε (1 GHz)	4.0	4.4	4.5	4.4	4.2	4.7	4.6	4.5	4.6	4.7	4.5
GPR ε (2.2 GHz)	4.53	4.50	4.82	4.87	4.91	5.01	4.93	4.80	4.80	5.04	4.86

Table 3.23. NDT Data with Core Results from Region 1 Demonstration

Core	1	2	3	4	5	6	7	8	9	10	11
IR Temp (°F)	237	263	232	217	196	244	269	242	267	243	249
Dielectric from 1 GHz	4.0	4.4	4.5	4.4	4.2	4.7	4.6	4.5	4.6	4.7	4.5
Dielectric from 2.2 GHz	4.5	4.5	4.8	4.9	4.9	5.0	4.9	4.8	4.8	5.0	4.9
Nuclear Density (lb/ft³)	134.1	139.1	142.6	142.5	142.8	144.6	143.9	142.6	145.4	145.3	142.9
Core Voids (%)	12.88	9.80	7.14	7.37	7.61	5.41	5.93	7.42	5.13	5.94	6.60
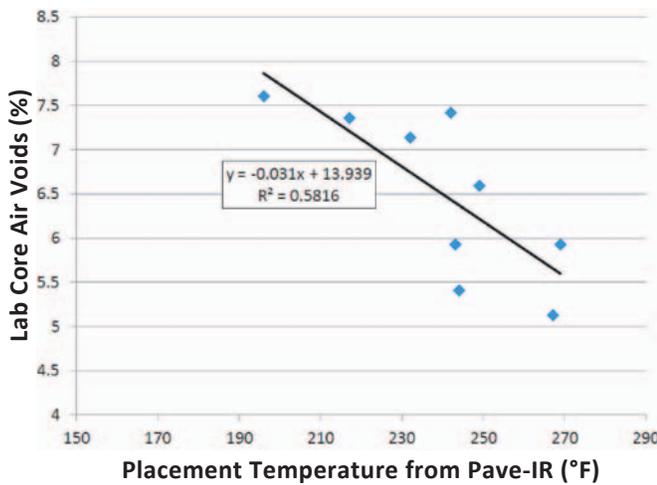
Figure 3.75. Air voids versus placement temperature from Region 1 data.
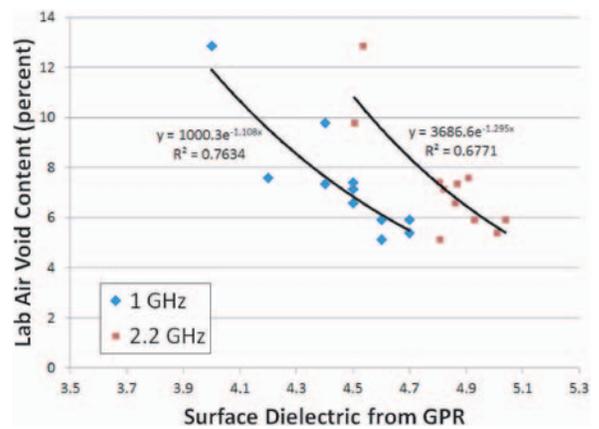
Figure 3.77. Calibrating GPR to predict in-place air voids for Region 1 demonstration.
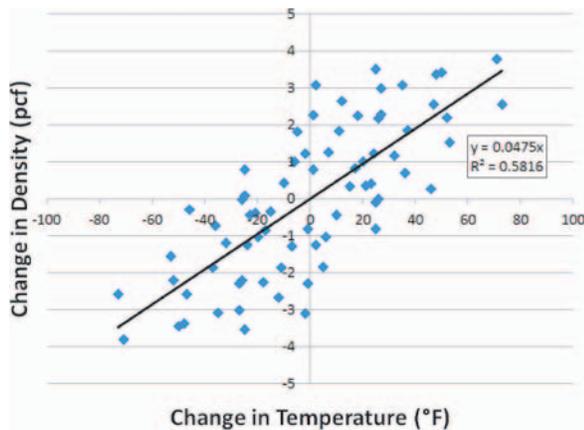
pcf = pounds per cubic foot

Figure 3.76. Density differentials versus temperature differentials from Region 1 demonstration.
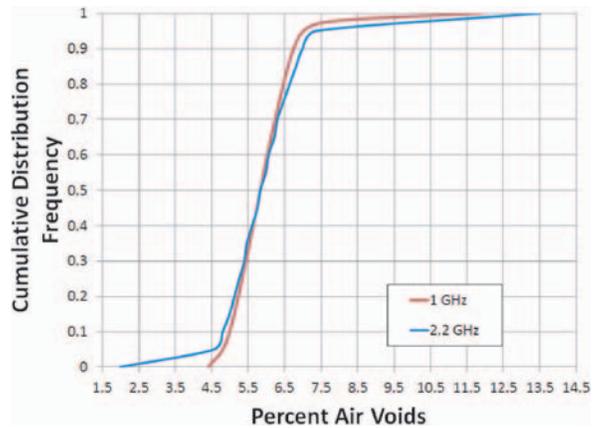

Figure 3.78. Expected air void distribution on Region 1 project.
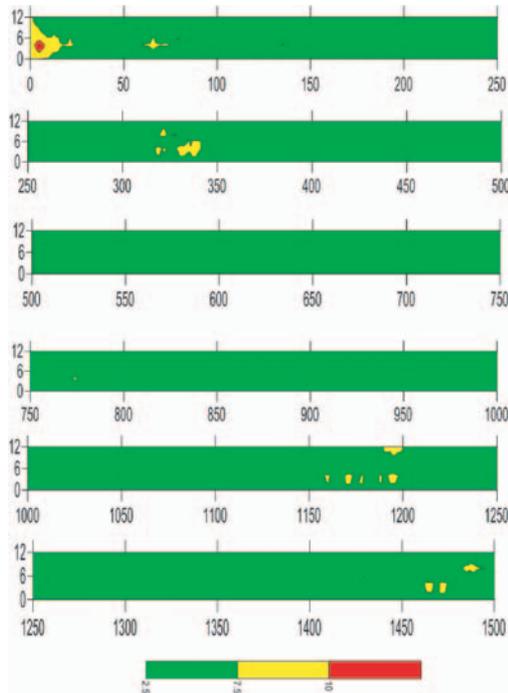
Figure 3.79. Geospatial distribution of air voids on Region 1 project from 1-GHz radar.


Figure 3.80. Geospatial distribution of air voids on Region 1 project from 2.2-GHz radar.

the main-lane area. The data showed a statistical correlation between the placement temperature data and the mix density. Although the thermal survey cannot capture the effects of rolling delays or other issues that may occur after placement, the GPR survey occurs after all finish rolling to serve as a final quality check. At this demonstration site, the GPR correlated well with in-place density and succeeded at providing a view of nearly 100% of the constructed area. After calibration to the project's cores, results from the 1-GHz and 2.2-GHz radar systems nearly matched. This observation is important because the 1-GHz system can no longer be obtained commercially in the United States. The similarity of results between the two radar systems shows the 2.2-GHz system, which is commercially available, should be a viable solution to perform uniformity evaluations on new asphalt mixture construction.

Both thermal and radar data suggested uniform construction with substantial compliance to the specifications. With the thermal data, if the two anomalies from paver stops are ignored, the largest temperature differential represented by the focused coring program is 37°F. With the radar data, a full-coverage assessment of the demonstration area indicates approximately 95% of the main-lane mat area contains air voids within the bonus region.

References

1. *Temperature Differentials and the Related Density Differentials in Asphalt Concrete Pavement Construction.* Washington State Department of Transportation, Olympia, Wash., 2001.
2. Scullion, T., and Y. Chen. *Using Ground-Penetrating Radar for Real-Time Quality Control Measurements on New HMA Surfaces.* Report 1702-5. Texas A&M Transportation Institute, College Station, Tex., 1999.
3. Read, S. *Construction Related Temperature Differential Damage in Asphalt Concrete Pavements.* University of Washington, Seattle, Wash., 1996.
4. Stroup-Gardiner, M., and E. R. Brown. *NCHRP Report 441: Segregation in Hot Mix Asphalt Pavements.* TRB, National Research Council, Washington, D.C., 2000.
5. Willoughby, K., S. Read, J. P. Mahoney, S. T. Muench, L. M. Pierce, T. R. Thompson, J. S. Uhlmeyer, R. Moore, and K. W. Anderson. *Construction Related Asphalt Concrete Pavement Temperature Differentials and the Corresponding Density Differentials.* Report WA-RD 476.1. Washington Department of Transportation, Seattle, Wash., July 2001.
6. Sebesta, S., and T. Scullion. *Using Infrared Imaging and Ground-Penetrating Radar to Detect Segregation in Hot-Mix Overlays.* Report 4126-1. Texas A&M Transportation Institute, College Station, Tex., 2002.
7. Ulmgren, N. 2000. Temperature Scanner—An Instrument to Achieve a Homogenous Asphalt Pavement. *Proceedings of Second Eurasphalt and Eurobitume Congress,* Barcelona, Spain, 2000, pp. 668–673.
8. Sebesta, S., and T. Scullion. Application of Infrared Imaging and Ground-Penetrating Radar to Detect Segregation in Hot Mix Asphalt Overlays. In *Transportation Research Record: Journal of the*

Transportation Research Board, No. 1861, TRB, National Research Council, Washington, D.C., 2003, pp. 37–43.

9. Sebesta, S., T. Scullion, W. Liu, and G. Harrison. *Pilot Implementation of PAVE-IR for Detecting Segregation in Hot Mix Asphalt Construction.* Implementation Report 5-4577-01-1. Texas A&M Transportation Institute, College Station, Tex., 2006.

10. Miller, S. R., A. G. Doree, H. L. ter Huerne, and B. W. Sluer. Paving the Way Forward: A Case Study in Innovation and Process Control. Presented at Fourth Annual Eurasphalt and Eurobitume Congress, Copenhagen, Denmark, May 21–23, 2008.

11. Sebesta, S., and T. Scullion. Infrared Imaging and Ground-Penetrating Radar as QC/QA Tools for Hot Mix Paving in Texas. In *Asphalt Paving Technology 2007: Journal of the Association of Asphalt Paving Technologists,* Vol. 76, Association of Asphalt Paving Technologists, Lino Lakes, Minn., 2007, pp. 1–40.

12. Scullion, T., and Y. Chen. *Using Ground-Penetrating Radar for Real-Time Quality Control Measurements on New HMA Surfaces.* Research Report 1702-5. Texas A&M Transportation Institute, College Station, Tex., 1999.

13. Ulriksen, C. P. F. Application of Impulse Radar to Civil Engineering. PhD Thesis. Lund University of Technology, Lund, Sweden, 1982.

14. Johansson, H. G. Användning av Georadar I Olika Vägverksprojekt. Vägverket, Serviceavdelning Väg och Brokonstruktion. Sektionen för geoteknik, Publ. 1987:59, Sweden, 1987.

15. Carlsten, P. P. *Geotechnical Properties and Up-to-Date Methods of Design and Construction.* Varia 215. Statens geotekniska institut, Linköping, Sweden, 1988.

16. Berg, F. *Ikke Destruktiv Måling af Lagstykkelser I Vejbefastelser.* Vejdirektoratet, Statens Vejlaboratorium, Notat 157, Denmark, 1984.

17. Saarenketo, T. Using Ground Penetrating Radar and Dielectric Probe Measurements in Pavement Density Quality Control. In *Transportation Research Record: Journal of the Transportation Research Board,* No. 1997, TRB, National Research Council, Washington, D.C., 1997, pp. 34–41.

18. Saarenketo, T. Ground Penetrating Radar Applications in Road Design and Construction in Finnish Lapland. *Geological Survey of Finland,* Special Paper 15, 1992, pp. 161–167.

19. Saarenketo, T., and P. Maijala. Applications of Geophysical Methods to Sand, Gravel and Hard Rock Aggregate Prospecting in Northern Finland. In *Aggregates—Raw Materials' Giant, Report on the Second International Aggregates Symposium* (G. W. Luttig, ed.), Erlangen, Germany, 1994, pp. 109–123.

20. Saarenketo, T., and T. Scullion. Ground Penetrating Radar Applications on Roads and Highways. Research Report 1923-2F. Texas A&M Transportation Institute, College Station, Tex., 1994.

21. Scullion, T., and T. Saarenketo. Implementation of Ground Penetrating Radar Technology in Asphalt Pavement Testing. Presented at Ninth International Conference on Asphalt Pavements, Copenhagen, Denmark, August 17–22, 2002.

22. Hobbs, C. P., J. A. G. Temple, and M. J. Hillier. Radar Inspection of Civil Engineering Structures. In *Proceedings of Conference on Non-destructive Testing in Civil Engineering* (J. Bungey, ed.), Liverpool, U.K., April 14–16, 1993, pp. 79–96.

23. Millard, S. G., J. H. Bungey, and M. R. Shaw. The Assessment of Concrete Quality Using Pulsed Radar. In *Proceeding of the Non-destructive Testing in Civil Engineering* (J. Bungey, ed.), University of Liverpool, Liverpool, U.K., Vol. 1, April 14–16, 1993, pp. 161–186.

24. Ballard, G. Under the Skin. *World Highways/Routes du Monde,* January/February 1992, pp. 37–39.

25. Ballard, G. Non Destructive Assessment of Pavement Design and New Build Quality. In *Proceedings of Conference on Non-destructive Testing in Civil Engineering* (J. Bungey, ed.), University of Liverpool, Liverpool, U.K., April 14–16, 1993, pp. 391–404.

26. Daniels, D. J. *Surface Penetrating Radar.* Institution of Electrical Engineers, London, 1996.

27. Hopman, V., and E. Beuving. Repeatability, Reproducibility and Accuracy of GPR Measurements. In *Proceedings of the Sixth International Conference on the Bearing Capacity of Roads, Railways and Airfields,* Lisbon, Portugal, June 24–26, Taylor & Francis, New York, 2002, pp. 637–645.

28. Saarenketo, T. Electrical Properties of Road Materials and Subgrade Soils and the Use of Ground Penetrating Radar in Traffic Infrastructure Surveys. *Acta Universitas Ouluensis,* Vol. A471, 2006.

29. Roimela, P. *Ground Penetrating Radar Surveys in Pavement Quality Control 1996–1997.* Tielaitoksen selvityksiä 4/1998. Rovaniemi, Finland (English abstract).

30. Roimela, P. *The Use of Pavement Radar in Quality Control of Bituminous Pavements.* Tielaitos, Konsultointi, Tielaitoksen selvityksiä 6/1999. Rovaniemi, Finland (English abstract).

31. Saarenketo, T., and P. Roimela. Ground Penetrating Radar Technique in Asphalt Pavement Density Quality Control. In *Proceedings of the Seventh International Conference on Ground Penetrating Radar,* May 27–30, University of Kansas, Lawrence, Kans., Vol. 2, 1998, pp. 461–466.

32. Scullion, T., and T. Saarenketo. Applications of Ground Penetrating Radar Technology for Network and Project Level Pavement Management Survey Systems. Presented at Fourth International Conference on Managing Pavements, Durban, South Africa, May 17–21, 1998.

33. Tiehallinto. Rakenteen parantamissuunnittelua edeltävät maatutkatutkimukset ja tulosten esitystapa—menetelmäkuvaus 09/2004. Tiehallinto, Helsinki (in Finnish).

34. Heikkilä, R., M. Jaakkola, T. Saarenketo, and F. Malaguti. Modelling Information Flows for Automated Road Rehabilitation Process. In *21st International Symposium on Automation and Robotics in Construction,* Jeju, Korea, September 21–25, 2004, pp. 85–93.

35. Scullion, T., C.-L. Lau, and T. Saarenketo. Performance Specifications of Ground Penetrating Radar. In *Proceedings of the Sixth International Conference on Ground Penetrating Radar,* Tohoku University, Sendai, Japan, September 30–October 3, 1996, pp. 341–346.

36. Saarenketo, T., and P. Kantia. Päällysteen Laadunvalvontamittaukset Maatutkalla—Testimittaukset 2005. Roadscanners Oy:n raportti Tiehallinnolle (in Finnish).

37. Pälli, A., S. Aho, and E. Pesonen. Ground Penetrating Radar as a Quality Assurance Method for Paved and Gravel Roads in Finland. In *Proceedings of the Third International Workshop on Advanced Ground Penetrating Radar* (S. Lambot and A. G. Gorriti, eds.), Delft, Netherlands, IEEE, New York, 2005, pp. 93–98.

CHAPTER 4

Conclusions and Suggested Research

Conclusions

This project demonstrated two nondestructive techniques for detecting defect areas in new HMA construction. Both technologies—IR imaging and GPR—test essentially 100% of the new surface, providing more inspection coverage than existing localized quality control methods.

The IR system produces a color-coded map showing placement temperatures for the entire mat area; the system also records and reports the locations of paver stops and their duration. The use of GPS technology also means that potential defect areas can be accurately located for follow-up validation testing. The system provides the color-coded temperature maps in real time to paving contractors, identifying potential construction problems so that corrective actions can be taken in the field. The IR profiling technology demonstrated in this project is ready for widespread implementation. The results presented in this project include the following highlights.

- The IR technology developed and demonstrated in this project is now commercially available through MOBA Corporation. This system worked very well to quantify possible problem areas. Figures 3.48 and 3.58 clearly show the relationship between placement temperature and final air voids. The lower the placement temperature, the higher the final air voids.
- A critical finding was that the final air voids obtained were also a function of other factors such as the rolling patterns and mix workability issues, including the amount and type of binder used. Regardless, this study found that cold placement temperatures resulted in higher air voids. Determining if these thermally segregated locations are out of density specifications will require additional testing.
- The use of warm-mix foaming technologies (at least with the two projects tested in this study) produced some interesting results. On one project (higher binder content and low RAP content), the WMA compacted well even at placement temperatures less than 200°F, whereas on another

WMA with higher RAP content, very high air voids (almost 15%) were found at similar placement temperatures.

- The severity of the thermal segregation problem was apparent to the research team on the I-295 project tested in AASHTO Region 1 in Maine. The project entailed a mill and overlay process. Figure 3.69 showed that the old HMA on this highway had very clear thermal segregation raveling and pothole failures at approximately 150-ft intervals, resulting in a poor ride. Between these failed locations, the HMA layer was in good condition. The new overlay was being placed primarily because of cyclical thermal segregation problems in the old mat. Testing of the new mat with IR imaging and GPR found it to be free of these thermal segregation defects, with very uniform in-place densities.
- Figures 3.63 and 3.76 clearly show that the computed surface dielectric values from GPR correlate well with the air voids measured on cores taken from the pavement. This means that GPR data collected at very short test intervals (possibly every foot) can readily be converted into surface air voids. GPR has the advantage over IR imaging in that it is directly correlated with the parameter of main interest to pavement engineers (mat density).
- The GPR hardware demonstrated in this project is commercially available, but developing a complete package including software will need some additional cooperative efforts. Appendix E includes a description of the recommended approach needed to convert GPR data into mat air void data. The steps required are highlighted in Section 5. These steps include the need for field coring at selected locations, laboratory testing, and determining regression equations relating field density to GPR dielectric. No standard relationship exists between dielectrics and air voids; this relationship is mix specific. The dielectric value is a function of aggregate type and binder content. However, from this project, it is clear that any mix increase in air voids will result in reductions in dielectrics. Project-specific calibrations are required for each job.

Recommendations on Specifications

Infrared Technology

Based on the findings of this project, thermal segregation detection using an IR bar should be considered for implementation into agency specifications for uniformity assessment. The system demonstrated in this report provides the agency with color profile maps of placement temperatures and the number and duration of paver stops. The additional use of GPS technology ensures that these potential problem areas can be accurately located for more follow-up testing. The following activities should be initiated to aid in expediting implementation of IR systems:

- Conduct additional demonstration projects including the full-scale validation coring as described in this report. At least six additional DOTs (including one from a Canadian province) contacted the research team during this study and asked to be included in the demonstration testing. The project, however, restricted demonstrations to four states. This level of interest clearly shows that thermal segregation is a recognized major concern for many, if not all, DOTs.
- Conduct webinars and other presentations at national conferences to inform potential users.
- Arrange for visits to specific states to meet with key decision makers. These key decision makers are typically state material engineers, paving contractor association representatives, IR equipment suppliers, and selected contractors. The purpose of these visits should be to explain this technology in detail and to provide information on implementation options. The specific goals of these visits should be to identify reporting requirements that will meet the DOT's objectives of constructing more uniform, longer-lasting overlays; developing draft specifications; establishing pilot implementation projects where the new technology can be used in parallel with existing processes; and identifying how the existing system can be customized to meet agencies' reporting needs.

Several states are already considering or have drafted specifications on how to incorporate IR technology into their specifications. The state that has made the most progress is Texas, and Appendix D presents its thermal profiling test procedure. No new penalties or bonuses are associated with the construction specification other than the existing temperature requirements (where temperature differentials exceeding 50°F can result in suspension of paving). For every station in the job, the IR test system categorizes the degree of thermal segregation into none, moderate, or severe. This system was targeted as a help to the contracting industry with the benefit of opening the paving window if the IR bar system is used and the mat is shown to be free of thermal segregation. The comments from contractors have been encouraging in that the system allows them to monitor their operations and determine if changes are required. The effect of paver stops on mat quality has clearly been demonstrated with the applications to date in Texas and Minnesota.

The TxDOT approach can be related to other DOTs, but they may have substantially different needs and approaches. Four different possible approaches include using the thermal profile

- For passive inspection, in which the thermal profile largely serves as information to the contractor and agency to promote uniformity;
- To trigger other action when thermal segregation exists, for example, locations with thermal segregation receive spot testing with a density profile to determine if substantial density differentials exist;
- To measure compliance with placement temperature tolerances, whereby the thermal profile simply measures if the placement temperatures stay within the range required by the agencies' specifications; and
- For focused coring, in which, instead of random coring, the engineer selects a core location for placement pay factors based on the thermal profile.

Ground-Penetrating Radar

From the findings in this research project, GPR has an advantage over IR imaging, because it is used on the final mat after compaction. If problems are found in the GPR analysis, these will be low-density areas where future failures can be anticipated. However, additional development is needed to streamline the steps from data collection to project uniformity evaluation before successful implementation can occur. This streamlining process will require partnering with industry and working with their radar systems to integrate the data collection and processing functions into a full-featured system tailored to uniformity assessment of new asphalt pavement layers.

Appendix C presents the Finnish specification (PANK 4122) for using GPR to compute asphalt layer densities. Appendix E provides a recommended approach for collecting and processing GPR for computing surface layer densities. Section 5 illustrates the steps needed to build a regression equation so that mat air voids can be computed. No DOT in the United States has pilot tested this approach for 100% coverage density measurements. Based on the results presented in this report, the GPR-based system provides many advantages over existing procedures, and with some cooperative efforts a commercially available system could be readily developed. The alternative approach for a DOT would be to pilot test this approach with GPR service providers.

54

Suggested Research

The findings from work conducted indicate the following topics exist for further exploration:

- Work is needed to identify if the IR and GPR technologies for uniformity assessment should be restricted to only certain mix types or certain placement operations. More work is needed to determine if these approaches are possible with stone mastic asphalt and permeable friction courses.

- Guidelines for minimum and maximum overlay thicknesses with each GPR system should be developed. The depth of influence of both the 1-GHz and 2.2-GHz systems used in this study was not clearly defined. It is suspected that if the lift thickness is less than 1 in., then the influence of the lower-layer mat affects the surface dielectric readings.
- Work is needed to streamline and make commercially available the GPR data-processing procedures.

APPENDIX A

Swedish National Road Administration Method for Defining Temperature Variation During Paving of Hot-Mix Asphalt

Summary

This method description is for defining temperature variation during the paving of hot-mix asphalt (HMA). Binders are specified based on low-temperature properties. When colder surfaces are meant to be located, an evaluation can be made of the risk for quality deficiencies in the pavement surface.

Conception

pavement pass. Width of the HMA after it has been laid by the paver with one pass. The edge of the pass is the same as the pavement surface edge after the pass.

line scanner. Digital equipment, such as an optical road laser, which gives information row by row.

average value. The average of all measurement values greater than 90°C inside the analysis area where the paver has been moving in the last 30 min.

thermal camera. Thermographic instrument made with the help of the line scanner technique to measure temperature via infrared radiation.

angle of approach. Perpendicular angle between the pavement surface and the central line of camera at measurement.

measuring width. Lane width from one edge of the pavement to the other after the pavement has been laid.

individual value. The measured value $x(i)$, which is registered under 2 s. The measured value is the average value of temperature from several target surfaces.

GPS. Global Positioning System, American positioning system that makes use of satellites.

target surface. Surface that is instantaneously read by a line scanner and gives measured values.

reference point. The center point of the target surface.

risk zone. Pavement surface that includes single points that are lower than 90% of the running average for the pass (risk

for insufficient compaction). Binders are specified based on low-temperature properties. Surfaces that are made colder than optimum temperature are also risk zones.

risk area. Entire surface area of risk zones for the analyzed pavement section.

risk part. Entire risk area for evaluated area in relation to total pavement surface, expressed in %.

RT90. Height coordinate system.

standard focus. Definition of objective with magnification 33:1 on the distance of 1.52 m.

scan. Width of measurement divided into 256 measurements points. These points (e.g., surfaces) seen along the object form 256 longitudinal scans.

Equipment

Temperature Measurements with the Help of Line Scanners (Thermal Camera)

Comment from Svante Johansson, SNRA: Measurement shall be done with infrared line scanner pointing at the pavement surface in an area 1 to 2 m behind the paver screed. The angle of approach shall be maximum 45 degrees.

The spot area shall be a maximum of 20 cm. The enlargement degree is allowed to vary between 33:1 and 100:1. The resolution shall be a minimum of 256 measurement values per line distributed over the measurement area (90 degrees of a rotation across the road direction). The measurement points are distributed over an angle of 90 degrees. Every measurement value represents an angle of 90/256 degrees. The thermal camera shall be fixed to the paver with a distance between the scanner and the aim point of 3 to 4.5 m.

Storing of data shall be done once every second and shall consist of the average value per measurement point for 256 passes. Measurements shall be done continuously during the ride.

Other Equipment

Storage shall be done either in the camera or in another storage device so that it is possible to present the data afterward.

Calibration, Control

Calibration is performed normally with the retailer's equipment. A rough control is done by comparing with point temperature gauges with accuracy of ±1°C. Gauge depth shall be between 10 and 20 mm. The control is performed immediately after the thermal camera has registered the value. It is a rough control because the temperature can fall up to 20°C/min after the HMA has been placed. The minimum number of measurements is one point from the first HMA load and one point from the last in the paving section, at least two times per day. Locations for these measurements shall be registered.

Measurement

The thermal camera shall be mounted to the paver. It shall read and save pavement temperatures successively as the paver moves forward.

Measurement data shall be registered at the same time with actual length measurements so that graphic printouts can be made afterward. Length measurements can be made with the help of a measurement wheel.

A minimum of two times per day, length data should be registered with GPS or some other method that is just as accurate. This should also be done with the start and end points of the section where the work is done. Positioning should be done in RT90 2.5 gon V 0:-15 national grid.

Limits

The database shall be checked during evaluation for unknown objects. These unknown objects are usually people that pass by the measurement area when the infrared radiation is reduced. Data from unknown objects that goes below 90°C shall be deleted either manually or automatically. It shall be clear that this measurement data is not relevant. Measurement values under 90°C from the HMA (i.e., from other objects such as machinery or people that are in the measurement area) are deleted.

Report of Examination Results

Reporting is performed from the entire width, but 30 cm from the edges of the pavement are left out of the evaluation area.

Measurement results shall be presented as a profile, where the x axis is the length measurement. In addition, a graph shall be presented from the measurements in two dimensions, where different colors represent different temperatures. The report should also include the project's location and results from the point temperature gauges. The report shall include risk zones (graphically), risk areas, and risk part.

The results table shall contain the following information:

- Measurement company's contact person;
- Measurement operator;
- Contractor's contact person;
- Object type;
- Road number;
- Pavement type;
- Pavement thickness;
- Data from investigation moment, time, weather, and so forth;
- Total length of section; and
- Measurement length (length of measurement line).

GPR Hardware Specifications for Systems Used in TxDOT

These specifications are based largely on the GPR reflection from a large metal plate. The amplitude of reflection is measured in volts typically from the maximum positive peak to the preceding negative.

Performance Specifications

1. Noise-to-signal ratio test: The antenna will be positioned at its recommended operating height above a minimum 16 square foot (4 ft × 4 ft) metal plate. The radar unit shall be turned on and allowed to operate for a 15-min warm-up period. After warm-up, the unit shall be operated at maximum pulse rate, and 50 radar waveform pulses shall be recorded. The recorded waveforms shall then be evaluated for noise-to-signal ratio. *No averaging or signal cleanup such as sky wave removal (and reflection subtraction) shall be allowed.* The noise-to-signal ratio is described by the following equation:

$$\frac{\text{Noise Level}\left(A_n\right)}{\text{Signal Level}\left(A_{mp}\right)} \le 0.05\,(5\%)$$

The signal level (A_{mp}) is defined as the average metal plate reflection in volts as measured from the peak to the preceding minimum. The noise level (A_n) is defined as the average maximum amplitude in volts occurring between 2 and 10 ns after the surface echo. The noise level is measured from any positive peak to either the preceding or the trailing negative, whichever is greater. The noise-to-signal ratio shall be less than or equal to 0.05 (5%).

2. Signal stability test: The same test configuration shall be used as described in the noise-to-signal ratio test. Fifty traces shall be recorded at the minimum data rate of 25 traces/s. The signal stability shall be evaluated using the following equation:

$$\frac{A_{max} - A_{min}}{A_{AVG}} \le 0.01\,(1\%)$$

where

A_{max} = maximum amplitude for all 50 traces,
A_{min} = minimum amplitude for all 50 traces, and
A_{AVG} = average trace amplitude of all 50 traces.

The signal stability test results for the GPR shall be less than or equal to 1%.

3. Long-term signal stability: The same test configuration shall be used as described in the noise-to-signal ratio test. The radar shall be switched on with no warm-up and allowed to operate for 2 h continuously. As a minimum, a single waveform shall be captured every 2 min, 60 in total. The amplitude of reflection shall be calculated and plotted against time. For the system to perform adequately the amplitude should remain constant after a short warm-up period. The stability criterion is as follows:

$$\frac{A_{any} - A_{20}}{A_{20}} \le 0.03\,(3\%)$$

where

A_{20} = amplitude measured at 20 min and
A_{any} = amplitude measured after 20 min.

4. Variations in time-calibration factor: The same test configuration shall be used as described in the noise-to-signal ratio test; 50 traces are collected and the height of the antenna is measured. The test is repeated at two other heights. Typically, heights of approximately 15, 20, and 25 in. are used. The time delay from the end reflection at the tip of the antenna to the metal plate reflection is measured for each trace, and their mean is time t_i (where the subscript represents height position at i). The difference between t_2 and t_1 represents the time to travel a fixed distance in air. For bistatic antennas the travel distance must be calculated based on the system geometry. The factor C_1 is calculated by dividing the distance by the time difference (inches per nanosecond). The factor C_2 represents

57

the same between heights 2 and 3. The variation in time-calibration factor is as shown below:

$$\frac{C_1 - C_2}{\text{Mean of } C_1 \text{ and } C_2} \leq 0.02\,(2\%)$$

The variation in time-calibration factor shall be less than or equal to 2%.

5. End reflection test: The same test configuration and results from the noise-to-signal ratio test shall be used. The amplitude of the end reflection directly preceding the metal plate reflection shall be measured. The size of the end reflection shall be

$$\frac{A_E}{A_{mp}} < 0.15\,(15\%)$$

where

A_E = amplitude of end reflection defined as any peak occurring from 1 to 5 ns before the metal plate reflection and

A_{mp} = mean of the amplitude of reflection from the metal plate.

The end reflection in the metal plate test shall be less than 15% of the amplitude of metal plate reflection.

6. Symmetry of metal plate reflection: The same test configuration as used in the signal-to-noise ratio test shall be used. Two different criteria have been established for symmetry, as described below:

6.1 The first criterion is the time from the maximum negative peak following the surface reflection to the zero crossing point. The required specification is

$$t_f \leq 0.7 \text{ ns}$$

6.2 The second criterion is based on the symmetry of the "legs" of the metal plate reflection. The amplitude is measured from the positive peak to both the preceding and trailing negative. The required specification is

$$A_{min}/A_{max} > 0.95\,(95\%)$$

where A_{min} and A_{max} are the minimum and maximum metal plate reflections measured using the preceding or trailing negatives. The ratio should be at least 95%.

7. Concrete penetration test: The antenna shall be placed at its recommended operating height above a 6-in.-thick concrete block. The concrete block shall be nonreinforced, a minimum age of 28 days, and a minimum 3,000 psi compressive strength. The block shall be 3 ft × 3 ft or greater to ensure that all the GPR energy enters the concrete. The concrete block shall be placed on top of a metal plate. Two hundred traces shall be recorded. The reflection amplitude from the top and bottom of the concrete block shall be measured. The concrete penetration test is defined by the following equation:

$$\frac{A_{bottom}}{A_{top}} \geq 0.25\,(25\%)$$

where

A_{top} = mean of the measured return amplitude from the top of the concrete slab and

A_{bottom} = mean of the measured return amplitude from the metal plate.

The concrete penetration test results for the GPR shall be greater than or equal to 25%.

APPENDIX C

Finnish PANK Method for Air Void Content of Asphalt Pavement with GPR

PANK 4122: Air void content of asphalt pavement, ground-penetrating radar method. Accepted first 10/26/1999 and revised 5/9/2008

1. Purpose of the Method

Ground-penetrating radar (GPR) technology is used to measure the dielectric value of the asphalt pavement, which is then used to calculate the air void content of the pavement.

2. Scope of Method Application

The method is suitable for measurement of air void content of new bituminous pavements regardless of the quality of the base course.

This method description describes the measurement protocols that have been used since 2004 and that were updated in 2008.

3. References

Tielaitoksen selvityksiä 4/1998, Päällystetutkimukset 1996–1997, TIEL 3200499 (in Finnish).

Tielaitoksen selvityksiä 6/1999, Päällystetutkatutka tiiviyden laadunvalvonnassa, TIEL 3200552 (in Finnish).

PANK 4114, Asfalttipäällysteen tyhjätila ja muut tilavuussuhteet (in Finnish).

Scullion, T., C. L. Lau, and T. Saarenketo. Performance Specifications of Ground Penetrating Radar. *Proceedings of Sixth International Conference on Ground-Penetrating Radar.* Tohoku University, Sendai, Japan, 1996, pp. 341–346.

4. Definitions

The term "air void content" is used to represent the ratio between pore volume and the total volume of pavement and is presented as percentage.

The term dielectric value or "relative dielectric permittivity" refers to the capacity of a material to store, and then allow the passage of, electromagnetic energy when an electrical field is imposed upon it. It can also be described as a measure of the ability of a material within an electromagnetic field to become polarized, and therefore respond to, propagated electromagnetic waves. The dielectric value of a material is a function of volumetric proportions of its material components and the dielectric properties of these components.

5. Test Method

5.1. Theory

In the method, air void content measurement is based on the measurement of dielectric value of the pavement surface. Dielectric value is one of the electrical properties of the materials. The dielectric value of a pavement is a function of the dielectric values and volumetric proportions of its individual components. Compaction decreases the air void content in the pavement, which leads to a decrease in the volume of low-dielectric-value component, air, and an increase in the proportional content of bitumen and rock. Thus, compaction leads to an increase in the dielectric value of the pavement.

A "surface reflection method," which can only be done with air-coupled antennae GPR systems, is used to determine the dielectric value of the asphalt surface. The dielectric value of pavement is obtained based on calculations of reflection amplitudes from electrical interfaces, such as the air/pavement interface. The air-coupled antenna transmits electromagnetic pulses and their reflections from electrical interfaces are registered by a receiver antenna. When the EM pulses transmitted by the antenna meet an electrical interface, for example the pavement surface, a part of the energy is reflected and this reflection is registered by a receiver antenna. The GPR unit measures the respective peak-to-peak amplitude A1 for pavement surface reflection. Figure C.1 illustrates the operational principle of a bistatic horn antenna system: the transmitter
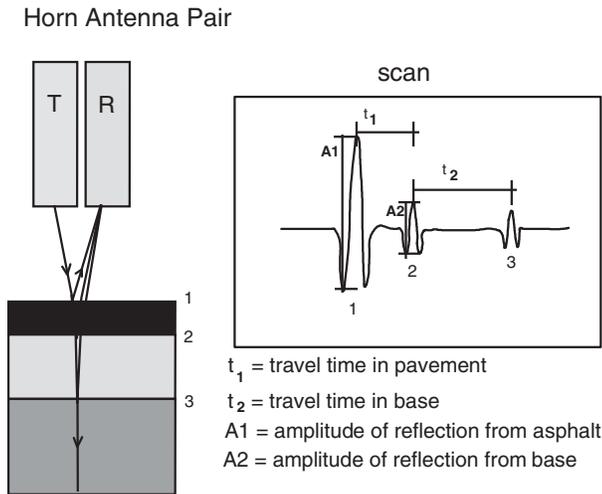
Horn Antenna Pair

Figure C.1. Operational principle of horn antenna.

antenna (T) and receiver antenna (R) and numbers 1, 2, and 3 represent layer interfaces in the pavement structure.

The relative dielectric value of the pavement can be calculated by using Equation C.1:

$$\varepsilon_a = \left(\frac{1 - A_a/A_m}{1 + A_a/A_m} \right)^2 \tag{C.1}$$

where

A_a = reflection amplitude from pavement surface and
A_m = reflection amplitude from a metal plate (complete reflection).

5.2. Required Equipment

The pavement GPR equipment includes

- A > 1.0 GHz horn antenna (or other air-coupled antenna) and antenna cable;
- Transmitter/receiver electronics (if not already built into the antenna);
- A central unit with display containing data storage system;
- A survey vehicle; and
- A computer (PC) for processing measurement data.

5.3. GPR System Specification and Calibration of the Equipment

The equipment used in surveys should pass annual antenna specification tests (Scullion et al., 1996). Equipment should be calibrated after each survey using air pulse and metal plate tests. Optional calibration can be done using a rubber plate.

5.4. Measurements

A minimum number of ten (10) measurements (scans) per meter are recorded. Measurement time (range) used is 20 ns. Maximum data-collection vehicle speed is defined according to the data-collection capability of the GPR system; generally it is greater than 60 km/h. One measurement covers an area of approximately 300 mm × 300 mm. Data collection is conducted as a continuous profile from the beginning to the end of the survey section. As a basic rule, one wheelpath is measured from each paved lane. When needed, the contractor and the client of the paving project can agree on the amount, length, and location of survey lines.

Limiting Factors

Measurements are not allowed during rain or when the pavement surface is wet. Likewise, measurements are not to be conducted when the pavement is frozen or when air temperature is below +1°C.

5.5. Calculation of Air Void Content

The calculation of air void values can be made using two separate methods:

A. When a new hot-mix asphalt (HMA) is paved at least 80 kg/m² over unbound or bound base course or over an old pavement, the calculation of the air voids content is based on the calculation of mean dielectric values. The method applies the results of laboratory tests conducted to define the function between the dielectric value and air void content (Roimela, 1998). The method includes, after GPR measurements and calculations of mean dielectric value have been done, taking one (1) calibration core sample from the pavement under survey (length at least 5 km) that represents well the mean dielectric value calculated after GPR data collection. In addition 2 + 2 representative samples are taken from other sections around mean dielectric value. The calibration coefficient calculated from the representative section can then be used on other paving sections in this contract if the asphalt plant, mixture, and aggregate are the same.

B. Air voids content of new REMIX and RC pavements is made using a "precise marking" method. In this method the survey vehicle is stopped during the data collection at the reference location and the point directly under the GPR antenna is marked on the pavement using paint. A marker is also added to the GPR data at the reference location and/ or the exact position along the survey line is documented in the survey memos. In that case the exact total length of the survey section also has to be documented just in case

the distance has to be scaled afterward. Drill core samples have to be taken at least once every survey line and/or on longer surveys one sample every 10 km has to be taken.

In both options air void content of the calibration cores is defined using laboratory methods approved by PANK. Using the air void content value obtained from the calibration samples, and their respective dielectric values, a calibration coefficient is determined for the calculation of air void contents of the pavement. The formula for calculation of air void content y is presented as Equation C.2:

$$y = 272.93e^{-1.3012k\varepsilon_x}, x \text{ between } 1 < x < n \tag{C.2}$$

where

k = calibration coefficient and
ε_x = measured dielectric value using GPR surface reflection method.

There is a more detailed description of the method in the publication "Päällystetutkatutkimukset 1996–1997" (Roimela, 1998).

6. Reporting the Survey Results

The results are presented in longitudinal diagrams or in table format if needed. Air void contents are presented in the longitudinal profiles and in addition the measured dielectric value and places for calibration drill cores and their results should be presented. Additionally, the results can be presented on a geographic information system map. This requires obtaining location information from the object that is consistent with the road register.

The survey report page must present, at the very least, the following information:

- Information on the measurement organization;
- Information on the final customer;

- Survey methods, GPR unit information, and software used in the calculations;
- Air voids content limits with proper references, such as
  - PANK Ry: Asphalt Standards 2000;
  - 0% to 5% for single samples;
  - 0% to 4% for mean values;
  - Mixture class with additional information, for instance why higher limits have been used compared to the standards;
  - Mixture type;
  - Project number;
  - Survey date;
  - General information on the project;
  - Project length (m);
  - Survey line length (used in calculation of sanctions);
  - Calculation section (if deviating from the measurement length); and
  - A table presenting the final calculation results: mean value, standard deviation, meter higher or lower than limits, percentage higher or lower than the limits and average dielectric value of the survey line. Separate calculations are made for each survey line and each project. The results of the whole project define if sanctions have to be applied.

If the ratio between dielectric value and air void content is exceptional, the report has to clearly present a reason for this. Figure C.2 provides an example of how to present results.

7. Measuring Accuracy

The measuring accuracy for air void content measurement using the GPR surface reflection technique is ±0.9%. This statistical analysis result has been achieved through comparison of core sample results and GPR measurements conducted as static shots over each individual measurement point ($R = 0.9223$).

GPR Ltd
Sportsmanstreet 7 - 9
00000 Mämmilä

Air Voids Content Report 2004

Customer   Road Administration / Tomi Tieto
                     Hallituskatu 21, 00000 Mämmilä

Project: Rova – Niemi   **Project nr:**   11-121
Road Nr: E4
Method: Voids Content Survey using GPR
Software: Road Doctor Pro v.2.2.

Air voids specs: PANK 2008   **Mixture type:** ABS
Road Class: Main road I   **Thickness:**   90 kg/m^2
Acceptance limits: 1, 5 - 5 % single value   **Date:**   9.6.2009
                       2 - 4 % mean value
Section length: 10 000   m   Section 1 start: 0   m
Survey length: 20 000   m   Section 1 end: 10 000   m
                                             Section 2 start: 0   m
                                             Section 2 end: 10 000   m

                                             Survey length   20 000   m

Reference samples: *Section 4/900 direction 1, 2, 2%, section 6 300 direction 2, 1, 9%*

Calibration coefficient: **0.6265**
Average air voids content used to calculate calibration coefficient   3.25
Average dielectric value equivalent to air voids content   6.97

Project info	Air voids content (%) Mean.	Std dev	Single value Under (%)	Single value Under (%)	Single value Over (%)	Single value Over (m)
Lane 11	2.93	0.65	4.48	13.13	3.93	314.40
Lane 12	2.33	0.29	15.06	1204.80	0.00	0.00
Lane 22	2.51	0.39	12.02	23.92	0.49	0.98
Lane 21	2.57	0.34	3.75	300.00	0.48	38.40
Total	**2.75**	0.50		1541.85		**352.80**

Additional info: _____

                          _____

                          _____

Company name, Date & Signature

Image courtesy of Roadscanners Oy.

Figure C.2. Example air void report from GPR survey.

A P P E N D I X   D

TxDOT Method TEX-244-F for Thermal Profile of Hot-Mix Asphalt

---

Test Procedure for

Thermal Profile of Hot-Mix Asphalt

Texas Department of Transportation

TxDOT Designation: Tex-244-F

Effective Date: May 2011

1.	SCOPE

1.1   Use this test method to obtain a thermal profile that identifies the presence of thermal segregation of an uncompacted mat of hot-mix asphalt. The thermal profile may be determined by using a handheld noncontact infrared thermometer, a thermal camera immediately behind the paver during uninterrupted paving operations, or a paver-mounted infrared bar (Pave-IR system).

1.2   The values given in parentheses (if provided) are not standard and may not be exact mathematical conversions. Use each system of units separately. Combining values from the two systems may result in nonconformance with the standard.

2.	APPARATUS

2.1   *Handheld Noncontact Infrared Thermometer, Thermal Imaging Camera, or Paver-Mounted Infrared Bar (Pave-IR System).*

2.1.1   Handheld noncontact infrared thermometer must be capable of

■   Measuring from 40°F to 475°F with an accuracy of ±2°F or ±1% of reading, whichever is greater;

■   Storing and recalling the maximum (and minimum temperature if available) from the most recent scan using a liquid-crystal display (LCD) viewing screen;

■   Measuring with a minimum 6:1 distance-to-spot ratio; and

■   Adjusting emissivity in increments of 0.01 or a fixed emissivity equal to or greater than 0.95.

63

64

2.1.2   Thermal imaging camera must be capable of

- Measuring from 40°F to 475°F with an accuracy of ±4°F or ±2% of reading, whichever is greater;

- Displaying the maximum temperature and minimum temperature using an LCD viewing screen with a minimum diagonal dimension of 3.5 in.;

- Storing a minimum of 50 images and capable of opening images while in operation;

- Measuring temperature with a minimum 6:1 distance-to-spot ratio; and

- Adjusting emissivity in increments of 0.01 or a fixed emissivity equal to or greater than 0.95.

2.1.3   Paver-mounted infrared bar (Pave-IR system) must be capable of

- Using a minimum of 10 infrared sensors spaced at most 13 in. apart, with each sensor located a maximum of 3 ft above the hot-mix asphalt pavement surface;

- Using infrared sensors measuring from 40°F to 475°F with an accuracy of ±2°F or ±1% of reading, whichever is greater;

- Measuring temperature with a minimum 6:1 distance-to-spot ratio;

- Profiling entire pavement width, excluding pavement edges;

- Measuring distance using a distance measuring instrument (DMI) and equipped with a Global Positioning System (GPS);

- Collecting, displaying, saving, and analyzing temperature readings while in operation, using the latest software available;

- Determining the low and high temperatures within each profile using the statistical 1 percentile and 98.5 percentile, respectively;

- Producing output files of pavement temperatures for each day's placement and daily summary output files in an approved test report that identifies locations of thermal segregation with a recording of the temperature at such locations;

- Providing software capable of developing and analyzing thermal profiles for the entire project; and

- Providing an operating system with at least one USB port to save test results to a portable USB memory device.

---

3.   REPORT FORMS

3.1   Tx244-4.xls, "Thermal Profile for Hot Mix Asphalt" (ftp://ftp.dot.state.tx.us/pub/txdot-info/cmd/sitemgr/tx244-4.xls).

---

4.   PROCEDURE

4.1   Operate the handheld noncontact infrared thermometer, thermal imaging camera, or paver-mounted infrared bar (Pave-IR system) in accordance with the manufacturer's recommendations.

4.2   Do not obtain thermal profiles in miscellaneous paving areas that are subject to handwork such as intersections, driveways, crossovers, turnouts, gores, tapers, and other similar areas.

4.3	Refer to Figures D.1 and D.2. Follow the requirements of Sections 4.3.1 to 4.3.6 while performing a thermal profile.

4.3.1   When using the handheld noncontact infrared thermometer or the thermal imaging camera, use spray paint or a permanent marker to mark the pavement edge at the beginning and ending location of each thermal profile.

Note 1—Refer to the summary output file for locations when using the Pave-IR system.

4.3.2   Record the beginning and ending station numbers of all thermal profiles.

Note 2—Instead of station numbers, use of GPS coordinates or other approved means of identifying the locations is acceptable.

4.3.3   Obtain all temperature measurements in units of degrees Fahrenheit.

4.3.4   Obtain all temperature measurements while the paver is moving.

4.3.5   Avoid taking temperature measurements within 2 ft of the edge of the uncompacted mat.

4.3.6   When performing a thermal profile, if the paver stops for more than 10 s, exclude the area 2 ft behind the screed and 8 ft in front of the screed (in the direction of travel) from the thermal profile.

4.3.7   Obtain a new maximum baseline temperature and minimum profile temperature for every thermal profile measured.

Note 3—Each thermal profile will be approximately 150 ft. This distance includes the 20 ft used to establish the maximum baseline temperature when profiling with a handheld thermometer or thermal imaging camera.

Note 4—Obtain the maximum baseline temperature when using the Pave-IR system by analyzing the temperature readings recorded throughout the entire 150-ft length.

4.4   Proceed to Section 4.5 when using a handheld noncontact infrared thermometer. Proceed to Section 4.6 when using a thermal imaging camera. Proceed to Section 4.7 when using a Pave-IR system.

4.5   *Using the Handheld Noncontact Infrared Thermometer:*

4.5.1   While the paver is moving, walk close to the edge of the uncompacted mat at approximately the same speed as the paver in order to maintain a distance of approximately 5 ft behind the paver to obtain temperature measurements.

4.5.2   Alternatively, stand on the paver screed to obtain temperature measurements.

Note 5—Follow all safety precautions and guidelines when standing on the paver screed.

4.5.3   Measure the temperature of the uncompacted mat by pointing the noncontact infrared thermometer, squeezing (and holding) the trigger, and scanning back and forth across the mat, transverse to the direction of paving.

Note 6—Do not attempt to obtain temperature measurements in areas of the mat that are more than 20 ft away from the handheld noncontact infrared thermometer or are outside the range recommended by the manufacturer.

4.5.4	Follow the requirements of Section 4.3 and determine the maximum temperature of the uncompacted mat over a paving distance of approximately 20 ft. This maximum temperature is called the maximum baseline temperature.

Note 7—The infrared thermometer will display the maximum temperature of the uncompacted mat surface when the trigger is released.

4.5.5	Determine the lowest allowable profile temperature by subtracting 25°F from the maximum baseline temperature measured in Section 4.5.4.

4.5.6	Follow the guidelines in Section 4.3 and use the procedures in Sections 4.5.1 to 4.5.3 to determine the minimum profile temperature over a paving distance of approximately 150 ft.

Note 8—The minimum profile temperature is the lowest temperature value measured throughout the thermal profile. (Refer to Figure D.2.)

Note 9—The infrared thermometer may have the capability to display the minimum temperature. Refer to the manufacturer's instructions.

4.5.7	Proceed to Section 4.8.

4.6	*Using the Thermal Imaging Camera:*

4.6.1	Configure the thermal camera to achieve the optimum brightness and contrast of the display image.

4.6.2	Configure the thermal camera to adjust the minimum and maximum temperature levels automatically while performing thermal profiles. Do not manually enter the minimum and maximum temperature levels.

Note 10—Thermal cameras are generally equipped with an auto-adjusting feature. This feature automatically adjusts the minimum and maximum temperature levels, brightness, and contrast.

4.6.3	Observe the paving operations to determine the approximate distance the paver travels until the roller compacts the mat.

Note 11—Refer to the manufacturer's instructions for determining the relationship between the field of view and distance to determine the length of pavement evaluated for the thermal camera in use.

4.6.4	Stand at the edge of the uncompacted mat at a distance of approximately 5 ft behind the paver or stand on the paver screed.

Note 12—Follow all safety precautions and guidelines when standing on the paver screed.

4.6.5	Measure the temperature of the uncompacted mat by pointing the thermal camera and squeezing the trigger facing the direction opposite of paving.

Note 13—Use the laser pointer equipped with the thermal camera as guidance to identify the area evaluated.

4.6.6	Follow the guidelines in Section 4.3 and determine the maximum baseline temperature over a paving distance of approximately 20 ft (6.1 m).

Note 14—Avoid measuring high-temperature areas caused by heating from the screed while the paver is stopped.

4.6.7	Save the image to the memory of the thermal camera.

Note 15—Additional images may be necessary to evaluate the total paving distance.

4.6.8	Follow the manufacturer's recommendations to determine the maximum temperature for the area evaluated and designate as the maximum baseline temperature.

4.6.9	Determine the lowest allowable profile temperature by subtracting 25°F from the maximum baseline temperature measured in Section 4.6.8.

4.6.10	Follow the requirements of Section 4.3 and Sections 4.6.1 to 4.6.5 to determine the minimum profile temperature over a paving distance of approximately 150 ft.

Note 16—The minimum profile temperature is the lowest temperature value measured throughout the thermal profile.

Note 17—Additional images will be necessary to evaluate the total paving distance.

4.6.11	Proceed to Section 4.8.
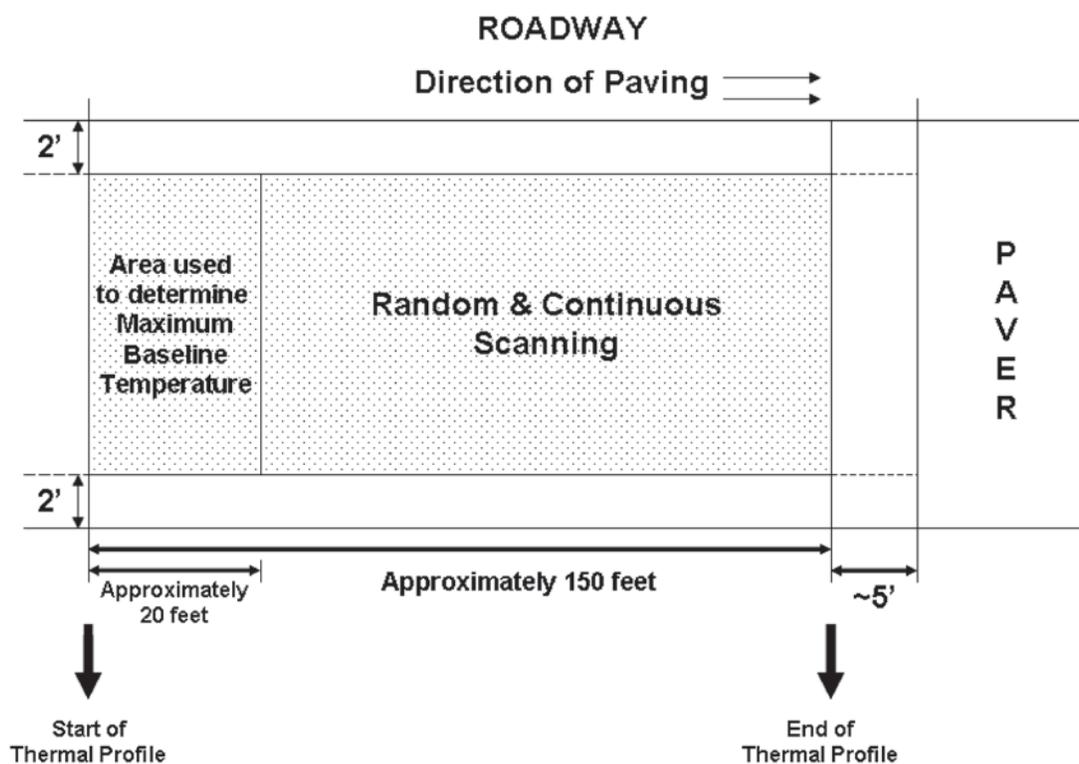
Figure D.1. Thermal profile when using a handheld noncontact infrared thermometer or a thermal imaging camera.

68

4.7	*Using the Pave-IR System:*
4.7.1	Install and operate the Pave-IR system to the paver screed following the manufacturer's recommendations.
4.7.2	Verify the calibration for each temperature sensor prior to collecting temperature measurements per manufacturer's recommendations.

Note 18—Calibrate each temperature sensor to a known standard on an annual basis.

4.7.3	Configure the Pave-IR system to record pavement temperatures at increments of no more than 6 in. of forward movement.
4.7.4	Refer to the automated test report produced by the Pave-IR system to obtain a summary of the results from the temperature readings measured in Section 4.7.3.

Note 19—The test report must include the locations (in station numbers, GPS coordinates, or other acceptable means) where thermal segregation exists.

4.8	Record the low temperature value obtained at the edge of the paving lane using spray paint or a permanent marker if the temperature of any area of the mat in the profile is less than the lowest allowable profile temperature established in Section 4.5.5, Section 4.6.9, or at the locations identified as having thermal segregation in Section 4.7.4.
4.9	Record the station number to identify the location of the mat for the low temperature measured in Section 4.5.6, Section 4.6.10, or Section 4.7.4.

Note 20—Instead of station numbers, use GPS coordinates or other acceptable means of identifying the location.
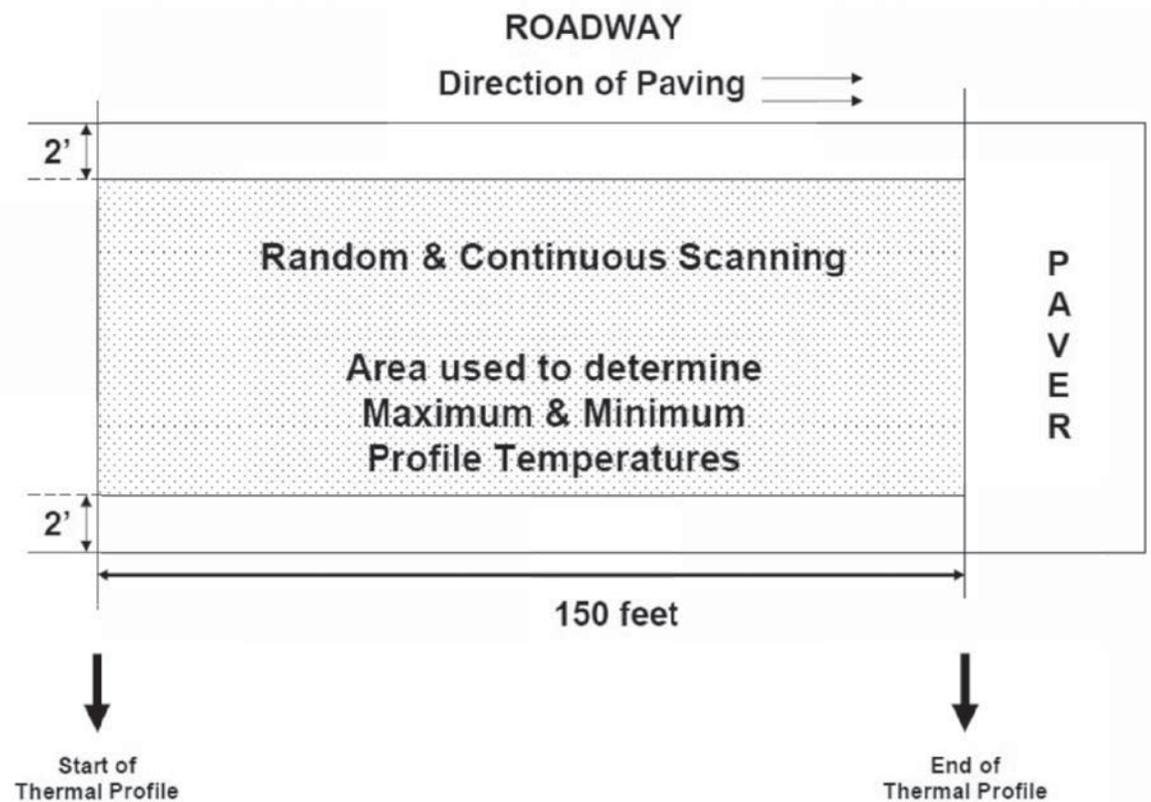
Figure D.2. Thermal profile when using the Pave-IR system.

5.   CALCULATIONS

5.1   Calculate and record the temperature differential of the uncompacted mat surface when using a handheld noncontact infrared thermometer or the thermal imaging camera:

Temperature Differential = Maximum Baseline Temperature – Minimum Profile Temperature

5.2   Calculate and record the temperature differential of the uncompacted mat surface when using the Pave-IR system:

Temperature Differential = Maximum Temperature Recorded – Minimum Temperature Recorded

Note 21—The minimum and maximum temperatures within each profile are determined using the statistical 1 percentile and 98.5 percentile, respectively.

6.   ARCHIVED VERSIONS

6.1   Archived versions are available.

Method for Detecting Segregation with GPR

Section 1. Overview

This method details procedures for using ground-penetrating radar (GPR) for detection of potentially segregated areas on a newly placed hot-mix asphalt overlay. This method requires the user to possess a working knowledge of the GPR data-collection equipment and radar data-collection software. This method uses variations in the surface dielectric constant to examine the project for segregation. This software has the capabilities of:

1. Producing a table of computed surface dielectric versus distance of travel along the project from the raw GPR data;
2. Using regression techniques to calculate the relationship between surface dielectric and air voids from a field coring operations; and

3. Converting the surface dielectric into in-place densities and reporting the results.

Section 5 shows an example of how this conversion is achieved using the TxDOT developed software packages.

Section 2. Apparatus

- An air-launched GPR system, capable of collecting signals in both distance and time modes, and capable of collecting a signal at least every foot;
- Field coring equipment;
- GPR data processing software to compute surface dielectric versus distance; and
- A GPR analysis program (conversion to air voids plus graphical mapping of the results from parallel runs).

Section 3. Procedure

Locating Potential Segregation with GPR

Step	Action
1	At the project site, set up the GPR data collection equipment and allow the antenna to warm up.
2	After placement and final rolling of the overlay at the project site, determine and document the limits where GPR data will be collected.

3	After placement and final compaction of the overlay, collect GPR data in a longitudinal pass covering the desired section limits. Collect this pass over the outside wheelpath.
	    Note: Data should be collected in distance mode with one trace recorded every foot.
	    If a more complete analysis of the project is desired, collect additional passes over the centerline and the inside wheelpath with the GPR system.

4	After collecting the desired longitudinal GPR passes, collect the metal plate file.
4a (Optional)	In the field, use GPR display software to examine the collected data and locate areas of high, low, and normal surface dielectric. Return to each of these locations and collect a stationary GPR reading over each location. Collect these data by positioning the antenna directly over the desired location, setting the GPR vehicle in park, and using the time data collection mode. Document each location with a unique label for future reference. Before moving to the next location, paint a circle approximately 12 in. in diameter directly underneath the antenna. Note: This step is necessary if an analysis of the in-place air voids over the section is desired.
4b (Required If 4a Performed)	At each of the previously marked locations from 4a, determine the bulk density, percent compaction, and percent air voids of the hot-mix asphalt through an approved method. Currently, cores should be taken from within each marked circle, returned to the laboratory, and tested with the appropriate part from Test Method Tex-207-F.
5	Using the GPR processing software, create a text output file from each GPR pass that contains, at a minimum, the surface dielectric (E1) value.

6	For a basic analysis, open the text file with Excel and determine the mean surface dielectric value of the tested section. Graph the surface dielectric value with distance. From this graph, determine if any areas of the project need investigation according to the following criteria:
	  • Coarse-graded mixes: locations not within ±0.8 of the mean dielectric value should be inspected for segregation.
	  • Dense-graded mixes: locations not within ±0.4 of the mean dielectric value should be inspected for segregation.

7	For a more advanced GPR analysis, predict air void content from the GPR-measured surface dielectric by using the calibration core data (from Step 4b) along with the following model:
	    % Air Voids = $A * e^{B*\text{Surface Dielectric (E1)}}$
	    where A and B are laboratory-determined constants.
	Use software to identify the percentage of measurements expected to have air voids with pay factors less than 1.0. If desired, use mapping software to display the geospatial location of measurements with pay factors less than 1.0.

8	Based on the results of the analysis, determine what, if any, corrective action should be taken.

Section 4. Reporting

Report the following information from the GPR survey:

- Project description, including mix type, contractor, and brief description of placement operation;
- Limits of the GPR survey;
- Graph of surface dielectric with distance;
- Mean, minimum, and maximum observed surface dielectric;
- Limits of potentially segregated areas;
- Results from core analysis and analysis of in-place air voids, if conducted; and
- Recommended corrective action.

To produce a color-coded map of in-place air voids, collect GPR data from a minimum of five parallel runs over the test site. Process each run to compute surface dielectrics, and compute in-place air voids from the calibration with core density. Then use digital mapping software to display the results and interpolate between values. Numerous such graphing packages are commercially available.

Section 5. Basics of GPR Data Processing

The following screens are from the software developed in TxDOT study 5-1702 (*1*).

The first step in the analysis of GPR data is to convert the measured amplitude of surface reflection into a surface dielectric. This uses exactly the same approach as that described in Appendix C (Equation C.1), where the ratio of amplitudes from the surface compared to that from a 100%
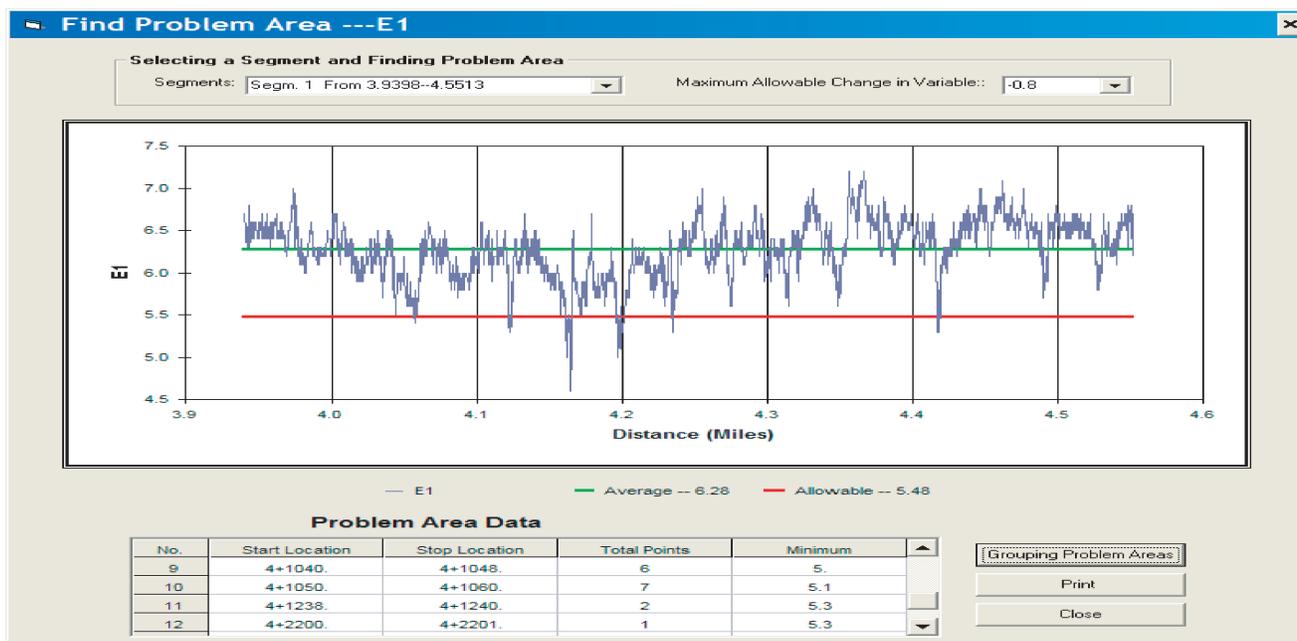
Figure E.1. Plot of computed surface dielectric versus distance along the project.

reflection (metal plate reflection) is used to computed the surface dielectric. Figure E.1 shows the plot of the computed surface dielectric from one pass of the system over the pavement.

Based on this plot, a minimum of three core locations are selected at locations of different surface dielectrics. Normally nuclear (or nonnuclear) nondestructive testing density gauge readings are taken at these locations, and 6-in.-diameter filed cores are also extracted. These are returned to the laboratory where in-place air voids are calculated. Typical results are shown in Figure E.2.

The next step is to develop regression equations relating the dielectrics and laboratory densities and air voids. This is shown in Figure E.3. Two options are available. The first uses nuclear density gauges and Rice maximum densities to estimate air voids. The second uses cores to determine air voids in the laboratory. The second method is more accurate and is recommended. In the example in Figure E.3, the regression parameters $A = 145.5$ and $B = -0.46$ were computed for the input data provided.

The next step is to use these regression equations to convert the dielectric plot shown in Figure E.1 into an air void plot as shown in Figure E.4.

The final step in the processing is to take multiple runs over the test section. Under normal operations, five parallel runs are made transversely across the 12-ft-wide lane (1 ft from the
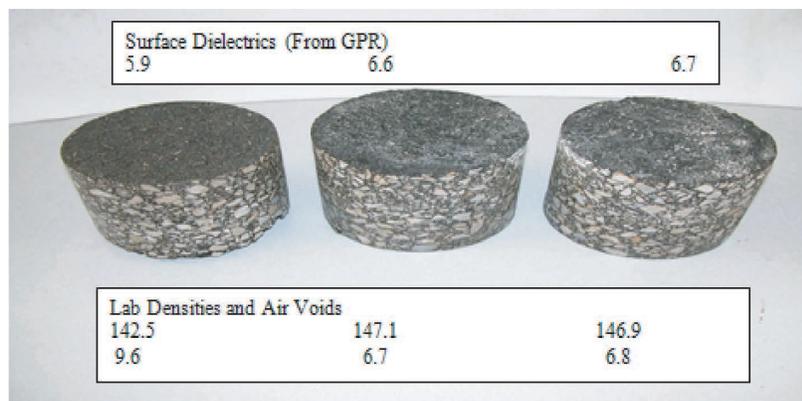
Figure E.2. Comparing field dielectrics with laboratory-measured properties.
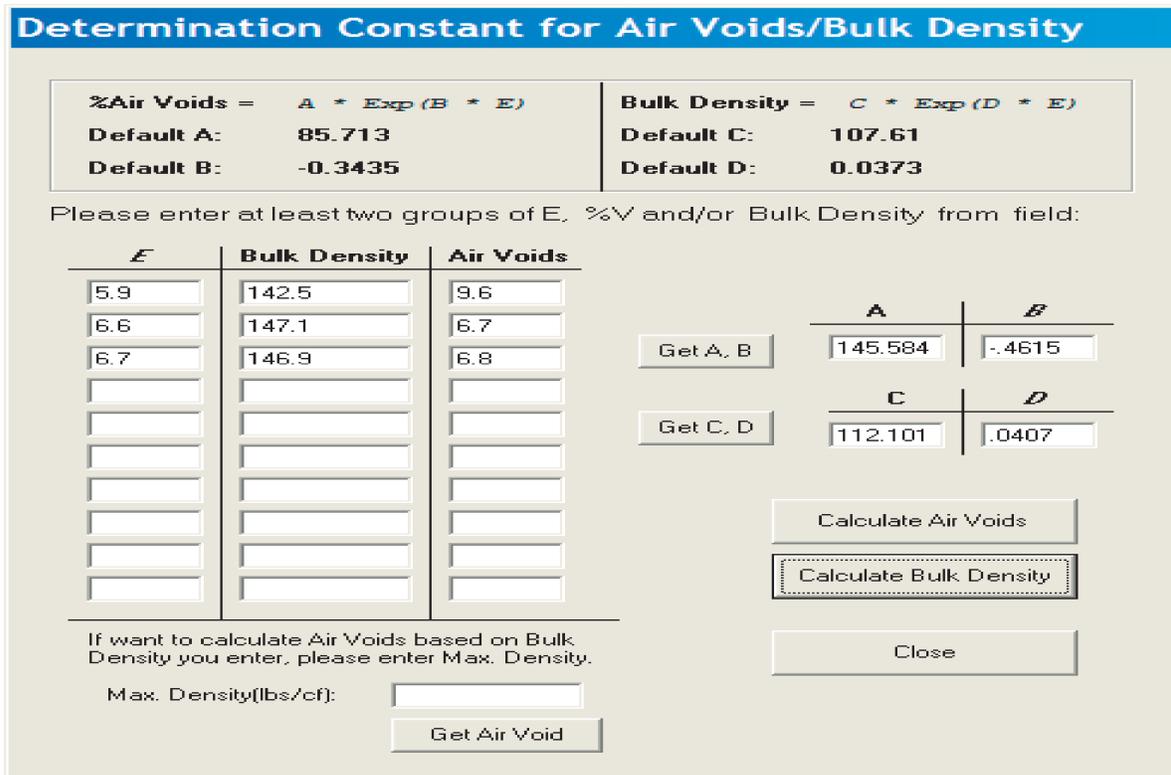
Figure E.3. Developing regression equations relating dielectrics to air voids.
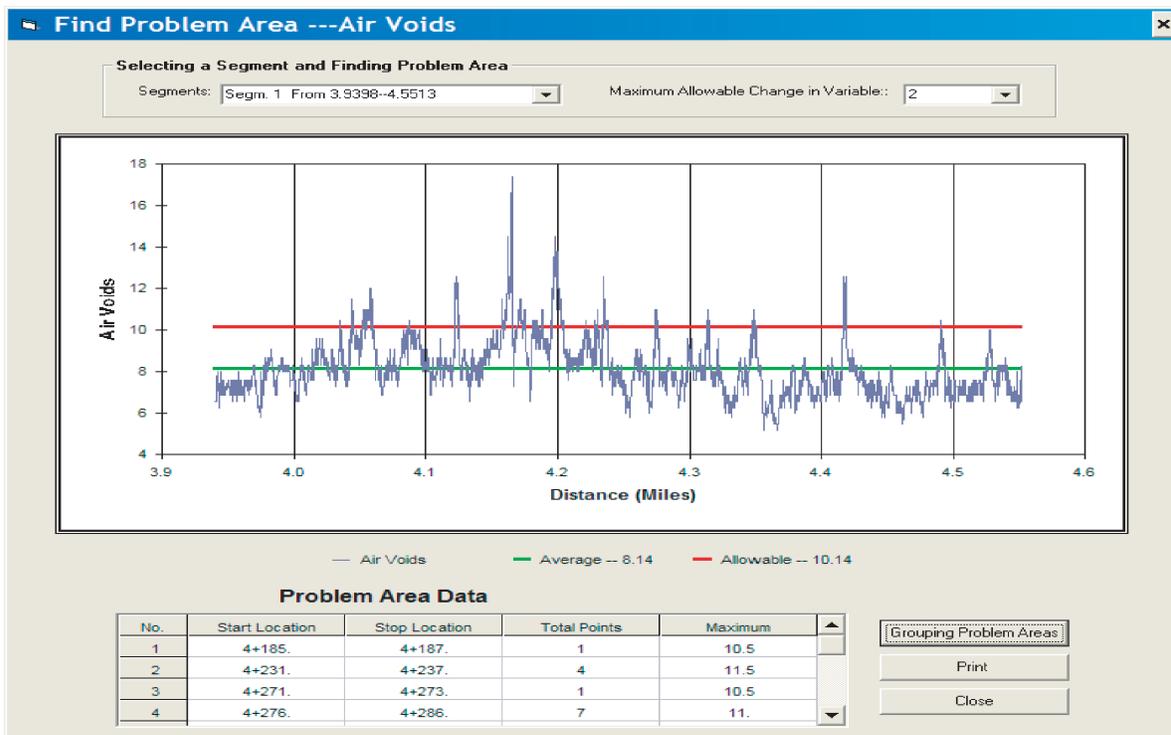
*Figure E.4. Plot of computed air voids for a single GPR run.*
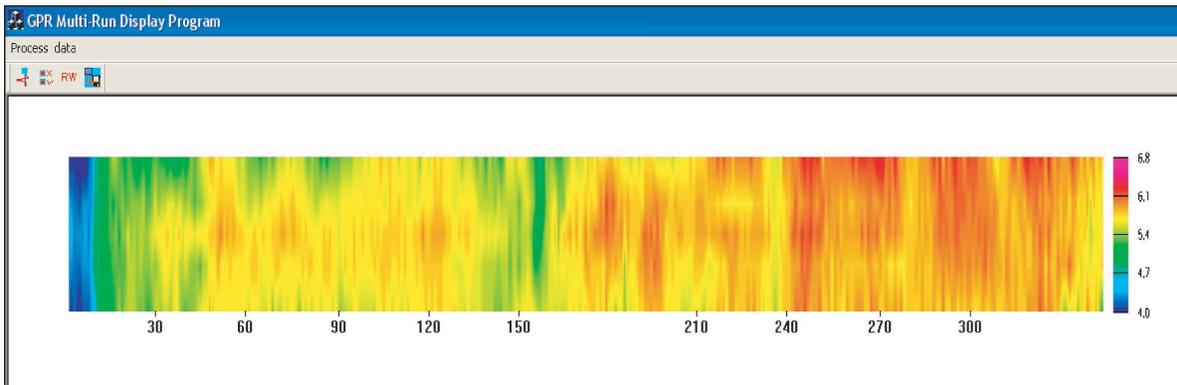
Figure E.5. Surface dielectric plot from five parallel GPR runs.

outer edge, wheelpath, center, wheelpath, and inside edge). These are then processed using the steps above and stacked side by side in a color-coded plot. The plot in Figure E.5 shows the color-coded plot of surface dielectric from a 400 ft × 12 ft section of pavement.

Reference

1. Wang, F., and T. Scullion. *RADSEG User's Manual: A GPR Analysis System for Detecting Segregation in New Asphalt Overlays.* TTI Report 5-1702-01-P7. Texas A&M Transportation Institute, College Station, Tex., October 2003.

Correlations of NDT and Core Data from Region 4 Demonstration

Correlation *R*-values and *P*-values

The following tables present the observed correlation *r*-values, and the *p*-values of the observed correlation, between nondestructive testing (NDT) and core data collected. Numbers in bold are statistically significant at the 95% confidence level.

Table F.1. Correlation R-Values Between NDT, Density, Permeability, and Asphalt Content

	Temperature	GPR ε	Nuke (lb/ft³)	Laboratory (lb/ft³)	Laboratory % Air Voids	Permeability	% AC
Temperature	1						
GPR ε	−0.20	1					
Nuke (lb/ft³)	0.16	**0.84**	1				
Laboratory (lb/ft³)	0.080	0.25	0.36	1			
Laboratory % Air Voids	−0.080	−0.25	−0.36	**−1.0**	1		
Permeability	−0.026	−0.49	**−0.70**	−0.21	0.21	1	
% AC	−0.46	0.31	0.04	−0.34	0.34	0.37	1

Table F.2. P-Values for Observed Correlations Between NDT, Density, Permeability, and Asphalt Content

	Temperature	GPR ε	Nuke (lb/ft³)	Laboratory (lb/ft³)	Laboratory % Air Voids	Permeability
Temperature						
GPR ε	0.28					
Nuke (lb/ft³)	0.33	**0.0012**				
Laboratory (lb/ft³)	0.41	0.24	0.15			
Laboratory % Air Voids	0.41	0.24	0.15	**0.00**		
Permeability	0.47	0.074	**0.012**	0.28	0.28	
% AC	0.09	0.19	0.46	0.17	0.17	0.15

Table F.3. Correlation R-Values Between NDT and Individual Percent Retained

	Temperature	GPR ε
Temperature	1	
GPR ε	−0.20	1
½ in.	0.069	−0.44
⅜ in.	−0.18	**−0.68**
No. 4	0.0071	**0.62**
No. 8	0.037	**0.72**
No. 16	−0.50	−0.079
No. 30	−0.31	0.094
No. 50	−0.42	−0.0055
No. 200	−0.47	−0.077

Table F.4. P-Values for Observed Correlations Between NDT and Individual Percent Retained

	Temperature	GPR ε
Temperature		
GPR ε	0.28	
½ in.	0.42	0.10
⅜ in.	0.31	**0.015**
No. 4	0.49	**0.029**
No. 8	0.46	**0.009**
No. 16	0.07	0.41
No. 30	0.19	0.40
No. 50	0.12	0.49
No. 200	0.086	0.42

Table F.5. Correlation R-Values Between NDT and Percent Passing

	Temperature	GPR ε
Temperature	1	
GPR ε	−0.20	1
½ in.	−0.069	0.43
⅜ in.	0.051	**0.68**
No. 4	0.071	0.45
No. 8	0.067	0.22
No. 16	0.19	0.27
No. 30	0.25	0.28
No. 50	0.32	0.30
No. 200	0.47	0.32

Table F.6. P-Values for Observed Correlations Between NDT and Percent Passing

	Temperature	GPR ε
Temperature		
GPR ε	0.28	
½ in.	0.42	0.10
⅜ in.	0.44	**0.015**
No. 4	0.42	0.097
No. 8	0.43	0.27
No. 16	0.30	0.23
No. 30	0.24	0.22
No. 50	0.8	0.20
No. 200	0.08	0.18

APPENDIX G

Correlations of NDT and Core Data from Region 2 Demonstration

Correlation *R*-values and *P*-values

The following tables present the observed correlation *r*-values, and the *p*-values of the observed correlation, between nondestructive testing (NDT) and core data collected. Numbers in bold are statistically significant at the 95% confidence level.

Table G.1. Correlation R-Values Between NDT and Core Data

	Temperature	GPR ε	Nuke (lb/ft³)	Laboratory (lb/ft³)	Laboratory % Air Voids
Temperature	1				
GPR ε	**0.897**	1			
Nuke (lb/ft³)	0.662	0.688	1		
Laboratory (lb/ft³)	**0.918**	**0.877**	**0.791**	1	
Laboratory % Air Voids	**0.918**	**−0.877**	**−0.791**	**−1**	1

Table G.2. P-Values for Observed Correlations Between NDT and Core Data

	Temperature	GPR ε	Nuke (lb/ft³)	Laboratory (lb/ft³)
Temperature				
GPR ε	0.0011			
Nuke (lb/ft³)	0.052	**0.0279**		
Laboratory (lb/ft³)	**0.0005**	**0.0008**	**0.0064**	
Laboratory % Air Voids	**0.0005**	**0.0008**	**0.0064**	**0.00**

77

APPENDIX H

Correlations of NDT and Core Data from Region 3 Demonstration

Correlation *R*-values and *P*-values

The following tables present the observed correlation *r*-values, and the *p*-values of the observed correlation, between non-destructive testing (NDT) and core data collected. Numbers in bold are statistically significant at the 95% confidence level.

Table H.1. Correlation R-Values Between NDT, Density, IDT, and Asphalt Content

	Temperature	GPR ε	Nuke (lb/ft³)	Laboratory % Air Voids	IDT (psi)	% AC
Temperature	1					
GPR ε	0.608	1				
Nuke (lb/ft³)	**0.775**	**0.915**	1			
Laboratory % Air Voids	**−0.813**	**−0.902**	**−0.939**	1		
IDT (psi)	**0.898**	**0.867**	**0.929**	**−0.968**	1	
% AC	0.575	0.490	0.596	−0.431	0.545	1

Note: IDT = indirect tension.

Table H.2. P-Values for Observed Correlations Between NDT, Density, IDT, and Asphalt Content

	Temperature	GPR ε	Nuke (lb/ft³)	Laboratory % Air Voids	IDT (psi)
Temperature					
GPR ε	0.062				
Nuke (lb/ft³)	**0.0085**	**0.00021**			
Laboratory % Air Voids	**0.0042**	**0.00036**	**5.8E-05**		
IDT (psi)	**0.00042**	**0.0012**	**0.00010**	**4.2E-06**	
% AC	0.082	0.15	0.069	0.21	0.10

Table H.3. Correlation R-Values Between NDT and Percent Passing

	Temperature	GPR ε
Temperature	1	
GPR ε	0.608	1
½ in.	0.622	0.428
⅜ in.	**0.820**	**0.672**
No. 4	**0.714**	0.564
No. 8	**0.747**	0.577
No. 16	**0.737**	0.559
No. 30	**0.639**	0.493
No. 50	0.380	0.325
No. 200	0.0882	0.130

Table H.4. P-Values for Observed Correlations Between NDT and Percent Passing

	Temperature	GPR ε
Temperature		
GPR ε	0.062	
½ in.	0.055	0.21
⅜ in.	**0.0036**	**0.033**
No. 4	**0.020**	0.089
No. 8	**0.013**	0.080
No. 16	**0.015**	0.093
No. 30	**0.047**	0.15
No. 50	0.28	0.36
No. 200	0.81	0.72

APPENDIX I

Correlations of NDT and Core Data from Region 1 Demonstration

Correlation *R*-values and *P*-values

The following tables present the observed correlation *r*-values, and the *p*-values of the observed correlation, between nondestructive testing (NDT) and core data collected. Numbers in bold are statistically significant at the 95% confidence level.

Table I.1. Correlation R-*Values Between NDT and Core Data*

	Temperature	GPR ε (1 GHz)	GPR ε (2.2 GHz)	Nuke (lb/ft³)	Laboratory (lb/ft³)	Lab % Air Voids
Temperature	1					
GPR ε (1 GHz)	**0.785**	1				
GPR ε (2.2 GHz)	−0.0230	**0.661**	1			
Nuke (lb/ft³)	0.574	**0.849**	0.846	1		
Laboratory (lb/ft³)	**0.763**	**0.871**	0.834	0.987	1	
Laboratory % Air Voids	**−0.763**	**−0.871**	−0.834	−0.987	**−1**	1

Table I.2. P-*Values for Observed Correlations Between NDT and Core Data*

	Temperature	GPR ε (1 GHz)	GPR ε (2.2 GHz)	Nuke (lb/ft³)	Laboratory (lb/ft³)
Temperature					
GPR ε (1 GHz)	**0.0122**				
GPR ε (2.2 GHz)	0.953	**0.0269**			
Nuke (lb/ft³)	0.106	**0.000951**	**0.00104**		
Laboratory (lb/ft³)	**0.0169**	**0.000480**	**0.00141**	**1.7E-08**	
Laboratory % Air Voids	**0.0169**	**0.000480**	**0.00141**	**1.7E-08**	**0.00**

Related SHRP 2 Research

Nondestructive Testing to Identify Concrete Bridge Deck Deterioration (R06A)

Evaluating Applications of Field Spectroscopy Devices to Fingerprint Commonly Used Construction Materials (R06B)

Nondestructive Testing to Identify Delaminations Between HMA Layers (R06D)

Real-Time Smoothness Measurements on Portland Cement Concrete Pavements During Construction (R06E)

Assessment of Continuous Pavement Deflection Measuring Technologies (R06F)

High-Speed Nondestructive Testing Methods for Mapping Voids, Debonding, Delaminations, Moisture, and Other Defects Behind or Within Tunnel Linings (R06G)